Identification of molecular mechanisms modulating nuclear abundance and co-repressor functions of CtBP1 in neurons

Dissertation

zur Erlangung des akademischen Grades

doctor rerum naturalium
(Dr. rer. nat.)

genehmigt durch die Fakultät für Naturwissenschaften
der Otto-von-Guericke-Universität Magdeburg

von M.Sc. Anika Dirks
geb. am 20.05.1987 in Quedlinburg

Gutachter: Prof. Dr. Eckart D. Gundelfinger
Prof. Dr. med. Frank Schmitz

eingereicht am: 24.10.2016
verteidigt am: 16.03.2017

I. Acknowledgement

My thesis is the result of committed work done at the Leibniz Institute for Neurobiology in Magdeburg, which would not have been possible without the support of my family, friends and lab members.

First of all, I would like to thank my supervisors Prof. Dr. Eckart D. Gundelfinger and Prof. Dr. Anna Fejtová for giving me the opportunity to work on this project and teaching me to become an independent scientist. I am grateful for their trust in my work and for their constructive discussions and guidance. Moreover, I would like to thank Dr. Michael Kreutz for being my second supervisor and for valuable discussions and suggestions.

I would particularly like to thank Dr. Daniela Ivanova. Besides sharing the office, she guided me through my thesis. Due to her helpful criticism and ideas my study gained in quality. I am grateful for the support of Anil Annamneedi who helped me with the slice-preparation, Dr. Carolina Montenegro who teached me all about mouse culture preparations and our technician Isabel Herbert for her valuable help in cloning. Thanks to all my other lab members Dr. Vesna Lazarevic, Franziska Altmüller, Maria Andrès-Alonso, Sandra Fienko, Eneko Pina, Santosh Pothula, Janina Juhle, Jeanette Maiwald, Peggy Patella and Bettina Kracht for daily talks and the creation of a very nice atmosphere in the lab. Not just group members, also friends supported me in the lab. I want to especially thank Dr. Rodrigo Herrera-Molina for his support with my final experiments- I did not expect that establishing a live-imaging setup and generating data would be possible within two months! Additionally, I am very grateful to have gotten the opportunity to meet Prof. Dr. Mike Fainzilber and to work with mice provided by his lab. Besides my work in the lab, Anna and Eckart gave me the opportunity to attend instructive international conferences and a summer school, which was supported by the DFG GRK 1167.

Abschließend möchte ich noch den wohl wichtigsten Menschen in meinem Leben danken: Meiner Familie und meinen Freunden. Anne Steinke hatte als meine langjährige beste Freundin immer ein offenes Ohr für mich und war für mich da, wann immer es nötig war. Meine Mittags- und Kaffeepausen mit Dr. Anne-Christin Lehmann, Sabrina Müller, Dr. Stefan Sokoll, Dr. Marie Woldeit und Sophie Ehrenberg haben mir sehr oft den Tag gerettet. Anne-Christin, vielen Dank für dein unermütliches Korrekturlesen meiner Doktorarbeit und deine aufmunternden Worte zur richtigen Zeit. Ich möchte auch von Herzen meinem Ehemann Toni Dirks für seine Unterstützung in den letzten Jahren danken. Zum Schluss bleibt mir nur noch mich bei meinen Eltern zu bedanken, die mir immer alles ermöglicht haben, mich zur Promotion ermutigt haben und mir mit Rat und Tat zur Seite standen, wenn ich einmal nicht weiter wusste.

II. Table of contents

1. Introduction **12**

1.1. Activity-dependent regulation of gene expression 12

1.1.1. Global Ca^{2+} routes 12

1.1.2. Synapse-to-nucleus communication mediated by protein messengers 16

1.1.3. Regulation of nuclear import and export 17

1.2. C-terminal binding proteins 19

1.2.1. Role of CtBP1 in gene expression 21

1.3. Objectives 23

2. Material and methods **24**

2.1. Material 24

2.1.1. Chemicals 24

2.1.2. Antibodies 24

2.1.2.1. Primary antibodies 24

2.1.2.2. Secondary antibodies 25

2.1.2.3. Fluorescent dyes 25

2.1.3. Animals 26

2.1.4. Bacteria strains and culture media 26

2.2. Methods 27

2.2.1. Biochemical methods 27

2.2.1.1. Isolation of cortex and hippocampus from mouse brain 27

2.2.1.2. Preparation of nuclear and cytoplasmic fraction from cortical cultures 27

2.2.1.3. Co-immunoprecipitation using magnetic anti-GFP microbeads 28

2.2.1.4. Immunoprecipitation of endogenous CtBP1 using sepharose coupled protein G 28

2.2.1.5. Amido black protein assay 29

2.2.1.6. Sodium dodecyl sulfate polyacrylamide gel electrophoresis (SDS-PAGE) 29

2.2.1.7. Western blotting and quantification 30

2.2.2. Cell culture 30

2.2.2.1. Cultivation and transfection of mammalian cell lines 30

2.2.2.2. Generation of lentiviral particles 31

2.2.2.3. Cultivation and infection of primary neuronal cultures 31

2.2.2.4. Treatment of cultured neurons 32

2.2.2.4.1. Chronical silencing and disinhibition of cultured cortical neurons 32

2.2.2.4.2. NMDA stimulation and viability assay of cultured primary neurons 33

2.2.2.4.3. Pharmacological treatments of cultured primary neurons 33
2.2.2.5. Slice preparation from mutant mice 35
2.2.2.6. Immunocytochemistry and imaging 35
2.2.2.6.1. Synaptotagmin 1 antibody live-uptake 36
2.2.2.6.2. Arc and BDNF promoter assay 36
2.2.2.6.3. Wide-field and confocal microscopy 36
2.2.2.6.4. Live-imaging 37
2.2.2.6.5. Image analysis 37
2.2.2.7. Statistical analysis 37
2.2.3. Molecular biological methods 38
2.2.3.1. Genotyping of mutant mice 38
2.2.3.2. DNA restriction 39
2.2.3.3. Agarose gel electrophoresis and DNA extraction from agarose gels 39
2.2.3.4. Cold Fusion™ Cloning 39
2.2.3.5. Transformation of chemically competent bacteria 41
2.2.3.6. Alkaline lysis preparation of plasmid DNA 41
2.2.3.7. Sequencing and sequence analysis 42
3. Results 43
3.1. CtBP1 synapto-nuclear distribution is controlled by neuronal activity 43
3.2. CtBP1 nucleo-cytoplasmic translocation is driven by network activity in excitatory neurons 47
3.3. Role of CtBP1 in regulation of activity-dependent genes 52
3.4. CtBP1 co-repressor function depends on Ca^{2+} signaling 55
3.4.1. GluN2B subunit containing NMDA receptors affect CtBP1 nuclear abundance 55
3.4.2. N-type voltage-gated calcium channels influence CtBP1 nuclear abundance in neurons 58
3.4.3. Intracellular Ca^{2+} in regulation of CtBP1 nuclear abundance 61
3.5. Activity-dependent nuclear export of CtBP1 in neurons is mediated by exportin 1 63
3.6. CtBP1 phosphorylation by PKA and Pak1 regulates its nuclear export in cortical neurons 69
3.7. Importin β1 and microtubules play a role in the activity-induced retrograde translocation and nuclear import of CtBP1 75

4. Discussion **80**

4.1. CtBP1 activity-regulated nuclear abundance is crucial for neuronal function 80

4.2. Mechanisms facilitating the nuclear export of CtBP1 in neurons 82

4.2.1. NMDA receptor signaling and global Ca^{2+} routes regulate the nuclear abundance of CtBP1 82

4.2.2. Exportin 1 mediates the activity-induced nuclear export of CtBP1 85

4.2.3. Posttranslational modifications of CtBP1 86

4.3. Nuclear import of CtBP1 in neurons 87

4.4. Conclusion 90

5. Literature **92**

6. Abbreviations **104**

7. Curriculum Vitae **106**

8. List of publications **107**

9. Eidesstattliche Erklärung **108**

III. List of figures

Figure 1.1: Routes for Ca^{2+} entry in neurons. 13

Figure 1.2: Model of nucleo-cytoplasmic transport of molecules. 18

Figure 1.3: C-terminal binding protein family members. 20

Figure 1.4: Domain structure of CtBP1-L. 21

Figure 1.5: CtBP in transcriptional repressor complexes mediating gene specific (A) and global (B) transcription repression. 22

Figure 2.1: Workflow of NMDA stimulation of cultured primary neurons, including application of pharmacological drugs. 33

Figure 3.1: Neuronal activity regulates the distribution of CtBP1 between presynapses and the nucleus in primary cortical cultures. 44

Figure 3.2: Time course of activity-induced translocation of CtBP1 into neuronal nuclei. 46

Figure 3.3: Fast adaptations of nuclear CtBP1 levels in response to changes in neuronal network activity. 48

Figure 3.4: Three-dimensional representation of CtBP1 distribution in mature cortical neurons. 49

Figure 3.5: Isolated nuclear fractions of mature cortical cultures showed an activity-dependent CtBP1 distribution. 50

Figure 3.6: CtBP1 activity-dependent nucleo/cytoplasmic-synaptic translocation is only observed in excitatory neurons. 51

Figure 3.7: Characterization of the CtBP1 KO mouse model. 52

Figure 3.8: Arc and BDNF promoters are regulated by CtBP1. 54

Figure 3.9: NMDA receptor signaling plays a crucial role in the nucleo-cytoplasmic translocation of CtBP1. 56

Figure 3.10: GluN2B containing NMDA receptors contribute to the nucleo-cytoplasmic translocation of CtBP1. 57

Figure 3.11: Ca^{2+} influx through N-type voltage-dependent calcium channels contributes to the Ca^{2+}-dependent nuclear depletion of CtBP1. 59

Figure 3.12: Ca^{2+} influx through N-type voltage-dependent calcium channels is required for the regulation of activity-dependent genes by CtBP1. 60

Figure 3.13: Intracellular Ca^{2+} is required for the nuclear depletion of CtBP1 after activation of NMDA receptors. 61

Figure 3.14: Ca^{2+} released from intracellular stores is required for the nuclear depletion of CtBP1. 62

Figure 3.15: Exportin 1 is crucial for the activity-dependent nuclear export of CtBP1 in cultured cortical neurons. 64

Figure 3.16: Characterization of the lentiviral construct CtBP1intEGFP_NESmut. 65

Figure 3.17: Mutation in the NES of CtBP1 prevents its activity-induced nucleo-cytoplasmic redistribution. 66

Figure 3.18: Live-imaging experiments performed in mature hippocampal neurons demonstrate the activity-induced nuclear export of CtBP1 dependent on its NES. 67

Figure 3.19: Co-immunoprecipitations of overexpressed CtBP1 constructs revealed CtBP1 interaction with exportin 1 mediated by its NES. 68

Figure 3.20: Potential phosphorylation sites of CtBP1 in neurons. 69

Figure 3.21: Potential signaling pathways involved in CtBP1 relocalization. 70

Figure 3.22: Nuclear export of CtBP1 requires both PKA phosphorylation and activity-induced adaptations of intracellular Ca^{2+} levels. 71

Figure 3.23: Characterization of CtBP1 constructs lacking phosphorylation sites of PKA and Pak1. 73

Figure 3.24: Phosphorylation of CtBP1 by PKA and Pak1 is required for the activity-induced nucleo-cytoplasmic translocation of CtBP1. 74

Figure 3.25: Importin β plays a key role in the nuclear import mechanism of CtBP1 in mature cortical neurons. 75

Figure 3.26: Microtubule transport machinery is required for the activity-induced synapse-to-nucleus translocation of CtBP1. 77

Figure 3.27: Shift of CtBP1 distribution towards presynapses in primary dissociated hippocampal cultures from KPNB1 Δ3´UTR subcellular KO mice. 78

Figure 3.28: Increased synaptic activity in KPNB1 Δ3´UTR subcellular KO mouse model. 79

Figure 4.1: Model for the activity-induced nuclear import and export of CtBP1 in neurons. 91

IV. List of tables

Table 1.1: Proteins that shuttle into the nucleus in response to neuronal activity. 17

Table 2.1: List of primary antibodies used for immunocytochemistry (ICC) and Western blotting (WB). 24

Table 2.2: List of secondary antibodies used for immunocytochemistry (ICC) and Western blotting (WB). 25

Table 2.3: List of fluorescent dyes used for immunocytochemistry (ICC). 25

Table 2.4: Culture media for bacterial cells. 26

Table 2.5: Pharmacological reagents. 32

Table 2.6: Pharmacological reagents. 34

Table 2.7: Master mix for genotyping of mutant mice. 38

Table 2.8: PCR program for genotyping of mutant mice. 38

Table 2.9: Generated constructs used in this study. 39

Table 2.10: Primers for cloning. Mutations are labeled in blue. 40

Table 2.11: PCR reaction and program. 40

Table 2.12: Cloning reaction. 41

V. Summary

Neuronal networks comprise millions of interconnected cells crucial for information processing, storage and transmission. Learning and memory formation requires alterations in elemental processes regulating these networks, many of which are based on the modulation of gene expression. Gene transcription is controlled in the nucleus, and its adjustments require the transmission of signals from the synaptic to the nuclear compartment. Upon synaptic membrane depolarization, Ca^{2+} influx via voltage- and ligand-gated calcium channels triggers the activation of signaling cascades towards the nucleus to induce changes in gene expression patterns. One major mechanism for communicating synaptic events to the nucleus is the synapse-to-nucleus shuttling of molecules. These protein messengers are present at synaptic terminals and in nuclei and most of them function as transcription modulators and/or chromatin modifiers.

Within the last decade, several postsynapse-to-nucleus and only few presynapse-to-nucleus translocating protein messengers were identified. Their shuttling between the synaptic and nuclear compartment is dependent on the neuronal network activity allowing the regulation of activity-induced gene expression. In particular, presynapse-to-nucleus translocating proteins are shown to be crucial for axon regeneration, presynaptic rearrangements, and long-term memory storage. Therefore, the control mechanisms underlying the nuclear abundance of shuttling gene expression modulators represent a unique regulation step of activity-dependent gene expression and are only poorly understood to-date.

One transcription modulator, present at presynapses, in the cytoplasm and the nucleus of neurons, is the C-terminal binding protein 1 (CtBP1). The present work describes CtBP1 as the first protein messenger to process pre- and postsynaptic signaling and gives novel insights into the regulation of its nuclear abundance and co-repressor function. The study shows that the three CtBP1 pools are interconnected, and that the transcription factor is able to translocate between the pools in an activity-dependent manner. The bidirectional shuttling of this protein messenger is crucial for its function in the regulation of activity-induced gene expression and depends on distinct neuronal signaling events which control its nuclear import and export. The study examines the role of GluN2B-containing NMDA receptor modulation, intracellular Ca^{2+}, posttranslational modifications and karyopherins for the CtBP1 nuclear abundance and co-repressor activity. The results link CtBP1-dependent gene expression to pre- and postsynaptic activity emphasizing the importance of gene regulation for neuronal plasticity and brain function.

VI. Zusammenfassung

Neuronale Netzwerke bestehen aus Millionen von miteinander verbundenen Zellen, was die Voraussetzung für die Verarbeitung, Speicherung und den Austausch von Informationen im Gehirn darstellt. Dabei basieren Lernen und Gedächtnisbildung auf Veränderungen dieser Prozesse, die häufig auf Anpassungen in der Genexpression zurückzuführen sind. Die Transkription von Genen wird im Zellkern gesteuert und ihre Adaptation benötigt die Weiterleitung von Signalen vom synaptischen zum nukleären Kompartiment. Aufgrund der Membrandepolarisation an den Synapsen kommt es zu einem Ca^{2+}-Einstrom durch Kalziumkanäle, wodurch Signalkaskaden zum Zellkern aktiviert werden, die Veränderungen in den Genexpressionsmustern von Nervenzellen induzieren. Ein bedeutender Mechanismus zur Übertragung von synaptischen Ereignissen in den Zellkern ist der Austausch von Proteinen zwischen den Synapsen und dem Zellkern. Diese Signalproteine sind sowohl an den Synapsen, als auch im Zellkern vorhanden und die meisten fungieren als Modulatoren der Transkription und/oder des Chromatins.

In den letzten Jahren wurden eine ganze Reihe von Postsynapse-zu-Zellkern und auch einige Präsynapse-zu-Zellkern wandernde Signalproteine identifiziert. Ihre Umverteilung zwischen dem synaptischen und nukleären Kompartiment ist von der Aktivität der Nervenzellen in ihrem Netzwerk abhängig, wodurch die Regulation der aktivitätsinduzierten Genexpression ermöglicht wird. Insbesondere die von der Präsynapse zum Zellkern wandernden Proteine sind essentiell für die Regeneration von Axonen, die Reorganisation von Synapsen und die Bildung eines Langzeitgedächtnisses. Dabei stellen Kontrollmechanismen, die die Konzentration dieser Modulatoren der Genexpression im Zellkern steuern, einen zentralen Regulationsschritt in der aktivitätsabhängigen Genexpression dar und sind noch nicht hinreichend verstanden.

Ein Modulator der Transkription, der in Nervenzellen sowohl an den Präsynapsen, im Zytoplasma und im Zellkern zu finden ist, ist das C-terminal bindende Protein 1 (CtBP1). Die vorliegende Arbeit beschreibt CtBP1 als erstes Signalprotein, welches in der Lage ist Informationen der Prä- und Postsynapse zu verarbeiten und sie gewährt neue Einblicke in die Regulation der nukleären Konzentration und Co-Repressor Funktion von CtBP1. Darüber hinaus konnte in dieser Arbeit gezeigt werden, dass die drei CtBP1 Pools miteinander verbunden sind und der Transkriptionsfaktor CtBP1 zwischen diesen Pools, in Abhängigkeit von der Zellaktivität, wandern kann. Diese bidirektionale Bewegung des Signalproteins ist wichtig für seine Funktion in der Regulation der aktivitätsinduzierten Genexpression, welche von bestimmten neuronalen Ereignissen abhängig ist, die auch den Kernimport und -export von

CtBP1 steuern. Diese Studie untersucht die Rolle von GluN2B-enthaltenden NMDA Rezeptoren, intrazellulärem Ca^{2+}, posttranslationalen Modifikationen und Karyopherinen auf die Konzentration von CtBP1 im Zellkern und dessen Co-Repressor Aktivität. Die Ergebnisse dieser Arbeit verknüpfen somit die CtBP1-abhängige Genexpression mit prä- und postsynaptischer Aktivität und verdeutlichen damit die Wichtigkeit der Regulation von Genen für die neuronale Plastizität und Hirnfunktion.

1. Introduction

The brain comprises millions of interconnected highly specified cells generating a network responsible for information processing, storage and transmission. Alterations in these fundamental processes provoked by environmental influences form the basis for learning and memory. Memory formation requires information storage in the nucleus where gene expression is controlled and adjusted. Synaptic input signals based on altered neuronal activity induce signaling cascades leading eventually to adaptations of gene transcription patterns. One major pathway to modulate gene expression in response to synaptic stimuli is the activation of signaling messengers.

1.1. Activity-dependent regulation of gene expression

The adaptation of gene expression patterns in response to altered network activity is important for many processes such as development, plasticity, and survival (Brunet *et al.*, 2005; Cohen and Greenberg, 2008; Goelet *et al.*, 1986; Rishal and Fainzilber, 2010), and requires the transduction of synaptic signals in the nucleus (Deisseroth *et al.*, 2003; West *et al.*, 2002). In neurons, several mechanisms are known to facilitate distal subcellular compartment-to-nucleus communication over long distances including Ca^{2+} signaling and the transport of protein messengers (Fainzilber *et al.*, 2011; Kam *et al.*, 2009). Most of the protein messengers are described as shuttling transcription factors able to pass the nuclear envelope, a highly regulated process crucial for activity-dependent gene transcription (Gorlich and Kutay, 1999; McBride *et al.*, 2002; Shen *et al.*, 2007).

1.1.1. Global Ca^{2+} routes

Ca^{2+} is the major intracellular messenger linking synaptic activity to gene transcription (Bengtson and Bading, 2012) by activating transcription modulators able to regulate nuclear gene expression crucial for learning and memory (Xiang *et al.*, 2007). Ca^{2+} flux into the cell in response to excitation can be mediated by voltage-gated calcium channels (VGCCs), Ca^{2+} release from internal stores, and ligand-gated calcium channels such as certain N-methyl-D-aspartate-type (NMDA) and α-amino-3-hydroxy-5-methyl-4-isoxazolepropionate-type (AMPA) glutamate receptors (Fig. 1.1).

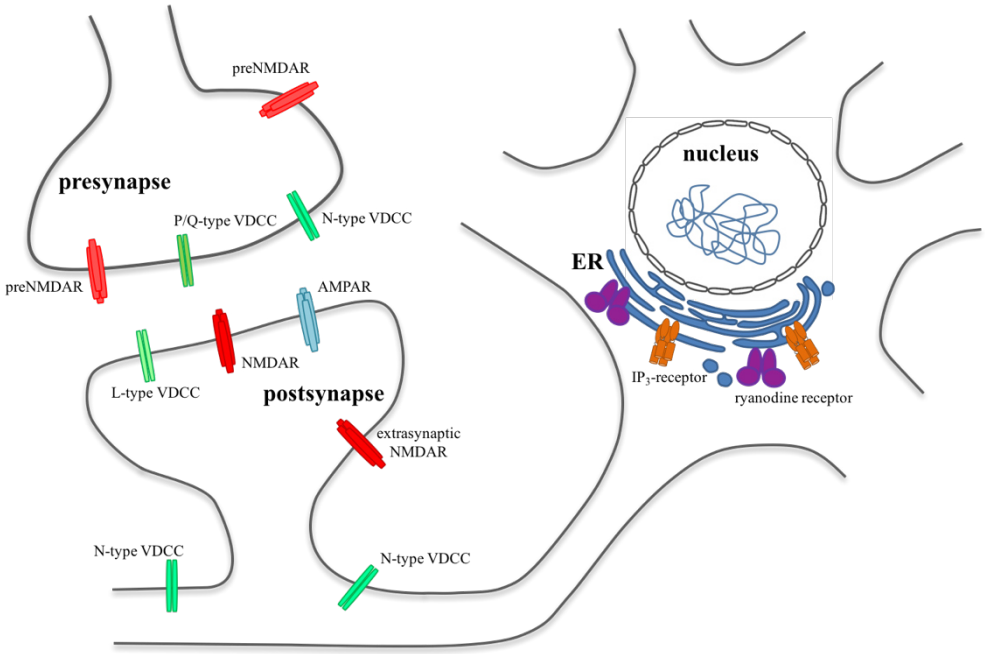

Fig. 1.1: Routes for Ca^{2+} entry in neurons. NMDA receptors (NMDAR) can be located in postsynaptic, presynaptic (preNMDAR), or extrasynaptic membranes, depending on their function. The indicated N-type, P/Q-type, and L-type voltage-gated calcium channels (VGCCs) are important for NMDA receptor-mediated signaling and can further trigger Ca^{2+} release from internal stores such as the endoplasmic reticulum (ER) via IP_3-receptors or ryanodine receptors. Ca^{2+}-permeable AMPA receptors (AMPAR) are primarily located at postsynapses.

AMPA receptors form a channel mostly permissive for sodium cations, whereas ionotrophic NMDA receptors are Ca^{2+}-permeable. Moreover, the latter possesses slow kinetics due to the gradual unbinding of glutamate (Cull-Candy and Leszkiewicz, 2004; Traynelis *et al.*, 2010). The activation of NMDA receptors requires membrane depolarization that leads to the removal of a magnesium ion from the pore and binding of glutamate and the co-agonists glycine or D-serine to their specific binding sites (Paoletti, 2011). Once the channel opens, influx of Ca^{2+} induces intracellular signaling cascades essential for neuronal excitability, synaptic strength and survival (Wang *et al.*, 2011). All these functions widely depend on the NMDA receptor subunit composition which varies across brain regions during development, in disease states, and due to changes in neuronal activity. So far, seven different subunits divided into three subfamilies according to their sequence homology can be classified: the GluN1 subunit, four GluN2 subunits (GluN2A through D) encoded by four separate genes, and two GluN3 subunits (GluN3A and GluN3B) derived from two different genes (Cull-Candy and Leszkiewicz, 2004; Paoletti, 2011; Traynelis *et al.*, 2010). Typically, NMDA receptors function as heterotetrameric complexes always containing two GluN1 and either two GluN2 subunits or a combination of one GluN2 with one GluN3 subunit. Especially in higher brain function areas such as the

hippocampus or cortex, GluN2A- and GluN2B-containing NMDA receptors play a pivotal role. The contribution of both subunits to the NMDA receptor complex is regulated during development. GluN2B-containing NMDA receptors are already present in developing neurons, and their absence results in death of GluN2B-deficient mice at postnatal day 1 (Kutsuwada *et al.*, 1996; Sheng *et al.*, 1994). On the contrary, GluN2A knock-out animals are viable and fertile. The expression of GluN2A subunits arises during synapse maturation and cortical circuit refinement (Monyer *et al.*, 1994; Sakimura *et al.*, 1995; Sheng *et al.*, 1994). The location of these NMDA receptor subtypes is still under discussion. However, both GluN2A and GluN2B subunits can be found at postsynaptic terminals, where GluN2A is located in the postsynaptic density, a meshwork of membranous and cytoplasmic proteins at the postsynaptic membrane of neurons (Gladding and Raymond, 2011). In contrast, GluN2B subunits are also found in peri- and extrasynaptic areas (Hardingham and Bading, 2010). In the last decade, studies also revealed a presynaptic localization of NMDA receptors, and there especially GluN2B-containing NMDA receptors are required for synaptic transmission and plasticity (Brasier and Feldman, 2008; Corlew *et al.*, 2008). As a consequence of NMDA receptor activity, several Ca^{2+}-dependent signaling pathways are activated to induce the expression of cell survival and plasticity genes.

Furthermore, gene transcription can be influenced by signaling cascades activated through the opening of voltage-gated calcium channels (VGCCs) (Dolmetsch *et al.*, 2001; Fields *et al.*, 2005). Additionally, Ca^{2+} influx through VGCCs initiates intracellular events such as synaptic transmission and posttranslational modifications of proteins (Catterall, 2011). The functional diversity of VGCCs in mammals is achieved by the existence of ten channel-forming α1 subunits, as well as four α2δ and four β auxiliary subunits (Dolphin, 2012). VGCCs are grouped in different classes according to their physiological and pharmacological characteristics. High-voltage-activated (HVA) calcium channels comprise L- (also named CaV1), P/Q- (CaV2.1), N- (CaV2.2), and R-type (CaV2.3) VGCCs. T-type (CaV3) VGCCs represent the group of low-voltage-activated (LVA) calcium channels. In neurons, L-type VGCCs are shown to be important for the activity-induced regulation of gene expression (Xiang *et al.*, 2007) and can be modulated by calcium/calmodulin-dependent protein kinase II (CAMKII) (Dzhura *et al.*, 2000). CAMKs are shown to become activated via a Ca^{2+} rise through the opening of NMDA receptors and L-type VGCCs or release from internal stores. These kinases modulate transcription by targeting the cyclic-AMP response element-binding protein (CREB) resulting in the recruitment of CREB-binding protein (CBP) and the activation of transcription (Das *et*

al., 1997; Lee *et al.*, 2005; Papadia *et al.*, 2005). Additionally, CAMKII can activate mitogen-activated protein kinase (MAPK) pathways important for the regulation of gene transcription for cell proliferation and differentiation (Morrison, 2012). Other targets of postsynaptic L-type VGCCs are shuttling transcription factors such as CRTC1 which translocate from distal subcellular compartments to the nucleus after Ca^{2+} influx to modulate activity-dependent gene expression (Ch'ng *et al.*, 2012). Moreover, selective influx of Ca^{2+} through presynaptic P/Q-type VGCCs is shown to activate the expression of syntaxin-1A, a presynaptic protein involved in neurotransmitter release (Sutton *et al.,* 1999). Another group of VGCCs which can facilitate Ca^{2+} signaling towards the nucleus are the N-type VGCCs. Besides their location at presynapses and function in neurotransmitter release (Dolphin, 2012), they can be found in the soma and in dendrites to facilitate Ca^{2+} waves in response to action potential firing of neurons (Catterall, 2011; Dolphin, 2012; Mills *et al.*, 1994; Scholz and Miller, 1995). The propagation of Ca^{2+} waves towards the nucleus can be supported by Ca^{2+} release from internal stores (Adams and Dudek, 2005; Bengtson *et al.*, 2010; Hardingham and Bading, 2010). Intracellular Ca^{2+} release can occur via calcium-induced-calcium-release from ryanodine receptors (Sandler and Barbara, 1999) or by the Ca^{2+}-dependent second messenger inositol 1,4,5-triphosphate (IP_3) which activates inositol 1,4,5-triphosphate (IP_3-) receptors (Berridge, 1998). Both types of receptors are located in the membranes of the smooth endoplasmic reticulum that surrounds the nucleus and extends into dendrites, and they were shown to influence activity-dependent gene expression (Berridge, 1998; Jaimovich and Carrasco, 2002; Powell *et al.*, 2001; Vali *et al.*, 2000).

Further, the propagation of Ca^{2+} waves to the nucleus influences the nuclear Ca^{2+} levels. It has emerged that nuclear Ca^{2+} is a key regulator in neuronal gene transcription on a more global level. An increase of nuclear Ca^{2+} levels leads to changes in the chromatin structure through histone acetylation and DNA methylation by influencing the nuclear abundance of class IIa histone deacetylases (Schlumm *et al.*, 2013). Another example for nuclear Ca^{2+} signaling as a regulator of gene transcription is the CREB-mediated gene expression of NMDA receptors (Hardingham *et al.*, 2001). Moreover, rises in intracellular Ca^{2+} levels are shown to influence gene transcription by modulating synapse-to-nucleus shuttling of transcription factors.

1.1.2. Synapse-to-nucleus communication mediated by protein messengers

The physical transport of signaling proteins includes the carriage of signaling endosomes, diffusion, and the active transport of protein messengers resulting in the integration of synaptic signals into the cytoplasm and nucleus. In case of signaling endosomes, entire signaling complexes on endosomes translocate from axon terminals towards the nucleus for the integration of synaptic signals. Upon NGF binding, TrkA receptors and bound signaling molecules have been shown to internalize into endosomes at presynapses, to travel along microtubules to the cytoplasm, and to signal to the nucleus (Howe and Mobley, 2005) to influence gene expression and survival (Cosker *et al.*, 2008; Harrington *et al.*, 2011).

Moreover, proteins may either migrate randomly via diffusion following a gradient or they are transported actively to their site of destination. In neurons, diffusion over long distances is only shown for few proteins such as ERK1/2 and Ras and presumably not efficient enough to mediate fast activity-induced adaptations in gene transcription (Harvey *et al.*, 2008; Lim *et al.*, 2016; Wiegert *et al.*, 2007). More frequently, synapse-to-nucleus transport of shuttling protein messengers is mediated by either actin filaments or microtubules (Franker and Hoogenraad, 2013). The last decade revealed several protein messengers located both at synapses and in the nucleus that act on modulation of activity-dependent gene transcription crucial for axon regeneration and synaptic plasticity. Several potential postsynapse-to-nucleus shuttling transcription factors such as AIDA-1, CREB2, Jacob, CRTC1 and Nf-κB were identified (Table 1.1) (Ch'ng *et al.*, 2012; Dieterich *et al.*, 2008; Jordan *et al.*, 2007; Kaltschmidt *et al.*, 1995; Karpova *et al.*, 2012; Karpova *et al.*, 2013; Lim *et al.*, 2016).

Moreover, analysis of presynapse-to-nucleus communication revealed shuttling transcription factors pivotal for cell survival and axon regeneration after nerve injury. Locally translated transcription factors such as STATs, SMADs, and ATFs are able to shuttle retrogradely from the axon lesion site into the nucleus and induce the transcription of pro-survival and axon growth genes (Baleriola *et al.*, 2014; Ben-Yaakov *et al.*, 2012; Korsak *et al.*, 2016; Moore and Goldberg, 2011; Zou *et al.*, 2009). Crucial for the function in the regulation of transcription of all described protein messengers in neurons is the regulation of their nuclear import and export.

Table 1.1: Proteins that shuttle into the nucleus in response to neuronal activity. The table contains proteins shown to be located in distal compartments of neurons and in the nucleus with the ability to shuttle between the pools in an activity-dependent manner. Additionally, their nuclear functions are indicated (modified from Karpova *et al.* (2012)).

Protein	Supposed function
Abi-1	regulates c-Myc transcription
Afadin	modification of histones
AIDA-1	nucleolar assembly
amyloid precursor protein (APP)	regulation of acetyltransferase Tip60
CAMAP	transcriptional co-activator of CREB1
CREB2	transcription factor
CRTC1	transcription co-activator
GRIP1	trafficking
HDAC4, HDAC5	histone deacetylases
JAB-1 (sub 3)	c-Jun co-activator
Jacob	regulates CREB transcription
LAPSER1	modulation of gene transcription
N-Cadherin	CBP downregulation, regulates CREB transcription
NF-AT4	transcription factor
NF-κB	transcription factor
α-Actinin-4	antagonist of HDAC7, regulation of MEF2 transcription
β-Catenin	regulates TCF transcription

1.1.3. Regulation of nuclear import and export

The nuclear import and export of proteins and mRNAs occurs either via the nuclear pore complex (NPC) mediated by karyopherins or via diffusion. Diffusion through nuclear pores is shown for proteins up to approximately 60 kDa in general, but even 90 kDa proteins can enter the nucleus in this manner (Ghavami *et al.*, 2016; Wang and Brattain, 2007). The nuclear import and export of proteins via the NPC and karyopherins is a highly regulated process (Gorlich and Kutay, 1999) important for the exact control of gene expression by precise timing of the presence of transcription factors in the nucleus (Hogan and Rao, 1999). Karyopherins bind their cargos by recognizing specific nuclear localization signals (NLS) or nuclear export signals (NES).

Importins recognize NLSs and mediate the transport of cargos through the NPC via interactions with NPC proteins, also known as nucleoporins. Once in the nucleus, dissociation of the importin-cargo complex is facilitated by the Ras-related GTPase Ran. Subsequently, importins are recycled back to the cytoplasm (Fig. 1.2). The classical receptor-mediated nuclear import pathway requires importin α and β complexes. Whereas importin α binds to the NLS of the cargo, importin β mediates tight cargo binding and the nuclear import (Pemberton and Paschal,

2005). In addition, importin β alone is shown to be efficient for the nuclear import of a various number of proteins such as Smad 3 (Chook and Suel, 2011; Palmeri and Malim, 1999; Xiao *et al.*, 2000). Moreover, importins are found in dendrites interacting with NMDA receptors (Lim *et al.*, 2016) and are known to facilitate retrograde transport of several synapse-to-nucleus shuttling transcription factors such as Jacob (Dieterich *et al.*, 2008). Jacob interacts via its NLS with importin α in a Ca^{2+}-dependent manner and is retrogradely transported and then imported into the nucleus in a complex with importin β to regulate gene transcription.

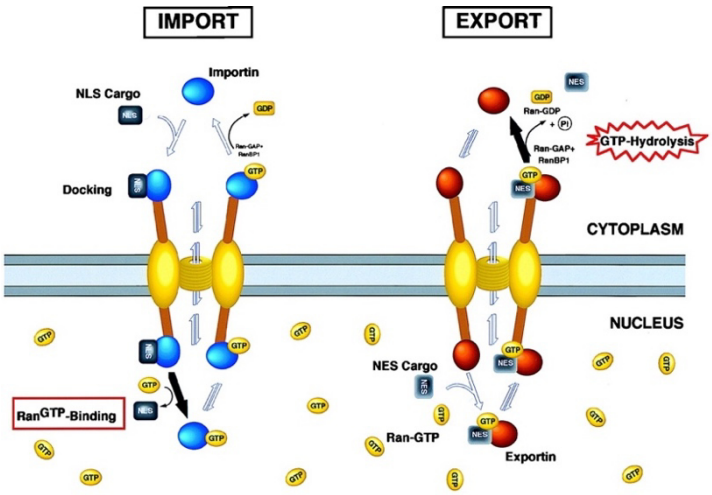

Fig. 1.2: Model of nucleo-cytoplasmic transport of molecules. The translocation through the nuclear pore requires multiple, reversible interactions between karyopherins (importins and exportins) as well as proteins of the nuclear pore complex (NPC) and the cargos. For both binding and release of cargo-karyopherin interaction, RanGTP activity is required (Goelet *et al.*, 1986; Nachury and Weis, 1999).

To enable fast adaptations in gene expression in response to changes in neuronal network activity, these complexes consisting of karyopherins and cargo might be efficient to mediate rapid nuclear import as soon as they arrive at the nuclear envelope (Lim *et al.*, 2016). Interestingly, the cytoplasmic and nuclear abundance of importins and exportins is highly regulated by Ca^{2+} suggesting Ca^{2+}-dependent nuclear import and export mechanisms in neurons (Kaur *et al.*, 2014). In particular, importin subunits are shown to accumulate in the nucleus upon NMDA receptor activation supporting the idea about Ca^{2+} signaling being crucial for the activity of importins (Thompson *et al.*, 2004).

Additionally, phosphorylation and dephosphorylation of NLSs or adjacent regulatory sequences might also regulate nuclear import. In *Aplysia*, PKA phosphorylation of the CAM-associated protein (CAMAP) induces accumulation of the protein in the nucleus (Jordan and Kreutz, 2009; Lee *et al.*, 2007). Further, PKA phosphorylation can enhance the binding of

importins to NLS-containing proteins (Briggs *et al.*, 1998; Jordan and Kreutz, 2009) and is shown to regulate gene transcription (Zanassi *et al.*, 2001). For example, nuclear import of NF-AT4 in response to increased intracellular Ca^{2+} levels is mediated by its dephosphorylation through calcineurin. This exposes its NLS and leads to subsequent nuclear import via importin α/β (Bhattacharya and Schindler, 2003; Hogan and Rao, 1999; Zhu and McKeon, 1999).
In case of nuclear export, exportin family members bind their cargos through an NES mediated by RanGTP activity (Fig. 1.2). Consequently, the ternary complex is exported and disassembled in the cytoplasm (Pemberton and Paschal, 2005). The nuclear export of NF-AT4 is mediated by phosphorylation and subsequent exposure of its NES and nuclear export via exportin 1 (Hogan and Rao, 1999; Zhu and McKeon, 1999). The nuclear export of STATs via exportin 1 in resting cells is an essential step in preparation of the next round of signaling-induced nuclear import of STATs. Interestingly, Stat3 is shown to comprise three NESs with one of them being important for the rapid nuclear export after stimulation (poststimulation export) and the other two for regulating the basal nuclear import of the transcription factor (Bhattacharya and Schindler, 2003).
Another transcription factor carrying a putative NES in its protein sequence is the C-terminal binding protein 1 (CtBP1) (Barnes *et al.*, 2003; Verger *et al.*, 2006).

1.2. C-terminal binding proteins

The CtBP protein family comprises CtBP1 and CtBP2, both existing in short (S) and long (L) isoforms, and RIBEYE (Fig. 1.3). The five proteins show high sequence homology (Fig. 1.3: purple region) and all except the latter function as transcriptional co-regulators interacting with sequence specific DNA-binding transcriptional repressors (Chinnadurai, 2007). Recent studies also suggest cytoplasmic functions of CtBP protein family members including macropinocytosis, fluid-phase endocytosis, coat protein complex I (COPI)-coated vesicle formation, and golgi partitioning during mitosis (Bonazzi *et al.*, 2005; Haga *et al.*, 2009; Hidalgo Carcedo *et al.*, 2004; Yang *et al.*, 2005). RIBEYE is encoded by the *CtBP2* gene and is the major structural component of synaptic ribbons (Schmitz *et al.*, 2000). CtBP2-L contains a nuclear localization signal (NLS) and is found predominantly in the nucleus where it functions as a transcriptional repressor. The splice variant CtBP2-S does not contain an NLS and is mostly located in the cytosol (Verger *et al.*, 2006). In 2012, Hübler *et al.* also revealed a synaptic localization of CtBP2 in primary hippocampal neurons which was previously only shown for CtBP1 (tom Dieck *et al.*, 2005).

Fig. 1.3: C-terminal binding protein family members. The *CtBP1* gene encodes for CtBP1-L (long) and CtBP1-S (short). The *CtBP2* gene codes CtBP2-L, CtBP2-S and the splicing variant RIBEYE. The purple B domain represents the highly homologous sequences, and the orange, yellow, and green marked regions highlight unique N-terminal regions of CtBP isoforms (analogous to Hübler *et al.*, 2012).

CtBP1 was identified interacting with the carboxyterminal end located PXDLS motif of the adenovirus E1A protein (Schaeper *et al.*, 1995). The multifunctional protein is present in the nucleus, the cytosol, and at synapses (Chinnadurai, 2007; Nardini *et al.*, 2003; Spano *et al.*, 1999; tom Dieck *et al.*, 2005). At presynapses, CtBP1 is shown to interact with the two highly homologous PXDLS motif containing presynaptic proteins Bassoon and Piccolo (Ivanova *et al.*, 2015; tom Dieck *et al.*, 2005). Furthermore, immunostainings in mice deficient for Bassoon and Piccolo revealed the significance of the two components of the cytomatrix at the active zone (CAZ) for the proper presynaptic localization of CtBP1 and consequently for the maintenance of the balance among the three CtBP1 pools (Ivanova *et al.*, 2015). In the cytoplasm, CtBP1 is involved in membrane fission, and in the nucleus it functions as transcriptional co-repressor. Mice lacking CtBP1 show deficits in a wide range of developmental processes emphasizing its essential role as transcriptional co-regulator (Hildebrand and Soriano, 2002). CtBP1 contains a substrate binding domain (SBD) and a nucleotide binding domain (NBD) (Fig. 1.4). The SBD allows its interaction with members of the transcription machinery and other proteins (Nardini *et al.*, 2003). Moreover, CtBP1 has dehydrogenase activity and is able to bind nicotinamide adenine dinucleotide NAD and NADH at its NBD with a higher affinity towards the latter. Changes in the redox status of the cell and thus changes in the intracellular NAD/NADH ratio correlate with altered neuronal activity (Brennan *et al.*, 2006; Kasischke *et al.*, 2004) which can be sensed by CtBP1 and cause its redistribution providing a link between the metabolic status of the cell and the regulation of gene expression (Garriga-Canut *et al.*, 2006; Ivanova *et al.*, 2016; Kumar *et al.*, 2002; Zhang *et al.*, 2002).

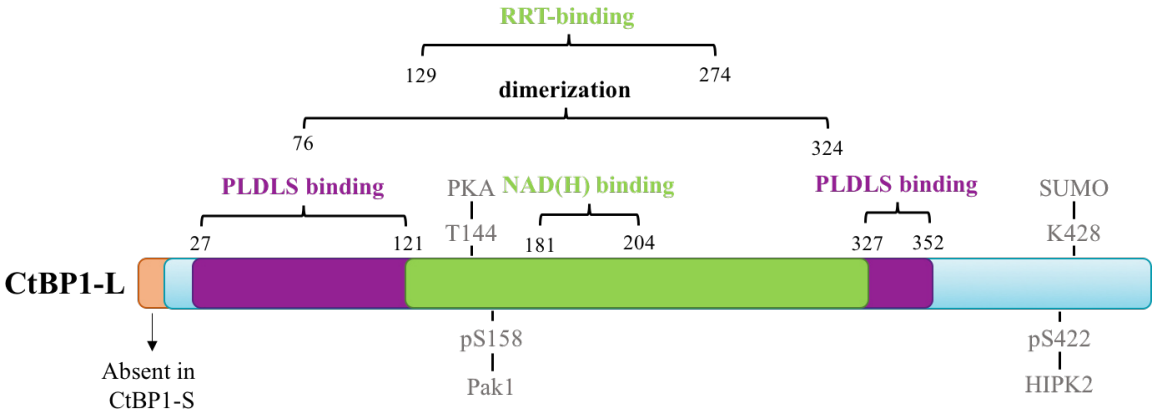

Fig. 1.4: Domain structure of CtBP1-L. The substrate binding domain (SBD, aa 27-121 and 327-352) is colored in magenta, and the nucleotide binding domain (NBD, aa 181-204) with the RRT binding motif is presented in green. Posttranslational modifications of CtBP1 by PKA, Pak1, HIPK2 and SUMO are shown in grey. Modified from Chinnadurai (2007).

Additionally, the co-repressor function of CtBP1 is regulated by the formation of dimers with a core of two NAD/NADH binding domains (Kuppuswamy *et al.*, 2008; Nardini *et al.*, 2003). The dimerization is possible either homologously or by heterologous interaction with other NLS containing proteins such as CtBP2, basic Krüppel-like factor (BKLF), or huntingtin indicating a putative mechanism for CtBP1 nuclear import, diminished cytoplasmic abundance and enhanced co-repressor function (Dammer and Sewer, 2008; Kegel *et al.*, 2002; Verger *et al.*, 2006).

1.2.1. Role of CtBP1 in gene expression

In the nucleus, CtBP1 acts as a dimer and is recruited to transcription repressor complexes by various DNA binding proteins either through the PLDLS-binding motif (located in the SBD of CtBP1) or via the RRT motif (located in its NBD) (Quinlan *et al.*, 2006a; Quinlan *et al.*, 2006b; Zhang *et al.*, 2003) (see Fig. 1.4). In addition, CtBP1 can be recruited to transcription factors like human double minute 2 homolog (HDM2) or the neuron-restrictive silencer factor/RE1-silencing transcription factor (NRSF/REST), that both lack the classical PLDLS and RRT binding motifs implying a third yet unknown mechanism how CtBP1 can interact with transcription repressors (Garriga-Canut *et al.*, 2006; Mirnezami *et al.*, 2003).

Analysis of CtBP1 nuclear transcriptional repressor complexes (Fig. 1.5 A) revealed CtBP1 in complex with both DNA-binding proteins - such as ZEB1/2 (Postigo and Dean, 1999), RREB-1 (Thiagalingam *et al.*, 1996) and Znf217 (Cowger *et al.*, 2007) - as well as with histone modifying enzymes (Shi *et al.*, 2003).

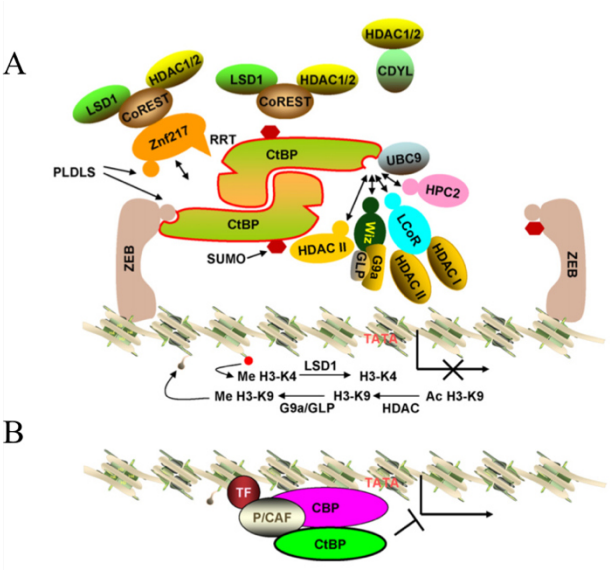

Fig. 1.5: CtBP in transcriptional repressor complexes mediating gene specific (A) and global (B) transcription repression. A: CtBP1 functions as a dimer to recruit a DNA-binding repressor (e.g. ZEB) with one PLDLS binding region and histone-modifying enzymatic factors (e.g. HDACs, G9a/GLP) with the second PLDLS binding cleft provided from the second monomer. Further transcription factors (e.g. Znf217, Co-Rest) can interact with CtBP through both PLDLS and RRT binding regions. **B**: CtBP antagonizes the trans-activation function of p300/CBP and associated HATs (e.g. P/CAF). Modified from Chinnadurai (2007) and Lim *et al.*, 2016.

So, the CtBP1 co-repressor complex contains enzymatic components important in epigenetic processes regulating deacetylation and methylation of histones. These processes are known to regulate the shift from euchromatin to the transcriptional inactive heterochromatin (Golbabapour *et al.*, 2011; Weichenhan and Plass, 2013). Besides histone deacetylases (HDACs) and histone methyltransferases (HMTs), CtBP1 co-repressor complexes are able to recruit further epigenetic factors like the histone acetyltransferase p300/CBP, a global transcription activator, and the lysine-specific demethylase LSD1 (Chinnadurai, 2007; Shi *et al.*, 2004) (Fig. 1.5 B) giving rise to the idea about an involvement of CtBP1 in epigenetic relevant gene regulation dependent on the activity state of the cell.

Nuclear abundance of CtBP1 can be regulated by posttranslational modifications as shown in non-neuronal cells. SUMOylation by homeodomain interacting protein kinase 2 (HIPK2) retains CtBP1 in the nucleus and enhances its repressor function, whereas phosphorylation by cAMP-dependent protein kinase A (PKA), serine/threonine-protein kinase PAK6, AMP-activated protein kinase (AMPK), or group I p21-activated kinase (Pak1) triggers its nuclear export and consequently the activation of transcription (Barnes *et al.*, 2003; Dammer and Sewer, 2008; Haga *et al.*, 2009; Kim *et al.*, 2013; Lin *et al.*, 2003; Thomas *et al.*, 2015) (also see Fig. 1.4). Liberali *et al.* (2008) studied the phosphorylation of CtBP1 by Pak1 in human A431 epidermoid carcinoma cells and revealed that Pak1 enzymatic activity induced nuclear export of CtBP1. In addition, phosphorylation of CtBP1 by PKA is shown to cause structural changes inducing CtBP1 nuclear export and gene expression of CtBP1 repressed genes in H295R adrenocortical cells (Dammer and Sewer, 2008). Moreover, in neurons, the neuronal

nitric-oxide synthase (nNOS) binds CtBP1 via its PDZ domain mediating CtBP1 cytoplasmic localization and transcription activation (Riefler and Firestein, 2001).

In summary, CtBP1 co-repressor function is shown to be regulated by posttranslational modifications such as phosphorylation and SUMOylation, by conformational changes (NAD/NADH binding) or by binding to other proteins influencing its nuclear abundance. However, the regulation of nuclear import and export of CtBP1 in neurons has not been fully understood and is part of the present study.

1.3. Objectives

CtBP1 is a ubiquitously expressed transcriptional co-repressor, and its nuclear abundance is regulated by posttranslational modifications, dimerization and binding to its interaction partners in non-neuronal cells. In neurons, CtBP1 is found in the nucleus, the cytoplasm and at presynapses.

Besides studying the activity-regulated nuclear function of CtBP1, the aim of this thesis was to shed more light on the **nuclear import and export mechanisms** of the transcription factor by using immunocytochemical and biochemical approaches. In this context, the **interaction partners** of CtBP1 for its nuclear import and export and the **regulation of its cytoplasmic pool size** were intensively studied. Moreover, this study addresses the underlying mechanism of the retrograde translocation of CtBP1 from presynapses to the nucleus.

Ca^{2+} has been shown to play a pivotal role in the activity-dependent regulation of many shuttling transcription modulators in neurons similar to CtBP1. Hence, its **sensitivity to Ca^{2+}-mediated signaling** through ligand- and voltage-gated calcium channels as well as through intracellular Ca^{2+} release was examined by pharmacological modulation and promoter assays.

Finally, CtBP1 phospho-mutants were employed to assess its nuclear abundance dependent on **activity-induced phosphorylations** in neurons.

2. Material and methods

2.1. Material

2.1.1. Chemicals

All chemicals were of analytical grade and received from BioRad, Invitrogen, Merck, Roth, Sigma-Aldrich, or Thermo Fisher Scientific. Specifically used chemicals and solutions are described in the corresponding methods.

2.1.2. Antibodies

2.1.2.1. Primary antibodies

Table 2.1: List of primary antibodies used for immunocytochemistry (ICC) and Western blotting (WB).

Antibody	Species	Company	Dilution
anti-CtBP1	ms monoclonal	BD Transduction Laboratories	ICC: 1:1000 WB: 1:1500
anti-CtBP1	rb polyclonal	Synaptic Systems	ICC: 1:1000 WB: 1:2500
anti-CtBP2	ms monoclonal	BD Transduction Laboratories	ICC: 1:1000 WB: 1:2000
anti-CtBP2	rb polyclonal	Synaptic Systems	ICC: 1:1000 WB: 1:2000
anti-βIII-Tubulin	ms monoclonal	Sigma	WB: 1:500
anti-Synaptophysin	gp polyclonal	Synaptic Systems	ICC: 1:500
anti-PKAcat	rb polyclonal	Santa Cruz	ICC: 1:50
anti-GAD65	ms monoclonal	Abcam	ICC: 1:500
anti-Synaptotagmin1 lumenal domain Oyster-550-labeled	rb polyclonal	Synaptic Systems	ICC: 1:100
anti-GFP	rb polyclonal	Abcam	ICC: 1:1000 WB: 1:5000
anti-GFP	ms monoclonal	self-made by W. Altrock	WB: 1:1000
anti-CRM1	rb polyclonal	Invitrogen	WB: 1:500
anti-KPNB1	rb polyclonal	EMELCA Bioscience	ICC: 1:200
anti-NeuN	rb polyclonal	Merck Millipore	WB: 1:200
anti-GAPDH	rb polyclonal	Abcam	WB: 1:1000

2.1.2.2. Secondary antibodies

Table 2.2: List of secondary antibodies used for immunocytochemistry (ICC) and Western blotting (WB).

Antibody	Species	Company	Dilution
anti-guinea pig Alexa Fluor™ 488	goat polyclonal	Jackson ImmunoResearch Laboratories	ICC: 1:500
anti-mouse Alexa Fluor™ 488	goat polyclonal	Jackson ImmunoResearch Laboratories	ICC: 1:1000
anti-mouse Cy3	goat polyclonal	Jackson ImmunoResearch Laboratories	ICC: 1:1000
anti-mouse Cy5	goat polyclonal	Jackson ImmunoResearch Laboratories	ICC: 1:1000
anti-mouse IgG Alexa Fluor™ 680	goat polyclonal	Invitrogen	WB: 1:20000
anti-rabbit Alexa Fluor™ 488	goat polyclonal	Jackson ImmunoResearch Laboratories	ICC: 1:1000
anti-rabbit Alexa Fluor™ 647	goat polyclonal	Jackson ImmunoResearch Laboratories	ICC: 1:1000
anti-rabbit Cy3	goat polyclonal	Jackson ImmunoResearch Laboratories	ICC: 1:1000
anti-rabbit Cy5	goat polyclonal	Jackson ImmunoResearch Laboratories	ICC: 1:1000
anti-rabbit IgG Alexa Fluor™ 770	goat polyclonal	Invitrogen	WB: 1:20000

2.1.2.3. Fluorescent dyes

Table 2.3: List of fluorescent dyes used for immunocytochemistry (ICC).

Dye	Company	Concentration
DAPI	Sigma-Aldrich	2.86 µM
propidium iodide	Sigma-Aldrich	5 µM

2.1.3. Animals

In this study, Wistar rats from the Leibniz Institute for Neurobiology (Magdeburg, Germany), CtBP1 (CtBP1^{tm1Sor}) and KPNB1 (KPNB1Δ3`UTR) mouse strains backcrossed to C57BL/6N were used for cell culture, slices and tissue preparation. CtBP1$^{tm1Sor}$ KO mice were obtained from Jackson Laboratory (Hildebrand and Soriano, 2002) and KPNB1Δ3`UTR mice were received from Mike Fainzilber, Department of Biological Chemistry, Weizmann Institute of Science, Rehovot 76100, Israel (Perry *et al.*, 2012).

2.1.4. Bacterial strains and culture media

For heat-shock transformations and plasmid DNA preparations the bacterial strain XL10-Gold from Stratagene with the genotype *endA1 glnV44 recA1 thi-1 gyrA96 relA1 lac Hte (mrA)183 Δ(mcrCB-hsdSMRmrr) 173 tetR F'[proAB laclqZΔM15 Tn10(TetR Amy CmR)]* was used.

Table 2.4: Culture media for bacterial cells.

Media	Composition
LB-medium	5 g/l yeast-extract; 10 g/l bacto-tryptone; 5 g/l NaCl
LB-plates	1000 ml LB-medium; 15 g agar
SOC-medium	5 g/l yeast-extract; 20 g/l bacto-tryptone; 10 mM NaCl; 2.5 mM KCl; 10 mM $MgSO_4$; 10 mM $MgCl_2$; 20 mM glucose

2.2. Methods

2.2.1. Biochemical methods

2.2.1.1. Isolation of cortex and hippocampus from mouse brain

Homogenization Buffer: **0.32 M Sucrose; 25 mM Tris/HCl; pH 7.4**
Protease inhibitors: **Complete®, Roche**

Mice were anesthetized and decapitated. Hippocampus and cortex were frozen on dry ice and stored at -80 °C until use. The tissue was homogenized with 10 ml/g Homogenization Buffer containing protease inhibitors (1 tablet/10 ml buffer) with a Homogenizer and Potter S for 12 strokes at 900 rpm and 4 °C. The sample was stored at -20 °C for SDS-PAGE and Western blotting.

2.2.1.2. Preparation of nuclear and cytoplasmic fraction from cortical cultures

10 x PBS: **1.4 M NaCl; 83 mM Na_2HPO_4; 17 mM NaH_2PO_4; pH 7.4**
CelLytic™ NuCLEAR™ Extraction Kit: **Sigma-Aldrich**

Nuclear extracts were obtained by using the CelLytic™ NuCLEAR™ Extraction Kit (Sigma-Aldrich). A modified protocol for the nuclear protein extraction from 100 µl of packed cell volume using a detergent was performed at 4 °C. Rat cortical neurons (5 Mio/75 cm^2 flask) were stimulated with NMDA as described (2.2.2.4.2.). The cells were washed twice with 1 x PBS and dissolved in 500 µl 1 x PBS. After five-minute centrifugation at 450 x g the packed cell volume (PCV) of the pellet was determined. The cell pellet was resuspended gently in 250 µl (5 x PCV) of 1 x Lysis Buffer (including 1 % DTT and 1 % protease inhibitors) and incubated for 5 minutes on ice. The lysis was checked with 2 µl of sample under the microscope (Olympus CK2). IGEPAL CA-630 solution was added to the swollen neurons to a final concentration of 0.6 %, immediately followed by a centrifugation for 30 seconds at 10,000 x g. The supernatant was collected as cytoplasmic fraction and stored at -20 °C until use. The crude nuclei pellet was resuspended in 2/3 PCV of the Extraction Buffer (containing 1 % DTT and 1 % protease inhibitors) and shaken at 800 rpm for 15 minutes. After the last centrifugation step (five minutes at maximum speed), the supernatant representing the nuclear fraction was transferred to a clean chilled tube, snap-frozen with liquid nitrogen and stored at -80 °C for Western blotting.

2.2.1.3. Co-immunoprecipitation using magnetic anti-GFP microbeads

µMACS™ Protein Isolation Kit:	**Miltenyi Biotec**
Lysis Buffer:	**50 mM NaCl; 0.5 % Triton X-100; 2 mM EDTA; 20 mM Tris/HCl; pH 7.4**
4 x SDS sample buffer:	**250 mM Tris; 1 % (w/v) SDS; 40 % (v/v) glycerol; 20 % (v/v) β-mercaptoethanol; 0.004 % (w/v) bromphenol blue; pH 6.8**
Protease inhibitors:	**Complete® (Roche)**
PhosSTOP:	**Phosphatase inhibitor cocktail EASYpacks (Roche)**

Cortical neurons (5 Mio/75 cm^2 flask) expressing GFP, CtBP1intEGFP or CtBP1intEGFP_NESmut were stimulated with NMDA as described (2.2.2.4.2.), followed by nuclear extraction (2.2.1.3.). The nuclear and cytoplasmic fractions were diluted 1:1 with Lysis Buffer containing protease inhibitors and PhosSTOP. The samples were subjected to co-immunoprecipitation as described in the manufacturers manual, except for the washing steps where the Lysis Buffer was used. Elution was done using 2 x SDS sample buffer. The samples were stored at -20 °C and analyzed by Western blotting.

2.2.1.4. Immunoprecipitation of endogenous CtBP1 using sepharose coupled protein G

Lysis Buffer:	**50 mM NaCl; 0.5 % Triton X-100; 2 mM EDTA; 20 mM Tris/HCl; pH 7.4**
4 x SDS sample buffer:	**250 mM Tris; 1 % (w/v) SDS; 40 % (v/v) glycerol; 20 % (v/v) β-mercaptoethanol; 0.004 % (w/v) bromphenol blue; pH 6.8**
Protease inhibitors:	**Complete® (Roche)**
PhosSTOP:	**Phosphatase inhibitor cocktail EASYpacks (Roche)**
GammaBindPlusSepharose:	**Amersham Pharmacia Biotech AB**

Cortical neurons (5 Mio/75 cm^2 flask) were stimulated with NMDA as described (2.2.2.4.2.), followed by the nuclear extraction (2.2.1.3.). The obtained nuclear and cytoplasmic fractions were diluted 1:1 with Lysis Buffer containing protease inhibitors and PhosSTOP. All steps of the immunoprecipitation were performed at 4 °C according the protocol described by Dillman and Pfister (Dillman and Pfister, 1994). After preclearing with GammaBindPlus Sepharose, the supernatant was diluted 1:1 with Lysis Buffer containing protease inhibitors, PhosSTOP and 0.25 % gelatine. The supernatant was incubated with 5 µg anti-CtBP1 antibody or rb IgG coupled to Protein G of the GammaBindPlus Sepharose for three hours at constant agitation. After removing uncoupled beads by centrifugation at 500 x g for two minutes and washing six times with 700 µl Lysis Buffer, precipitated proteins were eluted with 2 x SDS sample buffer for 10 minutes at 300 rpm and 70 °C with additional centrifugation for two minutes at 500 x g. The samples were stored at -20 °C and analyzed by Western blotting.

2.2.1.5. Amido black protein assay

Amido black solution:	**23 mM amido black 10B (Merck) in methanol : acetic acid**
methanol : acetic acid:	**methanol : acetic acid in a ratio of 9:1**
BSA:	**Interchim**

The amido black protein assay was used to quantify precipitated and in 2 x SDS sample buffer dissolved protein samples (Popov *et al.*, 1975). Thereby different dilutions of BSA served as standards and the concentrations of both protein and BSA samples were determined in triplicates. Samples were incubated with amido black solution at room temperature for 10 minutes in a 96-well plate and centrifuged for 10 minutes at 3,200 x g. The pellets were washed three times with methanol : acetic acid, dried and resuspended in 300 µl 0.1 N NaOH. For analysis of the data the optical absorbance was measured at 620 nm with the VERSAmax microplate reader (Molecular Devices) and further analyzed with the program Soft Max Pro 4.8.

2.2.1.6. Sodium dodecyl sulfate polyacrylamide gel electrophoresis (SDS-PAGE)

4 x SDS sample buffer:	**250 mM Tris; 1 % (w/v) SDS; 40 % (v/v) glycerol; 20 % (v/v) β-mercaptoethanol; 0.004 % (w/v) bromphenol blue; pH 6.8**
Electrophoresis Buffer:	**192 mM glycine; 0.1 % (w/v) SDS; 25 mM Tris; pH 8.3**
4 x Separating Buffer:	**0.4 % (w/v) SDS; 1.5 M Tris/HCl; pH 6.8**
Separation gel (20 %):	**8.25 ml Separation Buffer; 7.5 ml 87 % glycerol; 16.5 ml 40 % acrylamide; 330 µl 0.2 M EDTA; 22 µl TEMED; 120 µl 0.5 % bromophenol blue; 75 µl 10 % APS**
Separation gel (5 %):	**8.25 ml Separation Buffer; 17.94 ml dH_2O; 1.89 ml 87 % glycerol; 4.12 ml 40 % acrylamide; 330 µl 0.2 M EDTA; 22 µl TEMED; 118 µl APS**
4 x Stacking Buffer:	**0.5 M Tris; pH 6.8**
Stacking gel (5 %):	**6 ml Stacking Buffer; 7.95 ml dH_2O; 5.52 ml 87 % glycerol; 3.9 ml 30 % acrylamide; 240 µl 0.2 M EDTA; 240 µl 10 % SDS; 17.2 µl TEMED; 30 µl phenolred; 137 µl 10 % APS**
Protein ladder:	**Precision Plus Protein™ Prestained Standard All Blue (Bio-Rad)**

Following the established protocol by Laemmli (Laemmli, 1970) the separation of protein samples due to their molecular weight was achieved using one-dimensional SDS-PAGE. Protein samples were solubilized in 2 x SDS sample buffer and incubated at 95 °C for five minutes. For electrophoresis a continuous gradient running gel (5-20 % polyacrylamide) with 5 % stacking gel was used. After running at 11 mA the gel was subjected to Western blotting.

2.2.1.7. Western blotting and quantification

Blotting Buffer:	**192 mM glycine; 0.2 % (w/v) SDS; 20 % (v/v) methanol; 25 mM Tris; pH 8.3**
10 x PBS:	**1.4 M NaCl; 83 mM Na_2HPO_4; 17 mM NaH_2PO_4; pH 7.4**
PBS-T:	**0.1 % (v/v) Tween 20 in 1 x PBS**
Immobilon-FL PVDF membranes:	**Millipore**

The electrophoretic transfer of proteins to a PVDF membrane followed a protocol by Towbin *et al.* (Towbin *et al.*, 1979). The blotting was performed for 100 minutes at 4 °C and constant current of 200 mA in a blotting chamber by Hoefer. Primary antibodies, diluted in 5 % BSA, were incubated over night at 4 °C. Before and after one hour incubation of the secondary antibody, the membrane was washed three times 15 minutes with PBS-T. Quantitative immunoblots were obtained with Odyssey Infrared Scanner (LI-COR). The integrated density of signals (ID) was measured using ImageJ. Rectangular ROIs with identical dimensions within each experimental group analyzed on the same membrane were set around the bands. Each value was normalized to the respective loading control (GAPDH or βIII-Tubulin).

2.2.2. Cell culture

2.2.2.1. Cultivation and transfection of mammalian cell lines

HEK 293-T cells:	**American Type Culture Collection (ATCC)**
Culture dishes:	**Nunc**
Solution A:	**500 mM $CaCl_2$**
Solution B:	**140 mM NaCl; 50 mM HEPES; 1.5 mM Na_2PO_4; pH 7.05**
Culture Medium:	**DMEM; 10 % (v/v) fetal bovine serum (FBS); 2 mM L-glutamine; 100 U/ml penicillin; 100 µg/ml streptomycin (all Gibco)**
Culture Medium Neurons:	**Neurobasal™; 100 U/ml penicillin; 100 µg/ml streptomycin; 1 mM sodium pyruvate; 1 x B27; 4 mM GlutaMax (all Gibco)**

Human embryonic kidney (HEK) 293-T cells were used for production of viral particles. Cultures in 75 cm^2 flasks were maintained in an incubator at 37 °C, 5 % CO_2 and 95 % humidity. For cell line maintenance, cells were split 1:10 and for transfection cells were split 1:8 to achieve 70 % confluency within 48 hours.

Transfection of HEK 293-T cells for production of viral particles was performed using the calcium phosphate method. 1 ml Solution A was mixed with 20 µg of plasmid DNA. Exactly one minute after adding of 1 ml Solution B the mixture was given dropwise to the cells. After six hours the Culture Medium was replaced with Culture Medium for Neurons. Cells were harvested 48 hours after transfection.

2.2.2.2. Generation of lentiviral particles

Culture Medium:	**DMEM; 10 % (v/v) fetal bovine serum (FBS); 2 mM L-glutamine; 100 U/ml penicillin; 100 µg/ml streptomycin (all Gibco)**
Culture Medium Neurons:	**Neurobasal™; 100 U/ml penicillin; 100 µg/ml streptomycin; 1 mM sodium pyruvate; 1 x B27; 4 mM GlutaMax (all Gibco)**

Lentiviral particles were produced under S2 safety conditions in HEK 293-T cells using three vectors: FUGW-based transfer, psPAX2 packaging and pVSVG pseudotyping vector (Lois *et al.*, 2002). The plasmids were transfected into HEK 293-T cells using the calcium phosphate method (2.2.2.1.) with a molar ratio of 1:1:1. After six hours the Culture Medium was exchanged to Culture Medium for Neurons and after 48 hours the lentivirus was harvested by centrifugation at 800 x g for five minutes. The virus was aliquoted and stored at -80 °C until use.

Titration of the produced virus was performed to evaluate the optimal virus concentration for both hippocampal and cortical neurons. Depending on the experiment, the neurons were either infected at DIV4 or DIV9. All experiments were performed at DIV16.

2.2.2.3. Cultivation and infection of primary neuronal cultures

Plating Medium:	**DMEM; 10 % (v/v) fetal bovine serum (FBS); 2 mM L-glutamine; 100 U/ml penicillin; 100 µg/ml streptomycin (all Gibco)**
Culture Medium:	**Neurobasal™; 100 U/ml penicillin; 100 µg/ml streptomycin; 1 mM sodium pyruvate; 1 x B27; 4 mM GlutaMax (all Gibco)**
Culture Medium A:	**Neurobasal A™; 100 U/ml penicillin; 100 µg/ml streptomycin; 1 mM sodium pyruvate; 1 x B27; 4 mM GlutaMax (all Gibco)**
Poly-L-lysine:	**Sigma**
AraC:	**1.5 mM (Calbiochem)**
10 x trypsin:	**containing EDTA (Gibco)**
Culture dishes:	**Nunc**
Coverslips:	**Roth**
HBSS⁻⁻:	**Gibco**

Both primary hippocampal and cortical cultures from rat were prepared following the established protocol described in Frischknecht *et al.* (2009) and Lazarevic *et al.* (2011).

Preparation of primary hippocampal cultures from mice required newborn mice between DIV1 and DIV2 of desired genotypes (2.2.3.1.). They were sacrificed by decapitation, the hippocampi were isolated and transferred into HBSS⁻⁻ containing tubes. After 0.025 % trypsin treatment and mechanical dissection, the cell suspension was plated in Plating Medium onto poly-L-lysine coated round glass coverslips (18 mm diameter; 30,000 cells/coverslip). After one hour, the coverslips were transferred upside-down into petri dishes containing 70% confluent monolayer

of astrocytes (prepared one week in advance (Lazarevic *et al.*, 2011)) in Culture Medium A. At DIV1 and DIV3, AraC was applied to the neurons with final concentration of 1.2 µM.
Lentiviral infection of hippocampal and cortical cultures from rat was performed at either DIV4 for live-imaging experiments and immunocytochemistry or DIV9 for co-immunoprecipitations and pArc and pBDNFpI+II promoter assays. Therefore, concentrated virus solution was directly added to neuronal growth medium. The medium was exchanged after eight hours and the cultures were kept at 37 °C, 5 % CO_2 and 95 % humidity until DIV16.

2.2.2.4. Treatment of dissociated cultured neurons

2.2.2.4.1. Chronical silencing and disinhibition of cultured cortical neurons

Mature DIV21 cortical neurons were treated with 4-AP and bicuculline for eight hours or APV and CNQX for 24 hours to either disinhibit or silence the cultures. The compounds were directly added to the 24-well plate containing 50,000 cells/coverslip with concentrations indicated in table 2.5 and incubated at 37 °C, 5 % CO_2 and 95 % humidity. Control cells were treated with water and DMSO.

Table 2.5: Pharmacological reagents.

Compound	Biological Activity	Working Concentration	Company
4-Aminopyridin (4-AP)	selective inhibitor of Kv1 voltage-activated potassium channels	2.5 mM in H_2O	Sigma-Aldrich
6-Cyano-7-nitroquinoxaline-2,3-dione disodium (CNQX)	AMPA/kainate receptor antagonist	10 µM in DMSO	Tocris
Bicuculline	$GABA_A$ receptor antagonist	50 µM in DMSO	Sigma-Aldrich
D-(-)-2-Amino-5-phosphonopentanoic acid (APV)	competitive NMDA antagonist	50 µM in H_2O	Tocris

2.2.2.4.2. NMDA stimulation and viability assay of cultured primary neurons

Tyrodes Buffer:	**12.5 mM HEPES; 1.25 mM KCl; 15 mM glucose; 119 mM NaCl; 2 mM $MgCl_2$; 2 mM $CaCl_2$; pH 7.4**
10 x PBS:	**1.4 M NaCl; 83 mM Na_2HPO_4; 17 mM NaH_2PO_4; pH 7.4**
1000 x NMDA:	**100 mM in H_2O**
1000 x glycine:	**2 mM in H_2O**
4 % PFA:	**4 % (w/v) paraformaldehyde in 1 x PBS**
Propidium iodide:	**5 µM (Sigma-Aldrich)**

20 minutes before stimulation, the coverslips of DIV21 mature cortical and hippocampal neurons from mouse and rat were preincubated with pharmacological reagents in culture medium. After transferring coverslips into Tyrodes Buffer containing plates, the cells were treated with 100 µM NMDA and 2 µM glycine in Tyrodes Buffer. After three minutes of treatment the coverslips were transferred back into conditioned culture medium and incubated at 37 °C, 5 % CO_2 and 95 % humidity for one hour (Fig. 2.1) (Proepper *et al.*, 2007). Control cells were treated with water. These stimulated cultures were proceeded as described in 2.2.1.3., 2.2.1.4. and 2.2.2.6.

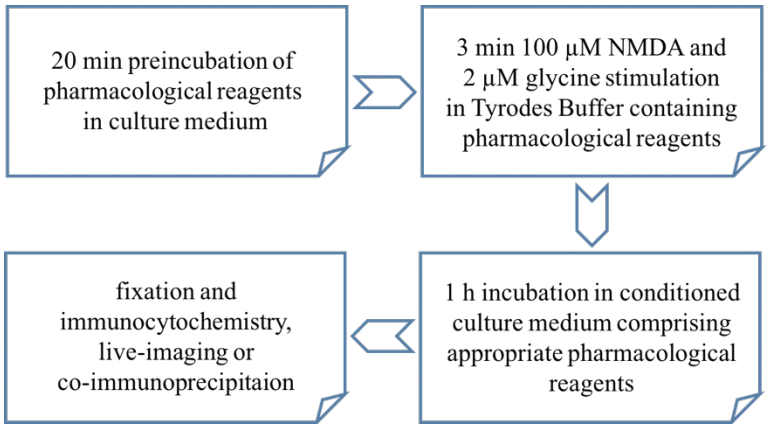

Fig. 2.1: Workflow of NMDA stimulation of cultured primary neurons, including application of pharmacological drugs (2.2.2.4.3.).

For the viability assay control and NMDA stimulated cortical neurons were treated with 5 µM propidium iodide at different time points (1, 6 and 24 hours) of incubation. The cells that served as a positive control were treated with 4 % paraformaldehyde for 10 minutes before application of propidium iodide for 20 minutes. After washing twice with 1 x PBS to remove unbound propidium iodide, cells were fixed, permeabilized and their nuclei were stained with DAPI (2.2.2.6.). The percentage of dead cells for each group was calculated as a ratio of propidium iodide positive versus total number of cells, masked by DAPI.

2.2.2.4.3. Pharmacological treatments of cultured primary neurons

Tyrodes Buffer:	**12.5 mM HEPES; 1.25 mM KCl; 15 mM glucose; 119 mM NaCl; 2 mM $MgCl_2$; 2 mM $CaCl_2$; pH 7.4**

The pharmacological reagents listed in table 2.6 were used for treatment of DIV16 or DIV21 dissociated neuronal cultures for immunocytochemistry (2.2.2.6.). Neurons were treated with

the pharmacological reagents 20 minutes prior chronical silencing, disinhibition or NMDA stimulation (Fig. 2.1). Control cells obtained the same experimental procedure with either water or DMSO as vehicle.

Table 2.6: Pharmacological reagents.

Compound	Biological Activity	Working Concentration	Company
anisomycin	inhibitor of protein synthesis	10 µM in DMSO	Sigma
BAPTA-AM	cell-permeable calcium chelator	10 µM in DMSO	Tocris
calmidazolium chloride (CCl)	inhibitor of CamKII	10 µM in DMSO	Sigma
EAA-090	preferentially inhibits GluN2A subunits of NMDA receptors	5 µM in H_2O	Sigma
forskolin	activator of PKA	50 µM in DMSO	Sigma
H89	inhibitor of protein kinase A	10 µM in H_2O	Sigma
ifenprodil	inhibitor of GluN2B subunits of NMDA receptors	10 µM in DMSO	Abcam
importazole	disrupts importin-β/RAN interaction	20 µM in DMSO	Sigma
IPA3	inhibitor of group I p21-activated kinase	20 µM in DMSO	Tocris
KT5720	selective inhibitor of PKA	1 µM in DMSO	Tocris
lactacystin	cell-permeable and irreversible proteasome inhibitor	0.5 µM in H_2O	Calbiochem
leptomycin B (LMB)	blocker of CRM1 mediated nuclear export by binding to CRM1	3 nM in ethanol	Merck Millipore
MG 132	cell-permeable and reversible proteasome inhibitor	10 µM in DMSO	Sigma
nifedipine	selective blocker of L-type VDCC	10 µM in DMSO	Tocris
nocodazole	disrupts microtubules by binding to β-tubulin	20 µM in DMSO	Sigma
NVP-AAM007	preferentially inhibits GluN2A subunits of NMDA receptors	50 nM in H_2O	Sigma
PD098059	specific inhibitor of MAPKK	50 µM in DMSO	Sigma
Ro25-6981	inhibitor of GluN2B subunits of NMDA receptors	1 µM in H_2O	Abcam
TTX	reversible, selective blocker of sodium channels	2 µM in H_2O	Sigma
xestospongin C	inhibitor of IP_3-dependent calcium release	1 µM in H_2O	Tocris
ω-agatoxin	selective blocker of P/Q-type VDCC	0.4 µM in H_2O	alomone
ω-conotoxin	selective blocker of N-type VDCC	1 µM in H_2O	alomone

2.2.2.5. Slice preparation from mutant mice

4 % PFA:	**4 % (w/v) paraformaldehyde in 1 x PBS**
10 x PBS:	**1.4 M NaCl; 83 mM Na_2HPO_4; 17 mM NaH_2PO_4; pH 7.4**
Sucrose Solution:	**0.5 M or 1 M sucrose in 1 x PBS; pH 7.4**
Isopentane:	**Sigma-Aldrich**

Anesthetized CtBP1 wild type and knock out mice were perfused transcardially first with 1 x PBS for 20 minutes and with 4% PFA for another 20 minutes. Heads were cut off and the skull was removed carefully without damaging the brain structures. Brains were post fixed overnight in 4 % PFA at 4°C and cryoprotected by incubating them in 0.5 M Sucrose Solution and then in 1 M Sucrose Solution. Brains were frozen using isopentane and liquid nitrogen and stored at −80°C until use. 30-40 µm thick sagittal or coronal sections were cut on a cryostat (Leica CM3050 S), collected freely floating, and used for immunological stainings, which were performed analogous to Hubler *et al.* (Hubler *et al.*, 2012).

2.2.2.6. Immunocytochemistry and imaging

Blocking Solution:	**10 % fetal calf serum; 0.1 % glycine; 0.3 % Triton X-100 in 1 x PBS**
4 % PFA:	**4 % (w/v) paraformaldehyde in 1 x PBS**
3 % FCS:	**fetal calf serum in 1 x PBS**
DAPI:	**Sigma Aldrich**
Mowiol:	**10 % (w/v) mowiol (Calbiochem); 25 % (v/v) glycerol; 100 mM Tris/HCl; pH 8.5**

Immunostainings of neurons were performed according the established protocol described in Lazarevic *et al.* (2011). Cells were fixed with 4 % PFA for five minutes at room temperature. The samples were blocked and permeabilized with Blocking Solution and incubated with the primary antibody, diluted in 3 % FCS, overnight at 4 °C. After washing three times with 1 x PBS for 10 minutes the cells were incubated with the secondary antibody in 3 % FCS for one hour at room temperature. After repeating the washing step, nuclei were stained with 2.86 µM DAPI for 30 minutes at room temperature. Before mounting the cells with Mowiol, they were washed three more times with 1 x PBS for 10 minutes and rinsed briefly with bidistilled water. All coverslips compared in one experiment were processed simultaneously using identical solutions.

2.2.2.6.1. Synaptotagmin 1 antibody live-uptake

Tyrodes Buffer: **12.5 mM HEPES; 1.25 mM KCl; 15 mM glucose; 119 mM NaCl; 2 mM $MgCl_2$; 2 mM $CaCl_2$; pH 7.4**

For the live staining of hippocampal mouse cultures with synaptotagmin 1 antibody (Syt 1 b Uptake), neurons were incubated 30 minutes with a fluorescence-labeled primary antibody towards the lumenal domain of synaptotagmin, diluted in Tyrodes Buffer (Kraszewski *et al.*, 1995; Lazarevic *et al.*, 2011). In order to prevent unspecific labeling, neurons were washed twice with Tyrodes Buffer prior fixation.

2.2.2.6.2. Arc and BDNF promoter assay

Both cortical and hippocampal cultures were infected at DIV9 with lentiviral particles containing constructs for GFP protein expressed under Arc promoter or BDNF promoter I + II (Hara *et al.*, 2009a; Ivanova *et al.*, 2015; Kawashima *et al.*, 2009). Treatments of neurons (2.2.2.4.) were done at DIV16, followed by immunocytochemistry (2.2.2.6.) using antibodies towards GFP and CtBP1. DAPI staining was used as mask for nuclear GFP fluorescence intensity as a readout for promoter activity.

2.2.2.6.3. Wide-field and confocal microscopy

Images of stainings were acquired on the Axio Imager A2 microscope (Zeiss) with Cool Snap EZ camera (Visitron Systems). The exposure time for each picture was 50 ms for nuclei and 200 ms for synapses. The imaging software VisiView (Visitron Systems GmbH) was used for image documentation.

Confocal images were received using a Leica SP5 confocal microscope (LAS AF software, version 2.0.2; 1024 x 1024 pixel display resolution, 12 bit dynamic range, 63 x objective, NA 1.40, 3 x optical zoom, approx. 60 nm pixel size). Stack imaging was acquired at a scan speed of 400 Hz by applying three times line and two times frame average using DPSS 561 and 405 Diode lasers (≤ 6 %) and corresponding HyD detectors. The z-step size came to 0.21 µm. For quantification of the cytoplasmic CtBP1 levels only one plane according to the middle plane of DAPI mask was imaged. For 3D reconstruction imaging, pixel display resolution was changed to 2048 x 2048, the dynamic range to 16 bit, and the z-step size to 0.1 µm.

2.2.2.6.4. Live-imaging

Tyrodes Buffer: **12.5 mM HEPES; 1.25 mM KCl; 15 mM glucose; 119 mM NaCl; 2 mM $MgCl_2$; 2 mM $CaCl_2$; pH 7.4**

All live-imaging experiments were performed in a heating chamber at constant 37 °C with perfusion system (flow 2 ml/min of Tyrodes Buffer) on inverted Leica TCS-SP5 Ti:Sapphire dual-colour STED microscope (512 x 512 pixel display resolution, 8 bit dynamic range, 40 x objective, 2 x optical zoom, approx. 120 nm pixel size, NA 1.40). At a scan speed of 400 Hz, a stream with imaging every five minutes over one hour was recorded. Thereby, the first image represents before and the second after NMDA stimulation (2.2.2.4.2.) via a perfusion system.

2.2.2.6.5. Image analysis

For quantitative immunofluorescence (IF) analysis only identical settings of microscope and camera were used for imaging coverslips of different groups within one experiment. For analyses of data ImageJ (NIH, rsb.info.nih.gov/ij) and OpenView (Tsuriel *et al.*, 2006) software were used. Threshold substraction of all images was done in ImageJ. Measurements of nuclear IF were performed using DAPI as mask. Cytoplasmic IF of confocal images were measured by setting rectangular regions of interest (ROI) with 1 x 1 µm in size and 3 µm distance around the nucleus restricted by DAPI staining. IF of synaptic puncta was calculated using synaptophysin as mask in OpenView software.

For 3D reconstruction, stacks of confocal images were subsequently deconvolved using the Huygens professional software package (Scientific Volume Imaging, version 4.4) and displayed in IMARIS (Bitplane).

2.2.2.7. Statistical analysis

Mean IF intensities were measured as described above (2.2.2.6.). All groups of one experiment were normalized to the corresponding control group to calculate mean values and standard error. For statistical analyses unpaired T-Test or OneWay Anova (Bonferroni: compare all pairs of column) of GraphPad Prism 5 software (GraphPad) were used. Statistical significance was reached by p-value ≤ 0.05.

2.2.3. Molecular biological methods

Most of the molecular methods followed established protocols described in Green and Sambrook (2012) and are described only briefly unless they were significantly altered.

2.2.3.1. Genotyping of mutant mice

Lysis Buffer: **10 mM Tris/HCl; 100 mM NaCl; pH 8.0**
Proteinase K: **0.4 mg/ml**
96-well plate: **Eppendorf**
dNTPs: **Deoxynucleoside triphosphate set (Thermo Scientific)**
PCR-Kit: **New England Biolabs**

For polymerase chain reaction (PCR) DNA was obtained by lysis of tailcuts from mice in Lysis Buffer containing proteinase K at 55 °C and 1000 rpm for 45 minutes, followed by 15 minutes at 95 °C to inactivate the enzyme. A 96-well plate was filled with 20 µl master mix (components described in table 2.7) and 5 µl DNA sample. The PCR program used is shown in table 2.8. The annealing temperature (T_m) was adjusted to primers utilized (see table 2.10). The samples were analyzed using agarose gel electrophoresis (2.2.3.3.).

Table 2.7: Master mix for genotyping of mutant mice.

Substance	Volume
5 x Reaction Buffer	5 µl
10 pmol primer for	0.5 µl
10 pmol primer rev	0.5 µl
10 mM dNTPs	0.5 µl
OneTaq-polymerase	0.125 µl
dH_2O	14.4 µl
total volume	21 µl

Table 2.8: PCR program for genotyping of mutant mice.

Step	Temperature	Time	Cycles
Initial Denaturation	94 °C	5 min	
Denaturation	94 °C	30 sec	
Annealing	T_m	40 sec	
Elongation	68 °C	2 min	go to step 2-4, 34 times
Final Extension	68 °C	5 min	
Hold	4 °C	HOLD	

2.2.3.2. DNA restriction

Restriction enzymes: Thermo Scientific

For digestion of DNA fragments as proof for insert of interest, several restriction enzymes were used according to the manufacturer´s protocol.

2.2.3.3. Agarose gel electrophoresis and DNA extraction from agarose gels

Agarose:	**Molecular biology grade (SERVA)**
50 x TAE:	**2 M Tris; 0.05 M EDTA**
Ethidium bromide:	**1 mg/ml (Roth)**
6 x Loading Dye:	**10 mM Tris/HCl; 0.03 % bromphenol blue; 0.03 % xylene cyanol FF; 60 % glycerol; 60 mM EDTA; pH 7.6**
GeneRuler 1kb DNA ladder:	**Thermo Scientific**
NucleoSpin ExtractII Kit:	**Macherey Nagel**

Agarose gel electrophoresis was used for separation of DNA fragments for analytical and preparative purposes. 1 % agarose gels containing 0.5 µg/ml ethidium bromide were used for DNA fragment separation at 80 mV in 1 x TAE buffer.

For Cold Fusion reaction (2.2.3.4.), DNA fragments were cut out from the gel and extracted using the NucleoSpin ExtractII Kit according to the manufacturers protocol.

2.2.3.4. Cold Fusion™ Cloning

Cold Fusion™ Cloning kit:	**Systembiosciences**
dNTPs:	**Deoxynucleoside triphosphate set (Thermo Scientific)**
PCR-Kit:	**Qiagen**

For all expression studies CtBP1-S (NM_019201.3, NP_062074.2) was used. CtBP1intEGFP expressed from FUGW was generated by insertion of the EGFP sequence between amino acids 361 and 362 of CtBP1 sequence (Ivanova *et al.*, 2015). All constructs utilized in this work (table 2.9) were generated by Cold Fusion™ Cloning system from CtBP1intEGFP subcloned into FUGW (Lois *et al.*, 2002) viral vector and sequenced.

Table 2.9: Generated constructs used in this study.

Name	Mutation	Function
CtBP1intEGFP_NESmut	Leu75Ala and Leu81Ala	nuclear export of CtBP1
CtBP1intEGFP_T133A	Thr133Ala	PKA interaction site
CtBP1intEGFP_S147A	Ser147Ala	PAK1 interaction site
CtBP1intEGFP_T133A_S147A	Thr133Ala and Ser147Ala	PKA and PAK1 interaction site

For cold fusion reaction, FUGW vector was linearized by using BamHI and XhoI (2.2.3.2.), and inserts carrying the point mutations were amplified by PCR. All required primers and PCR reactions were listed in table 2.10 and 2.11.

Table 2.10: Primers for cloning. Mutations are labeled in blue.

Name	Sequence	T_m
P1: cf_FUGW-EcoRI-CtBP1_for	GTCGACTCTAGAGGAATTCGCCACCATGTCA	53.8 °C
P2 (mut): cf_CtBP1_T133A_rev	TTCCCGAAGTGCCTGGTGTAGCCAggcAGTTCGTCG	81.2 °C
P2 (wt): cf_CtBP1_T133wt_rev	TTCCCGAAGTGCCTGG	53.3 °C
P3 (mut): cf_CtBP1_S147A_for	GCACTTCGGGAAGGCACTCGGGTCCAGgctGTAGAG	80.1 °C
P3 (wt): cf_CtBP1_S147wt_for	GCACTTCGGGAAGGCAC	57.2 °C
P4: cf_ FUGW-XI-CtBP1_rev	GTTTTTCTAGGTCTCGAGCTACAACTGGTC	56.1 °C
P5: cf_CtBP1_L75A_rev	GCTTTAAACTTCTCcgcATCTTCTC	64.1 °C
P6: cf_CtBP1_L81A_for	GAAGTTTAAAGCTgccAGAATCATCG	64.7 °C

Table 2.11: PCR reaction and program.

Substance	Volume
Template 1:100	1 µl
P1/P3 (wt/mut)/ P5/ P6	1 µl
P2 (wt/mut)/ P4/ P1/P4	1 µl
5 x Reaction Buffer	10 µl
10 mM dNTPs	1 µl
OneTaq-polymerase	0.25 µl
dH_2O	37.75 µl
total	50 µl

Step	Temperature	Time	Cycles
Initial Denaturation	94 °C	5 min	
Denaturation	94 °C	30 sec	
Annealing	T_m	40 sec	
Elongation	68 °C	2 min	go to 2-4, 31 times
Final Extension	68 °C	5 min	
Hold	4 °C	HOLD	

DNA fragments were extracted from agarose gel (2.2.3.3.) and used in cold fusion reaction together with master mix and linearized vector (table 2.12). After five minutes at room temperature and 10 minutes on ice, 50 µl *E.coli* XL10-GOLD were transformed (2.2.3.5.). Single clones were incubated in an overnight culture to isolate DNA (2.2.3.6.) and validate the sequence (2.2.3.7.).

Table 2.12: Cloning reaction.

Substance	Volume
Linearized FUGW (10-100 ng/µl)	1 µl
PCR inserts (20-200 ng/µl each)	2 x 1 µl
5 x master mix	1 µl
dH_2O	1 µl
total	5 µl

Both pArc and pBDNFpI+II (Hara et al., 2009b) were subcloned upstream of EGFP in FUGW vector for analysis of Arc and BDNF promoter activity (Ivanova *et al.*, 2015) upon pharmacological treatments (2.2.2.6.2.) and in dissociated hippocampal cultures from CtBP1 mutant mice.

2.2.3.5. Transformation of chemically competent bacteria

For replication of DNA, 5 µl of fusion reaction were transferred into 50 µl *E.Coli* XL10-GOLD suspension (2.1.4.) and incubated for 10 minutes on ice, followed by a heat shock at 42 °C for 45 seconds and a two-minute incubation on ice. Afterwards, the cell suspension was transferred into 1 ml preheated SOC-medium and incubated for one hour at 37 °C and constant shaking before plated on LB-agar plates with ampicillin and incubation overnight at 37 °C.

2.2.3.6. Alkaline lysis preparation of plasmid DNA

Buffer P1: **50 mM Tris; 10 mM EDTA; 100 µg/ml RNase A; pH 8.0**
Buffer P2: **200 mM NaOH; 1 % (w/v) SDS**
Buffer P3: **3 M potassium acetate; pH 5.5**
Maxi preparation: **NucleoBond® Xtra Maxi (Macherey-Nagel)**

Plasmid DNA mini scale preparation was used in cloning procedure to identify positive clones. Therefor single colonies were incubated overnight in 3 ml LB-medium containing 0.02 % (v/v) ampicillin at 37 °C and 175 rpm. Analogous to Birnboim and Doly (Birnboim and Doly, 1979), bacteria were resuspended in 200 µl Buffer P1, lysed with 200 µl Buffer P2 and neutralized with 200 µl ice-cold Buffer P3. After 10-minutes incubation at room temperature, precipitated proteins were removed by five-minute centrifugation at 16,000 x g and 4 °C. The DNA in the supernatant was precipitated with 70 % isopropanol. After centrifugation for five minutes at 16,000 x g and 4 °C the DNA pellet was washed with 70 % ethanol. After drying, the DNA was dissolved in 50 µl 10 mM Tris/HCl (pH 8.0).

Large amounts of DNA with high purity were isolated from 500 ml overnight culture using the endotoxin-free NucleoBond® Xtra Maxi kit according to the included manual.
Concentrations of DNA were measured using NanoDrop photometer (Intas) and 10 mM Tris/HCl (pH 8.0) as blank.

2.2.3.7. Sequencing and sequence analysis

The control sequencing of produced DNA constructs was performed by SeqLab and the results were analyzed using the Standard Nucleotide Blast (NCBI).

3. Results

3.1. CtBP1 synapto-nuclear distribution is controlled by neuronal activity

Within the last decade, many activity-dependent postsynapse-to-nucleus and only few presynapse-to-nucleus translocating protein messengers were studied (Ben-Yaakov *et al.*, 2012; Ch'ng *et al.*, 2012; Dieterich *et al.*, 2008; Jordan *et al.*, 2007; Kaltschmidt *et al.*, 1995; Karpova *et al.*, 2013; Korsak *et al.*, 2016; Moore and Goldberg, 2011; Zou *et al.*, 2009). Most of them function as regulators of gene transcription and their shuttling between the synaptic and nuclear compartment depends on neuronal network activity.

My study focused on CtBP1, which was shown to be ubiquitously expressed and to function predominantly as transcriptional co-repressor (Chinnadurai, 2007). In neuronal cells of both hippocampus and cortex, CtBP1 is enriched in the nucleus, the cytoplasm and at presynapses (Hubler *et al.*, 2012; Ivanova *et al.*, 2015). The presynaptic and nuclear pools of CtBP1 are interconnected and CtBP1 is able to shuttle between these pools as shown by live-tracked overexpressed photoactivatable CtBP1paEGFP in cultured neurons (Ivanova *et al.*, 2015).

At first, I addressed the influence of neuronal activity on the shuttling of CtBP1 based on studies from other transcriptional factors translocating after changes in neuronal activity. Such modulation of neuronal networks can be achieved by chronic silencing of network activity by application of the glutamate receptor antagonists 2-amino-5-phosphovaleric acid (APV) and 6-cyano-7-nitroquinoxaline-2,3-dione (CNQX) for 48 hours. This was shown to induce homeostatic adaptations of the presynaptic strength (Lazarevic *et al.*, 2011). Another way to modulate neuronal activity is the treatment with the potassium channel blocker 4-aminopyridine (4AP) in combination with the GABAergic antagonist bicuculline (bicucu) shown to induce excitation and expression of activity-regulated genes, such as BDNF, which can be regulated by the co-repressor CtBP1 (Garriga-Canut *et al.*, 2006; Vashishta *et al.*, 2009; Xiang *et al.*, 2007). These compounds were applied to day-*in-vitro* (DIV) 21 cortical cultures, and CtBP1 was visualized by immunostaining with a specific antibody. Nuclei were marked with DAPI and synapses with synaptotagmin 1.

The quantification of anti-CtBP1 antibody nuclear immunofluorescence (IF) intensities revealed a significant increase in the nuclear levels of CtBP1 after application of APV (50 µM) and CNQX (10 µM) for 48 hours (Fig. 3.1 A, B: 143.5 ± 3.8 %, normalized to control cells). The same treatment resulted in a significant decrease in the anti-CtBP1 antibody IF at presynapses (Fig. 3.1 C, D: 69.7 ± 4.0 %, normalized to control cells).

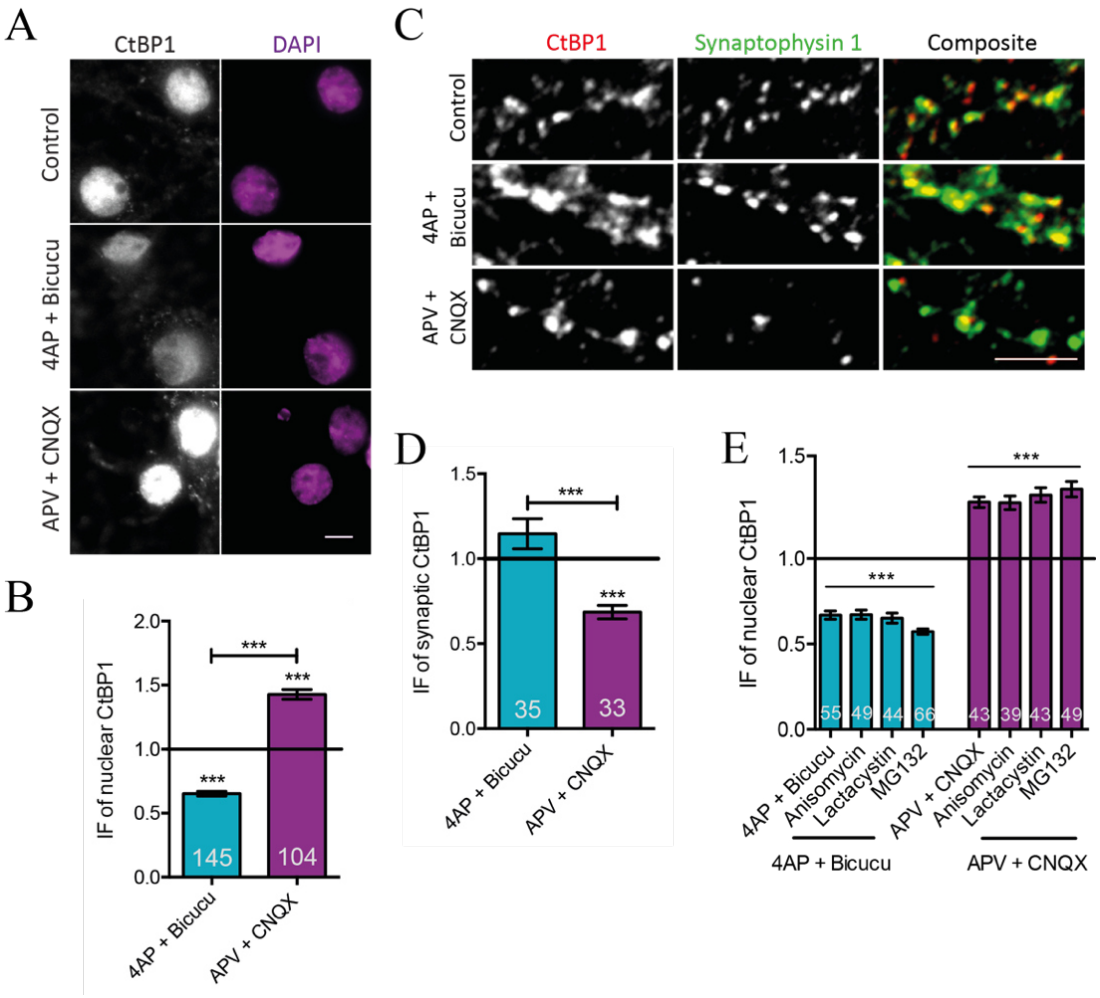

Fig. 3.1: Neuronal activity regulates the distribution of CtBP1 between presynapses and the nucleus in primary cortical cultures. A: Representative images of cell bodies and nuclei stained with antibody towards CtBP1 and DAPI as a mask. Scale bar: 10 µm, applies for all panels. **B**: Analysis of the experiment shown in A. **C:** Presynaptic distribution of CtBP1 upon disinhibition (4AP and bicucu for 8 hours), chronic silencing (APV and CNQX for 48 hours), or control (water) of DIV21 mature cortical neurons. Synaptophysin 1 was used as presynaptic marker. Analysis shown in **D**. **E:** Translocation of CtBP1 in presence of protein synthesis (anisomycin) and proteasome (lactacystin, MG132) inhibitors. For each graph n is indicated and stands for number of cells (at least 20 synapses per cell analyzed) of at least three independent experiments (cultures were prepared from at least three different animals). Data are shown as mean ± SEM. Statistical analyses were done by one-way ANOVA with unpaired t-test (B, D) or Bonferroni post hoc test (E), p*** < 0.0001. These experiments were done in collaboration with Dr. Daniela Ivanova.

This activity-dependent redistribution of CtBP1 was not sensitive to inhibition of protein synthesis (anisomycin, 10 µM (Cimato *et al.*, 1997)) or proteasomal degradation (lactacystin, 0.5 µM and MG 132, 10 µM (Johnson *et al.*, 2012; Yang *et al.*, 2005)) for six hours prior to cell fixation (Fig. 3.1 E: APV + CNQX + Aniso: 133.2 ± 4.0 %; APV + CNQX + Lacta: 137.1 ± 4.3 %; APV + CNQX + MG 132: 141.7 ± 4.5 %, normalized to control cells).

Disinhibition of cortical cultures for eight hours by treatment with the potassium channel blocker 4AP (2.5 mM) in combination with the GABAergic antagonist bicuculline (50 µM) revealed decreased nuclear and increased synaptic CtBP1 levels (Fig. 3.1 A, B: 65.4 ± 1.8 %; C, D: 115.2 ± 8.0 %, normalized to control cells). This could not be prevented by proteasomal degradation and protein synthesis inhibition (Fig. 3.1 E: 4AP + Bicucu + Aniso: 67.0 ± 2.7 %; 4AP + Bicucu + Lacta: 65.3 ± 1.6 %; 4AP + Bicucu + MG 132: 57.5 ± 1.6 %, normalized to control cells). The activity-induced changes in CtBP1 nuclear accumulation were observed already two hours after increased network activity by 4AP and bicuculline (Fig. 3.2 A, B 2 h: 73.2 ± 1.9 %, normalized to control cells) and 24 hours after silencing of cultures with APV and CNQX (Fig. 3.2 C, D 24 h: 1.5 ± 6.5 %, normalized to control cells). Silencing of neuronal cultures was also achieved by applying the sodium channel blocker tetrodotoxin (TTX, 2 µM). The treatment led to increased CtBP1 nuclear level already within one hour (Fig. 3.2 E, F: 1h: 127.9 ± 2.4 %, normalized to control cells). The observed redistribution of CtBP1 upon modulation of neuronal network activity implies CtBP1 as shuttling signal messenger between its nuclear and presynaptic pools with a cytoplasmic moiety as an intermediate pool.

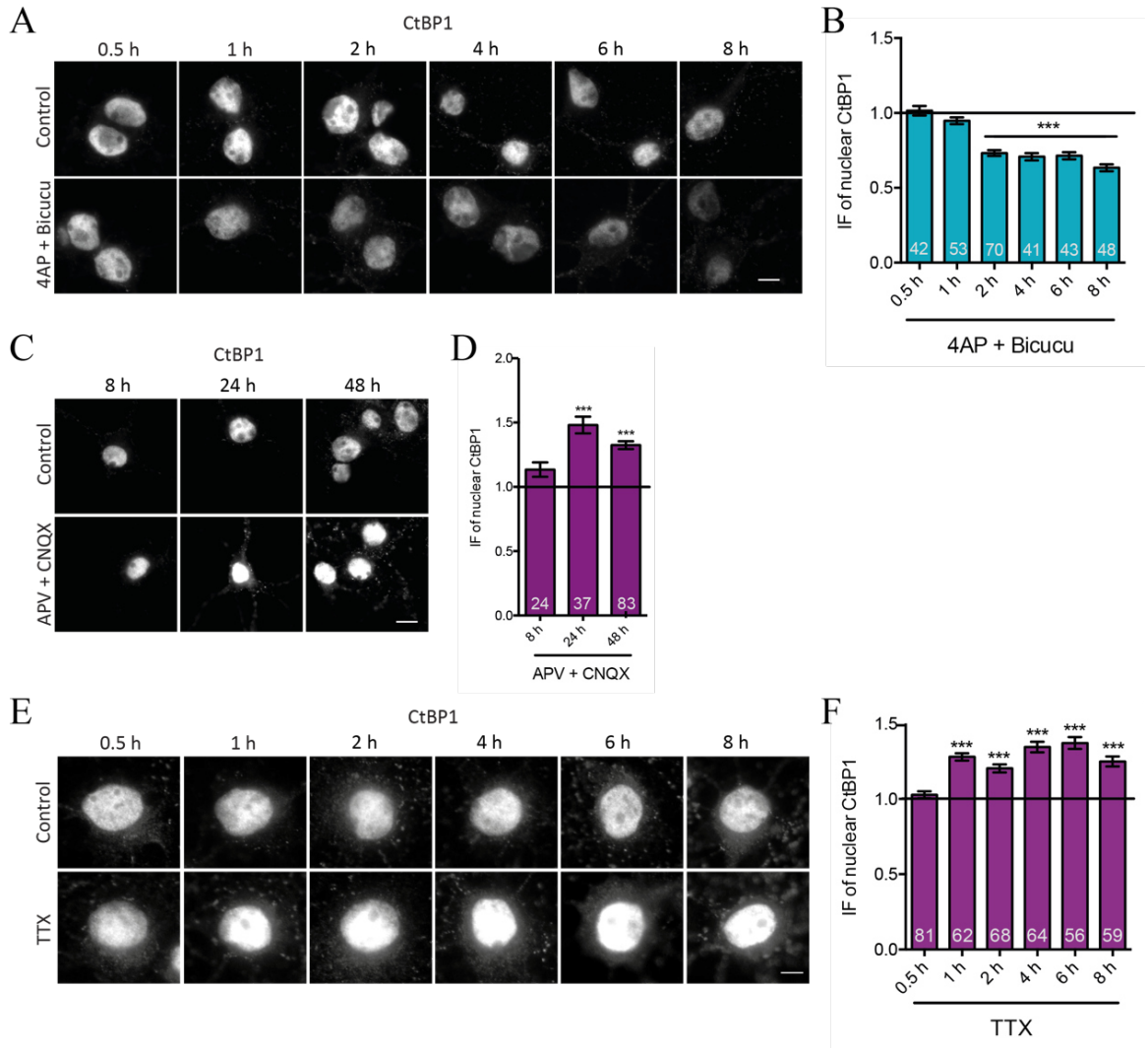

Fig. 3.2: Time course of activity-induced translocation of CtBP1 into neuronal nuclei. **A, C, E:** Representative images of cell bodies and nuclei stained with antibody towards CtBP1 indicating CtBP1 distribution upon disinhibition (4AP and bicucu for 8 hours), chronic silencing (APV and CNQX for 48 hours), TTX treatment (2 µM), or Control (water) of DIV21 mature cortical neurons. Scale bar: 10 µm, applies for all panels. **B, D, F:** Analysis of nuclear CtBP1 immunofluorescence (IF) using DAPI as a mask. For each graph n is indicated and stands for number of cells of at least three independent experiments (cultures were prepared from at least three different animals). Data are shown as mean ± SEM. Statistical analyses were done by one-way ANOVA with unpaired t-test, p*** < 0.0001.

3.2. CtBP1 nucleo-cytoplasmic translocation is driven by network activity in excitatory neurons

Besides the nuclear and presynaptic pools of CtBP1 a third – so called cytoplasmic pool – exists where CtBP1 functions as a regulator in membrane fission (Corda *et al.*, 2006; Ivanova *et al.*, 2015; Valente *et al.*, 2013). Moreover, this pool might be essential for the regulation of the nuclear and presynaptic pool size of CtBP1 in neurons. To study activity-induced changes in the nuclear and cytoplasmic (focusing on the perikaryon) pools of CtBP1, specific protocols for activation and silencing of neuronal networks were established. As mentioned above, blocking of action potentials by applying 2 µM TTX caused changes of CtBP1 nuclear pool size in cultured cortical neurons within one hour (Fig. 3.3 C: TTX 1 h: 142.9 ± 2.4 %, normalized to control cells) independent of protein synthesis or degradation as shown by application of the protein synthesis inhibitor anisomycin (Aniso, 10 µM) or the proteasome inhibitors lactacystin (Lacta, 0.5 µM) and MG 132 (10 µM) (Fig. 3.3 C: TTX: 139.1 ± 5.9 %; TTX + Aniso: 144.3 ± 4.5 %; TTX + Lacta: 142.9 ± 6.4 %; TTX + MG132: 143.3 ± 4.9 %, normalized to control cells). The NMDA receptor agonist NMDA was used to increase the excitation in neuronal cultures and was previously shown to induce synapse-to-nucleus shuttling of transcriptional factors within one hour (Jordan *et al.*, 2007). To estimate the time-course for CtBP1 shuttling, NMDA (100 µM) always in combination with the NMDA receptor co-activator glycine (2 µM) was applied for two, three, or five minutes in extracellular solution (Tyrodes Buffer). After an additional incubation time of 15, 30, 45, or 60 minutes, CtBP1 nuclear levels were quantified in DIV21 cortical neurons (Fig. 3.3 A: NMDA stimulation: 3 min: 64.6 ± 3.2 %; 3 min NMDA stimulation + 60 min: 52.6 ± 3.2 % of normalized control cells) (workflow of NMDA stimulation in Fig. 2.1, analogous to Proepper *et al.* (2007)). According to this test, an NMDA incubation time of three minutes followed by one-hour incubation of cells in medium was selected to induce robust CtBP1 translocation into the nucleus. NMDA treatments are known to induce excitotoxicity and cell death (Hardingham and Bading, 2002; Zhou *et al.*, 2013). Therefore, I performed a viability assay to evaluate the effect of the applied NMDA treatment on cell survival. To that end, cells were incubated for three minutes with NMDA and glycine and incubated in medium without NMDA for one, six, or 24 hours. The number of dead cells was examined by counting propidium iodide positive cells normalized to 4 % PFA treated cells and was not significantly altered after selected NMDA treatment as compared to untreated controls (Fig. 3.3 B: Control: 9.3 ± 1.3 %; NMDA: 9.9 ± 1.7 %, normalized to PFA treated cells). Same as above described treatments, CtBP1 shuttling by pulse NMDA receptor

stimulation was independent of protein synthesis or degradation (Fig. 3.3 C: NMDA: 67.4 ± 3.0 %; NMDA + Aniso: 68.7 ± 3.2 %; NMDA + Lacta: 62.8 ± 1.8 %; NMDA + MG 132: 67.0 ± 2.2 %, normalized to control cells).

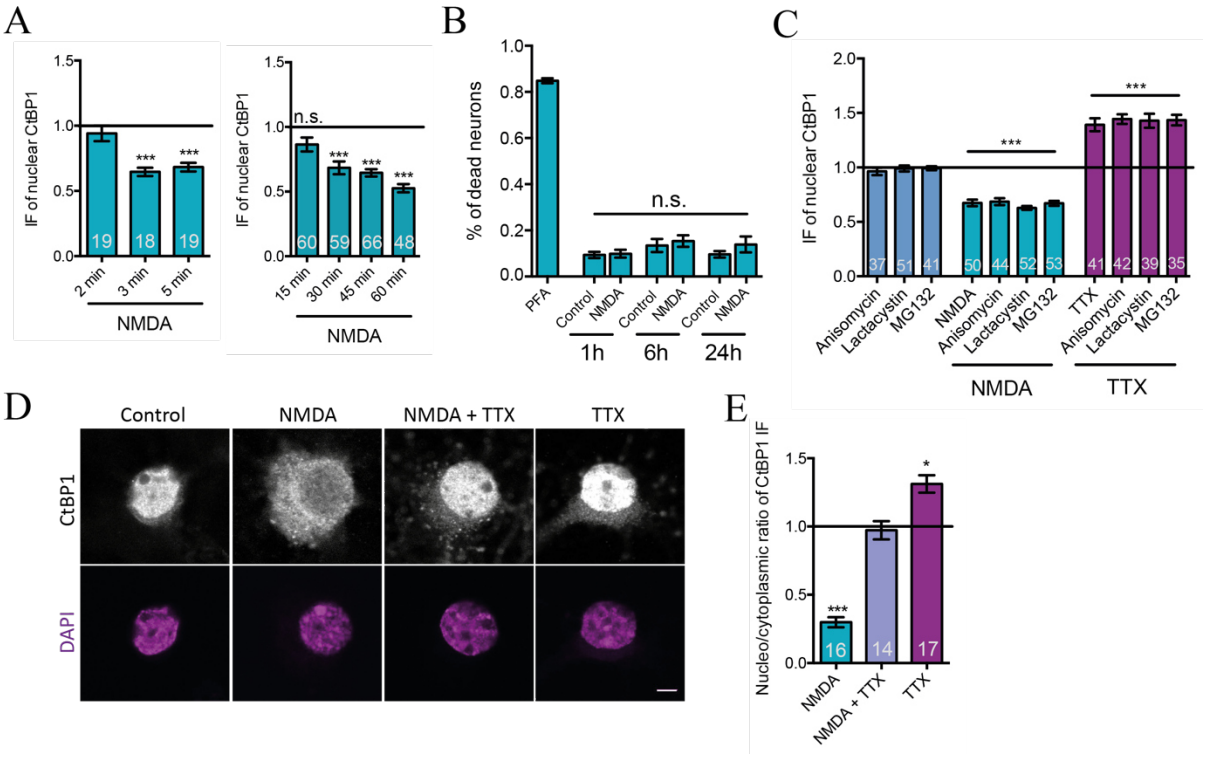

Fig. 3.3: Fast adaptations of nuclear CtBP1 levels in response to changes in neuronal network activity. **A**: Time lapse analysis of NMDA receptor stimulation with 100 µM NMDA and 2 µM glycine. **B**: Viability assay of mature cortical cultures upon NMDA receptor stimulation for three minutes and additional incubation for one, six or 24 hours. Dead cells were identified as propidium iodide positive cells. **C**: Nuclear abundance of CtBP1 in presence of protein synthesis (anisomycin) and proteasome (lactacystin, MG132) inhibitors. **D**: Confocal images of cell bodies and nuclei stained with antibody towards CtBP1 and the nuclear marker DAPI. Scale bar: 5 µm, applies for all panels. **E**: Single middle planes, defined by DAPI staining, were analyzed and the nucleo/cytoplasmic ratio was calculated after activation (NMDA + glycine) and silencing (TTX) of DIV21 primary cortical cultures for one hour. For each graph n is indicated and stands for number of cells of at least three independent experiments (cultures were prepared from at least three different animals). Data are shown as mean ± SEM. Statistical analysis was done by unpaired t-test (A, B) or one-way ANOVA with Bonferroni post hoc test, $p^* < 0.05$ and $p^{***} < 0.0001$.

The effect of changes in network activity on the cytoplasmic pool size of CtBP1 was examined by quantitative immunofluorescence analysis of endogenous CtBP1 in mature cortical cultures by confocal imaging. The middle plane of the received stack images was identified by DAPI staining and used for further analyses. The cytoplasmic levels of CtBP1 were measured by setting six rectangular regions of interest (ROIs) per cell with 1 x 1 µm in size and at 3 µm distance from the nucleus defined by DAPI. The nuclear levels of CtBP1 were quantified as

already described with DAPI as a mask for the nucleus. CtBP1 nucleo/cytoplasmic ratio was significantly decreased after NMDA (Fig. 3.3 D, E: 22.4 ± 4.0 %, normalized to control cells) and increased after TTX treatment (Fig. 3.3 D, E: 131.2 ± 6.4 %, normalized to control cells). Interestingly, the effects were diminished by simultaneous application of NMDA and TTX (Fig. 3.3 A, B: 97.3 ± 6.7 %, normalized to control cells) suggesting CtBP1 nucleo-cytoplasmic shuttling depend on both NMDA receptor signaling and neuronal network activity.

In addition, the imaged confocal stacks were deconvolved, and three-dimensional images representing CtBP1 nuclear distribution after NMDA and TTX treatment were created using IMARIS (Fig. 3.4). The images document the large effect of neuronal activity changes on the nuclear levels of CtBP1.

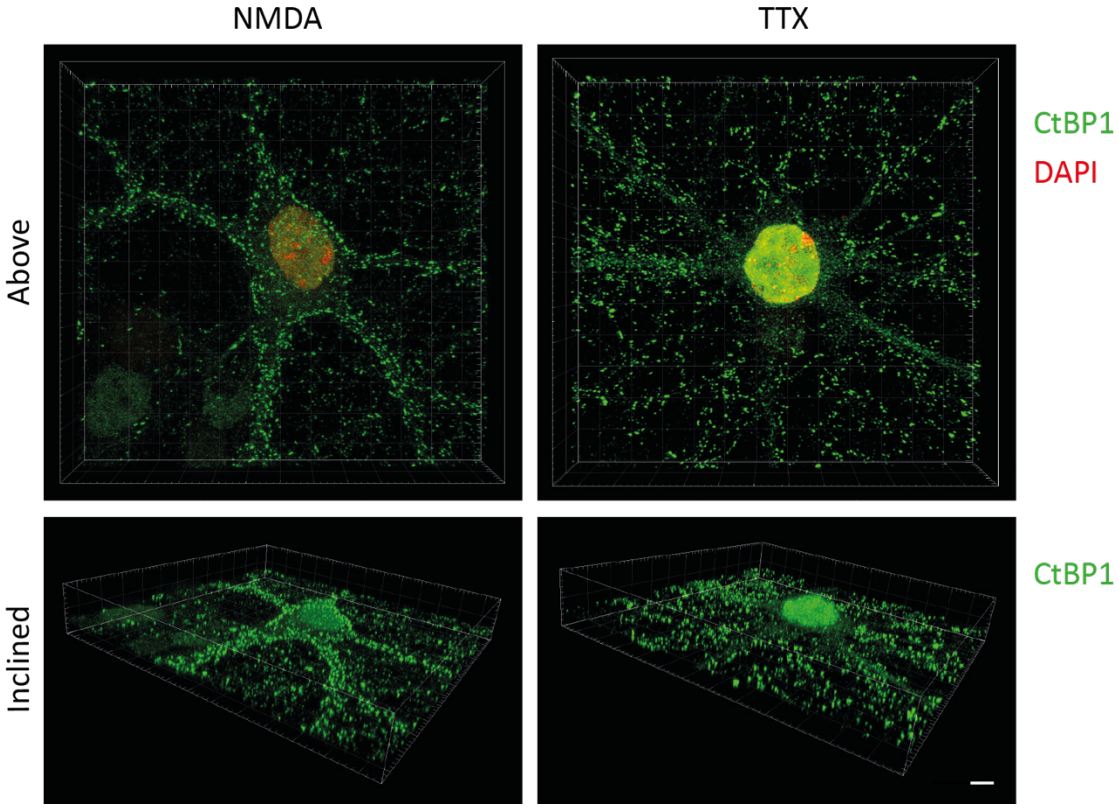

Fig. 3.4: Three-dimensional representation of CtBP1 distribution in mature cortical neurons. Deconvolved confocal images stained with antibody towards CtBP1 and the nuclear marker DAPI. Scale bar: 5 µm, applies for all panels. Images represent CtBP1 distribution after stimulation (NMDA + glycine) and silencing (TTX) of DIV21 cortical cultures.

To further explore the changes of CtBP1 nuclear level in response to NMDA receptor activation, western blot analyses were performed (Fig. 3.5). After stimulation of DIV16 cortical neurons with NMDA + glycine or vehicle (control), the nuclear (NF) and cytoplasmic (CF, contains cytoplasmic and synaptic proteins) fractions were separated biochemically, and equal

protein amounts (40 µg) were analyzed regarding the distribution of the nuclear-enriched neuronal nuclear antigen (NeuN) (Mullen *et al.*, 1992) and the cytoplasmic-enriched βIII-tubulin. As expected, NeuN (46 and 48 kDa) is enriched in the nuclear and βIII-tubulin (50 kDa) in the cytoplasmic fraction (Fig. 3.5 A). Endogenous CtBP1 (50 kDa) is present in both fractions, however, the relative amount of CtBP1 is lower in the CF compared to the NF (Fig. 3.5 A). The quantification of CtBP1 signal in the nuclear fraction in control and NMDA treated cells confirmed the decreased nuclear CtBP1 level after NMDA receptor activation obtained by immunocytochemistry (Fig. 3.5 B, C: 65.5 ± 4.1 %, normalized to GAPDH level).

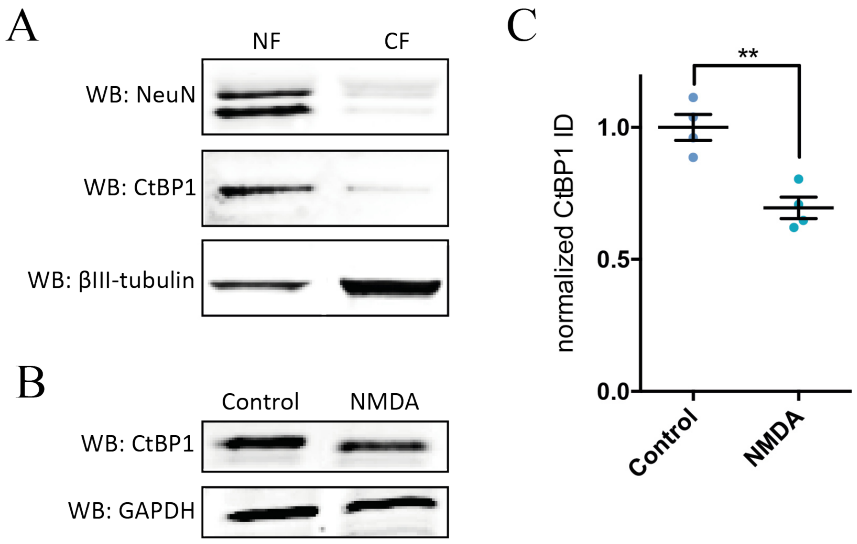

Fig. 3.5: Isolated nuclear fractions of mature cortical cultures showed an activity-dependent CtBP1 distribution. **A**: Western blot analysis of biochemical isolated nuclear (NF) and cytoplasmic (CF) fraction with antibodies towards NeuN (nuclear marker, bands at 46 and 48 kDa), βIII-tubulin (cytoplasmic, 50 kDa) and CtBP1 (50 kDa). **B**: Western blot of the nuclear fraction with CtBP1 antibody after NMDA receptor stimulation (NMDA + glycine). **C**: For analysis integrated densities (ID) of four independent experiments from individual cultures (loaded in triplicates) were normalized to GAPDH. Data are shown as mean ± SEM. Statistical analysis was done by unpaired t-test, p** < 0.01.

In every experiment, approximately 20 % of the imaged cells did not show the nucleo-cytoplasmic translocation of CtBP1 in response to stimuli. Experiments in mature cortical cultures using double-labeling with CtBP1 and GAD65 as a marker for GABAergic neurons revealed that CtBP1 is present in both inhibitory (inhib.) and excitatory (excit.) neurons, however, its expression levels in excitatory neurons were significantly lower (Fig. 3.6 A: 80.4 ± 2.6 %, normalized to excitatory cells). Furthermore, the activity-dependent increase

in nuclear IF of CtBP1 was only observed in excitatory, GAD65 negative, neurons (Fig. 3.6 B, C: NMDA inhib.: 98.2 ± 5.3 %; TTX inhib.: 94.9 ± 3.0 %; NMDA excit.: 64.9 ± 2.9 %; TTX excit.: 128.8 ± 4.9 %, normalized to control cells).

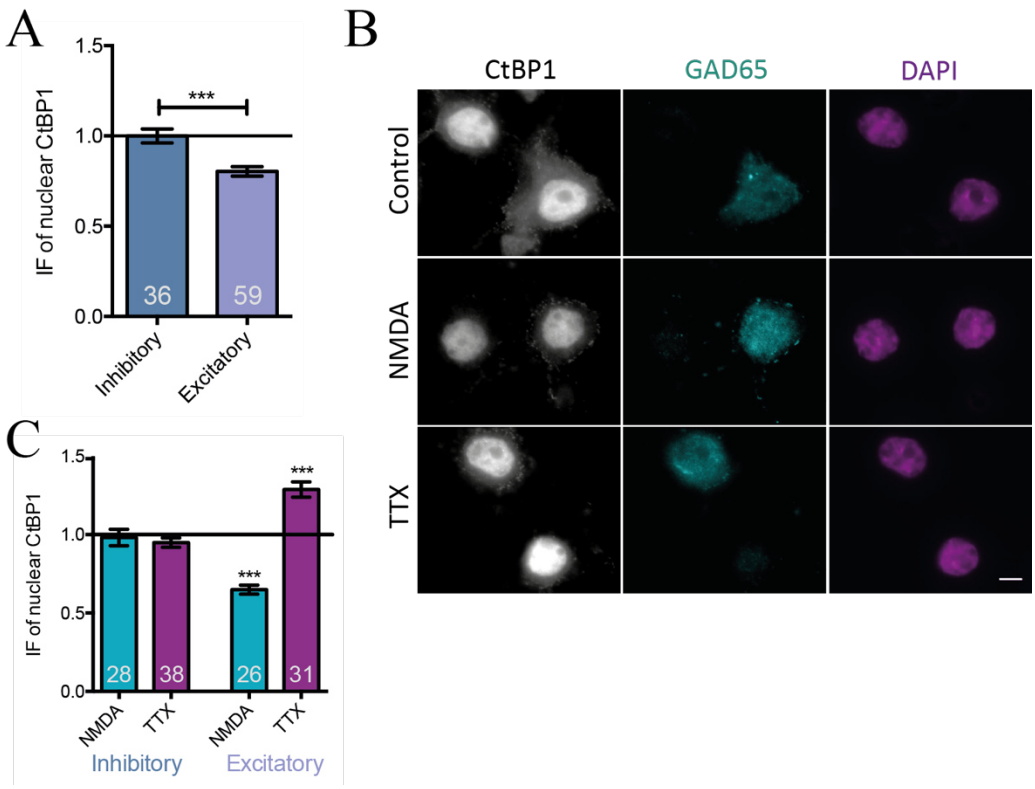

Fig. 3.6: CtBP1 activity-dependent nucleo/cytoplasmic-synaptic translocation is only observed in excitatory neurons. A: Comparison of entire CtBP1 level between glutamatergic and GABAergic neurons in DIV21 cortical cultures. **B, C**: Representative images and analysis of CtBP1 nuclear abundance in GAD65 positive (inhibitory) and negative (excitatory) mature cortical neurons after stimulation (NMDA + glycine) and silencing (TTX). Scale bar: 10 µm, applies for all panels. For each graph n is indicated and stands for number of cells of at least three independent experiments (cultures were prepared from at least three different animals). Data are shown as mean ± SEM. Statistical analyses were done by one-way ANOVA with Bonferroni post hoc test, p*** < 0.0001.

All these findings imply that neuronal network activity and NMDA receptor signaling are crucial for CtBP1 nucleo-cytoplasmic translocation in excitatory neurons. To prove the functional significances of the NMDA-induced nuclear reduction of CtBP1 levels, its impact on the co-repressor function of CtBP1 was examined.

3.3. Role of CtBP1 in regulation of activity-dependent genes

Changes in CtBP1 nuclear abundance due to altered neuronal network activity and NMDA receptor modulation might result in its altered co-repressor activity. To investigate the necessity of CtBP1 in activity-induced gene expression, a constitutive knock-out (KO) mouse model of CtBP1 was used.

Western blot analysis of hippocampus and cortex of eight-week old mice (Fig. 3.7 A: CtBP1: 50 kDa; CtBP2: 49 kDa; GAPDH: 36 kDa), slice preparation of 12-week old mice (Fig 3.7 B) and immunocytochemical experiments on DIV21 primary hippocampal neurons (Fig. 3.7 C) confirmed CtBP1 full knock-out in the KO mice (Fig. 3.7 A: 1.0 ± 0.0 %, normalized to GAPDH of WT mice; C: 10.1 ± 0.6 %, normalized to wild-type cells).

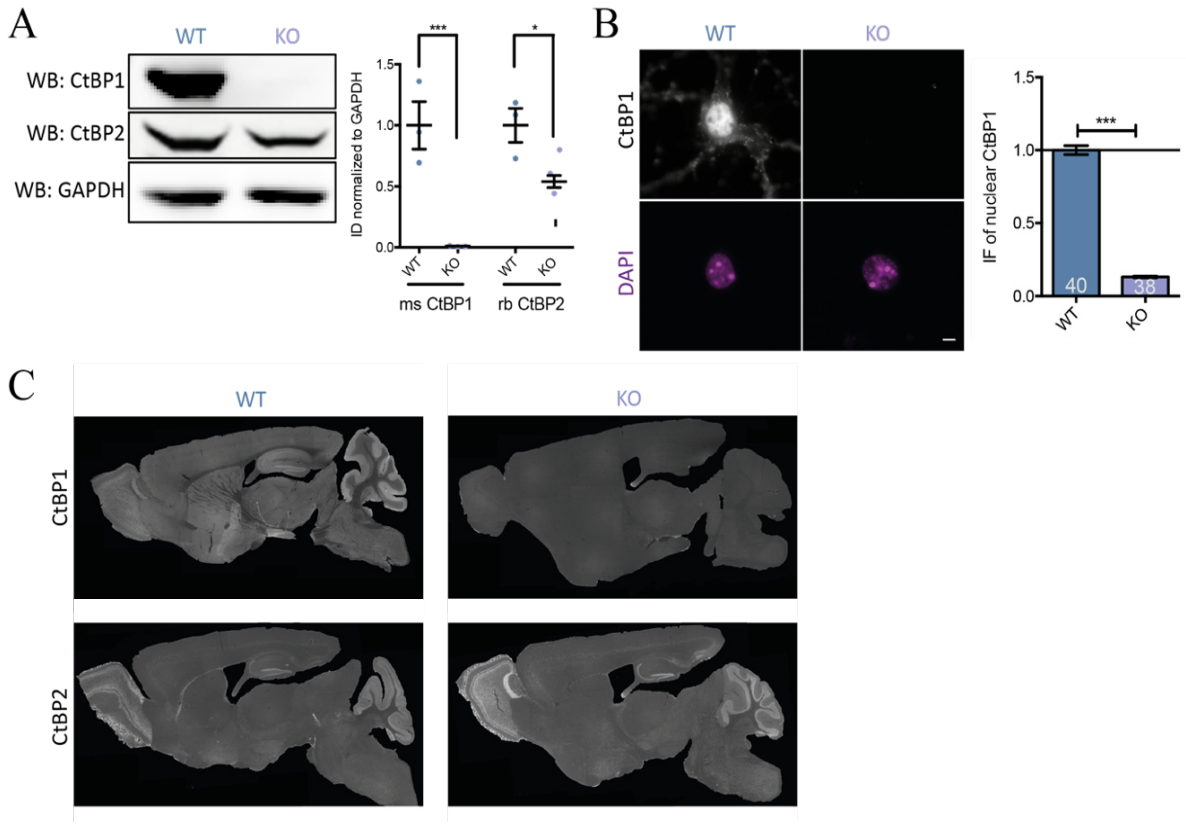

Fig. 3.7: Characterization of the CtBP1 KO mouse model. A: Western blot analysis of CtBP1 (50 kDa) and CtBP2 (49 kDa) abundance in 12 weeks old wild-type (WT) and knock-out (KO) mice. Three mice per genotype were analyzed in triplicates and normalized to the loading control GAPDH (36 kDa). **B:** 30 µm thick sections of 12 weeks old CtBP1 WT and KO mice were prepared with the help of Anil Annamneedi, showing CtBP1 and CtBP2 distribution throughout the brain. **C**: Immunocytochemistry of CtBP1 WT and KO mice. For analysis of nuclear CtBP1 immunofluorescence (IF) intensities DAPI was used as a mask. Scale bar: 10 µm, applies for all panels. For each bar n is indicated and stands for number of cells of at least three independent experiments (cultures were prepared from at least three different animals). Data are shown as mean ± SEM. Statistical analyses were done by unpaired t-test, $p^* < 0.05$ and $p^{***} < 0.0001$.

The protein levels of the CtBP1 paralog CtBP2, shown to have similar functions and large sequence homology (Hubler *et al.*, 2012), seemed to be upregulated in the dentate gyrus of CtBP1 KO mice (Fig. 3.7 B), but downregulated in all other brain areas (Fig. 3.7 A: 54.0 ± 5.0 %, normalized to GAPDH of WT mice). That implies no compensatory effect of CtBP2 in CtBP1 KO mice and makes the KO mouse model suitable for studying the role of CtBP1 in the regulation of activity-dependent genes.

CtBP1 acts as repressor of *Arc* and *BDNF* expression in neurons (Ivanova *et al.*, 2015). Therefore, I investigated the expression levels of these two genes in neurons from CtBP1 KO animals using fluorescent promoter activity reporters (Fig. 3.8). Cultured cortical neurons were infected at DIV9 with lentiviral vectors expressing GFP either under the activity-inducible Arc promoter (Kawashima *et al.*, 2009) or the activity-sensitive BNDF promoters I and II (Hara *et al.*, 2009). At DIV16, NMDA (stimulation) or TTX (silencing) treatments were performed. After one hour, cells were fixed and stained with an antibody against GFP, and DAPI was used as a nuclear mask. In wild-type neurons expressing GFP regulated by BDNF promoter I and II, NMDA receptor stimulation (100 µM NMDA + 2 µM glycine; workflow of stimulation in Fig. 2.1) led to 1.5-fold increase in the nuclear GFP IF compared to control (Fig. 3.8 A, B: 147.8 ± 7.3 %, normalized to control cells) correlating with the observed CtBP1 nuclear depletion after NMDA treatment (Fig. 3.3 C). The opposite effect was observed after silencing of the cultures with the sodium channel blocker TTX (2 µM) (Fig. 3.8 A, B: 67,1 ± 4.4 % of normalized control cells). In CtBP1 KO neurons, the activity-dependent induction of gene expression was abrogated resulting in increased BDNF promoter activity already under control conditions (Fig. 3.8 A, B: Control: 151.3 ± 13.3 %, normalized to control cells). Moreover, pharmacological modulation of the cultures did not alter the expression levels of the GFP reporter (Fig. 3.8 A, B: NMDA: 153.9 ± 20.5 %; TTX: 151.1 ± 13.5 %, normalized to control cells). Similar results were obtained for experiments analyzing the Arc promoter activity. In wild-type neurons, NMDA-induced nuclear depletion of CtBP1 resulted in increased GFP expression, whereas TTX-induced nuclear accumulation of CtBP1 led to its increased co-repressor function and decreased GFP signal (Fig. 3.8 C, D: NMDA: 170.9 ± 10.6 %; TTX: 73.3 ± 3.3 %, normalized to control cells). As for the BDNF promoter assay, CtBP1 activity-regulated *GFP* expression was no longer observed in the absence of the transcriptional co-repressor resulting in increased GFP nuclear IF intensities independent of changes in neuronal network activity (Fig. 3.8 C, D: Control: 125.8 ± 7.6 %; NMDA: 127.9 ± 11.9 %; TTX: 127.9 ± 10.9 %, normalized to control cells).

These results indicate that CtBP1 plays an important role in the regulation of activity-induced gene expression of *Arc* and *BDNF* which can be modulated by NMDA receptor signaling and network activity.

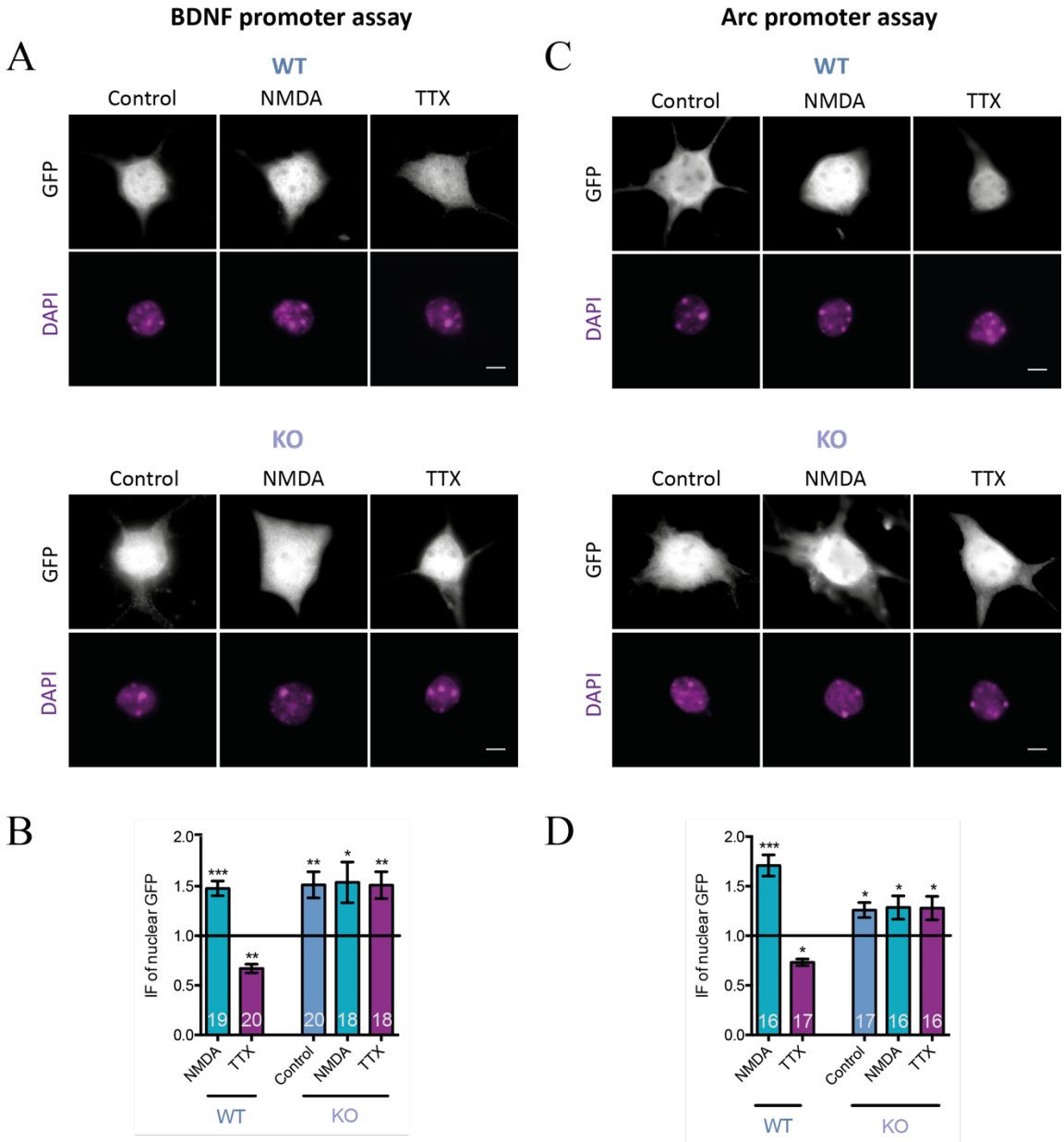

Fig. 3.8: Arc and BDNF promoters are regulated by CtBP1. A, B: Representative images of GFP immunofluorescence (IF) intensities in DIV16 dissociated hippocampal CtBP1 wild-type (WT) and knock-out (KO) cultures infected with a GFP construct under activity-inducible BDNF promoters I and II. Analysis of nuclear GFP IF after stimulation (NMDA + glycine) or silencing (TTX) is shown in **B**, DAPI was used as a mask. **C, D**: Representative images of GFP IF in dissociated hippocampal CtBP1 wild-type (WT) and knock-out (KO) cultures infected with a GFP construct under Arc activity-dependent promoter. Analysis of nuclear GFP IF is shown in **D**. Scale bar: 10 µm, applies for all panels. For each graph n is indicated and stands for number of cells of at least three independent experiments (cultures were prepared from at least three different animals). Data are shown as mean ± SEM. Statistical analyses were done by one-way ANOVA with Bonferroni post hoc test, $p^* < 0.05$, $p^{**} < 0.01$ and $p^{***} < 0.001$.

3.4. CtBP1 co-repressor function depends on Ca^{2+} signaling

My previous experiments revealed NMDA receptor activation to be a potent stimulus for the nucleo-cytoplasmic translocation of CtBP1. In neurons, NMDA receptor modulation and consequent Ca^{2+} signaling were shown to be important for downstream signaling events such as regulation of activity-induced gene expression (Greer and Greenberg, 2008; Jordan *et al.*, 2007; Kaur *et al.*, 2014). Therefore, the role of Ca^{2+} originating from different entry routes on the nucleo-cytoplasmic translocation of CtBP1 was determined.

3.4.1. GluN2B subunit containing NMDA receptors affect CtBP1 nuclear abundance

The composition of NMDA receptors has been shown to be critical for its function. Especially the - in hippocampus and cortex most abundant - GluN2A and GluN2B subunits of NMDA receptors might be of interest in studying the signaling pathway involved in the nucleo-cytoplasmic translocation of CtBP1.

So far, my results indicated NMDA receptor activation as origin of CtBP1 nuclear depletion. That was confirmed by quantitative analysis of nuclear immunofluorescence intensities of anti-CtBP1 antibody in DIV21 cortical neurons treated with both NMDA agonist (100 µM NMDA + 2 µM glycine) and antagonist (50 µM APV), respectively (Fig. 3.9 A, B, C: NMDA: 68.9 ± 1.6 %; NMDA + APV: 93.0 ± 2.3 %, normalized to control cells).

Neither the treatment with CNQX (10 µM) to block postsynaptic AMPA receptors nor the specific block of GluN2A subunits of NMDA receptors by using NVP-AAM007 (de Marchena *et al.*, 2008) (NVP, 50 nM) or EAA-090 (Sun *et al.*, 2004) (5 µM) influenced the NMDA-induced decrease of nuclear CtBP1 level (Fig. 3.9 A-C: NMDA + CNQX: 70.1 ± 3.6 %; Fig. 3.11 D: NMDA: 59.7 ± 2.3 %; NMDA + EAA-090: 66.2 ± 2.9 %; NMDA + NVP: 70.2 ± 3.0 %, normalized to control cells). These results suggest that AMPA and GluN2A-containing NMDA receptors are not required for the activity-induced nucleo-cytoplasmic shuttling of CtBP1.

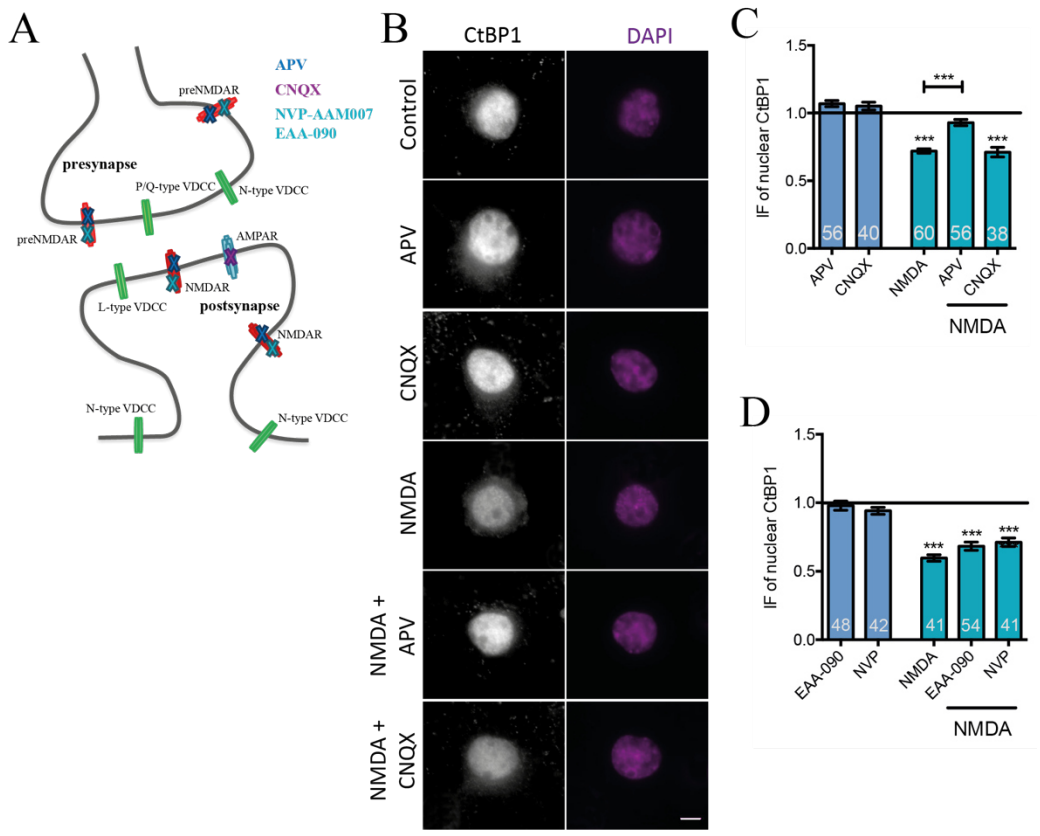

Fig. 3.9: NMDA receptor signaling plays a crucial role in the nucleo-cytoplasmic translocation of CtBP1. A: Scheme of targets of applied pharmacological reagents. CNQX blocks AMPA receptors, APV blocks NMDA receptors (NMDAR, including pre-, post- and extrasynaptic), and both NVP-AAM007 and EAA-090 specifically block GluN2A subunits of NMDA receptors. **B, C, D**: Images and analyses of stimulated (NMDA + glycine) DIV21 cortical neurons additional treated with APV, CNQX or GluN2A blockers. Scale bar: 10 µm, applies for all panels. For each graph n is indicated and stands for number of cells of at least three independent experiments (cultures were prepared from at least three different animals). Data are shown as mean ± SEM. Statistical analyses were done by one-way ANOVA with Bonferroni post hoc test, p*** < 0.001.

To define the role of GluN2B subunits of NMDA receptors, selective GluN2B inhibitors were applied to mature cortical cultures (Fig. 3.10 A). Staining with anti-CtBP1 antibody and DAPI allowed the quantitative analysis of immunofluorescence intensities of nuclear CtBP1 levels revealing no NMDA-induced nuclear depletion of CtBP1 after application of the specific GluN2B subunit inhibitors ifenprodil (Ifen, 10 µM) and Ro25-6981 (Ro, 1 µM) (Fig. 3.10 B, C: NMDA: 68.2 ± 2.1 %; NMDA + Ifen: 99.2 ± 2.5 %; NMDA + Ro: 95.7 ± 4.5 %, normalized to control cells).

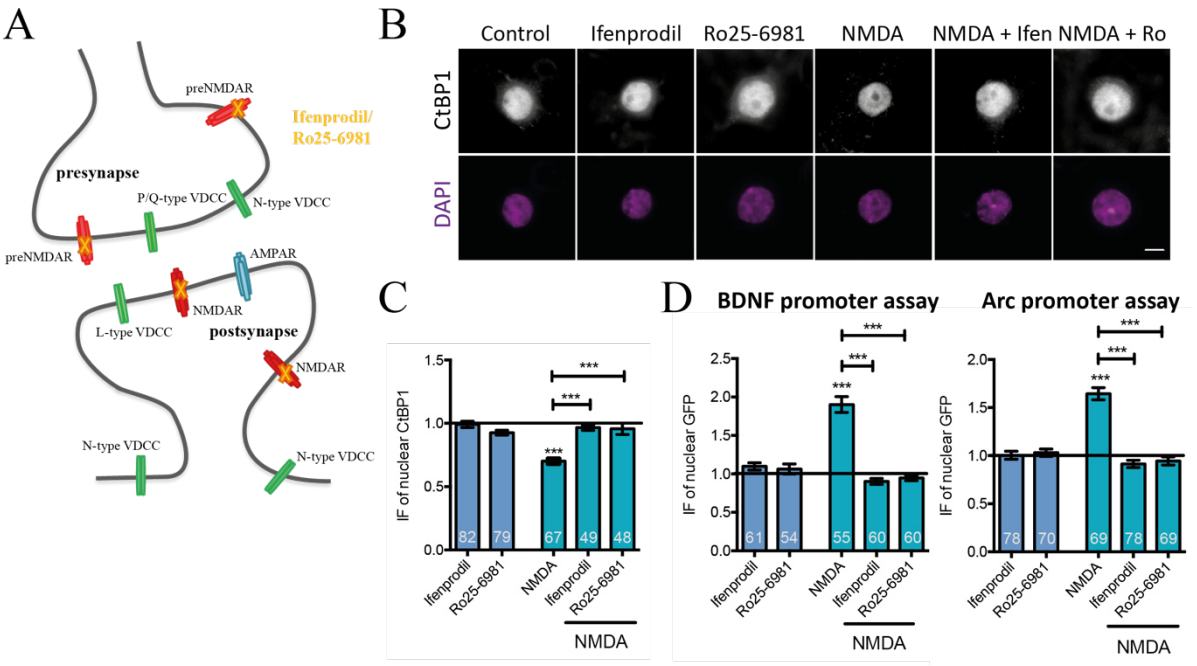

Fig. 3.10: GluN2B-containing NMDA receptors contribute to the nucleo-cytoplasmic translocation of CtBP1. **A**: Scheme of targets of applied pharmacological reagents. Ifenprodil and Ro25-6981 specifically block GluN2B subunits of NMDA receptors (NMDAR, including pre-, post- and perisynaptic). **B, C**: Images and analysis of stimulated (NMDA + glycine) DIV21 cortical cultures additional treated with GluN2B blockers. Scale bar: 10 µm, applies for all panels. **D**: BDNF and Arc promoter reporter assays. Nuclear GFP immunofluorescence (IF) intensities were analyzed after indicated treatments. For each graph n is indicated and stands for number of cells of at least three independent experiments (cultures were prepared from at least three different animals). Data are shown as mean ± SEM. Statistical analyses were done by one-way ANOVA with Bonferroni post hoc test, p*** < 0.0001.

To examine functional consequences of inactive GluN2B subunits, Arc and BDNF promoter reporter assays were performed. DIV9 rat cortical cultures were infected with lentiviral vectors for expressing GFP reporter controlled by activity-inducible Arc or BDNF promoters shown to be regulated by the transcriptional co-repressor CtBP1 (Fig. 3.8 and Ivanova *et al.* (2015)). Experiments were performed with DIV16 cortical cultures and revealed increased nuclear GFP expression (analyzed by using DAPI staining as nuclear mask) under Arc promoter and BDNF promoter I and II after NMDA treatment (100 µM NMDA + 2 µM glycine, for stimulation protocol see Fig. 2.1) (Fig. 3.10 D: BDNF: NMDA: 190.2 ± 10.4 %; Arc: NMDA: 164.3 ± 6.3 %, normalized to control cells expressing GFP). This correlates negatively with the already

shown reduced CtBP1 nuclear abundance and co-repressor function under these conditions (Fig. 3.3 and Fig. 3.8). The activity-induced gene expression of the GFP reporter was completely abolished under conditions where CtBP1 was not exported from the nucleus (Fig. 3.10 D: BDNF: NMDA + Ifen: 90.2 ± 6.8 %; NMDA + Ro: 94.7 ± 3.6 %; Arc: NMDA + Ifen: 91.4 ± 3.8 %; NMDA + Ro: 94.5 ± 4.3 % of normalized control cells expressing GFP).

In summary, CtBP1 nuclear abundance and its function as transcriptional co-repressor are influenced by NMDA receptor modulation and signaling. In particular, activated GluN2B-containing NMDA receptors play a pivotal role in the reduction of nuclear CtBP1 levels presumably by elevating intracellular Ca^{2+} levels.

3.4.2. N-type voltage-gated calcium channels influence CtBP1 nuclear abundance in neurons

Elevation in intracellular Ca^{2+} concentrations can be sensed by different VGCCs (Dolmetsch *et al.*, 2001; Fields *et al.*, 2005), another promising target in CtBP1 signaling. My study focused on high-voltage-activated calcium channels such as postsynaptic L- (also named CaV1) as well as presynaptic P/Q- (CaV2.1) and N-type (CaV2.2) VGCCs (Catterall, 2011). Postsynaptic L-type VGCCs are shown to be important for the regulation of postsynapse-to-nucleus shuttling of transcriptional factors such as CREB or CRTC1 (Ch'ng *et al.*, 2012; Deisseroth *et al.*, 1996) and to be involved in the regulation of many activity-dependent genes (Xiang *et al.*, 2007). P/Q- and N-type VGCCs are present at presynapses, connected to the active zone, and required for neurotransmitter release (Dolphin, 2012).

To explore if VGCCs influence the CtBP1 shuttling and thereby its nuclear localization, I applied potent toxins to specifically inhibit Ca^{2+} influx through P/Q-, N-, or L-type VGCCs to NMDA stimulated (100 µM NMDA + 2 µM glycine) or non-stimulated mature cortical cultures (Fig. 3.11). Interestingly, neither the presynaptic P/Q-type VGCC blocker ω-agatoxin (Aga, 0.4 µM) nor the postsynaptic L-type VGCC blocker nifedipine (Nife, 10 µM) were able to influence the NMDA-induced nuclear depletion of CtBP1 (Fig. 3.11 A, B, C: NMDA: 66.9 ± 1.2 %; NMDA + Aga: 70.8 ± 2.0 %; NMDA + Nife: 70.9 ± 3.1 %, normalized to control cells).

Due to the abrogated nuclear depletion of CtBP1 after ω-conotoxin (Cono, 1 µM) application (Fig. 3.11 A, B, C: NMDA + Cono: 95.5 ± 2.4 %, normalized to control cells), Ca^{2+} influx through N-type VGCCs seems to specifically contribute to the regulation of CtBP1 nuclear abundance in response to NMDA stimulation. The finding is in line with the results received by Arc and BDNF promoter reporter assays (Fig. 3.12) which were performed as described above (see 3.4.1 and Fig. 3.10).

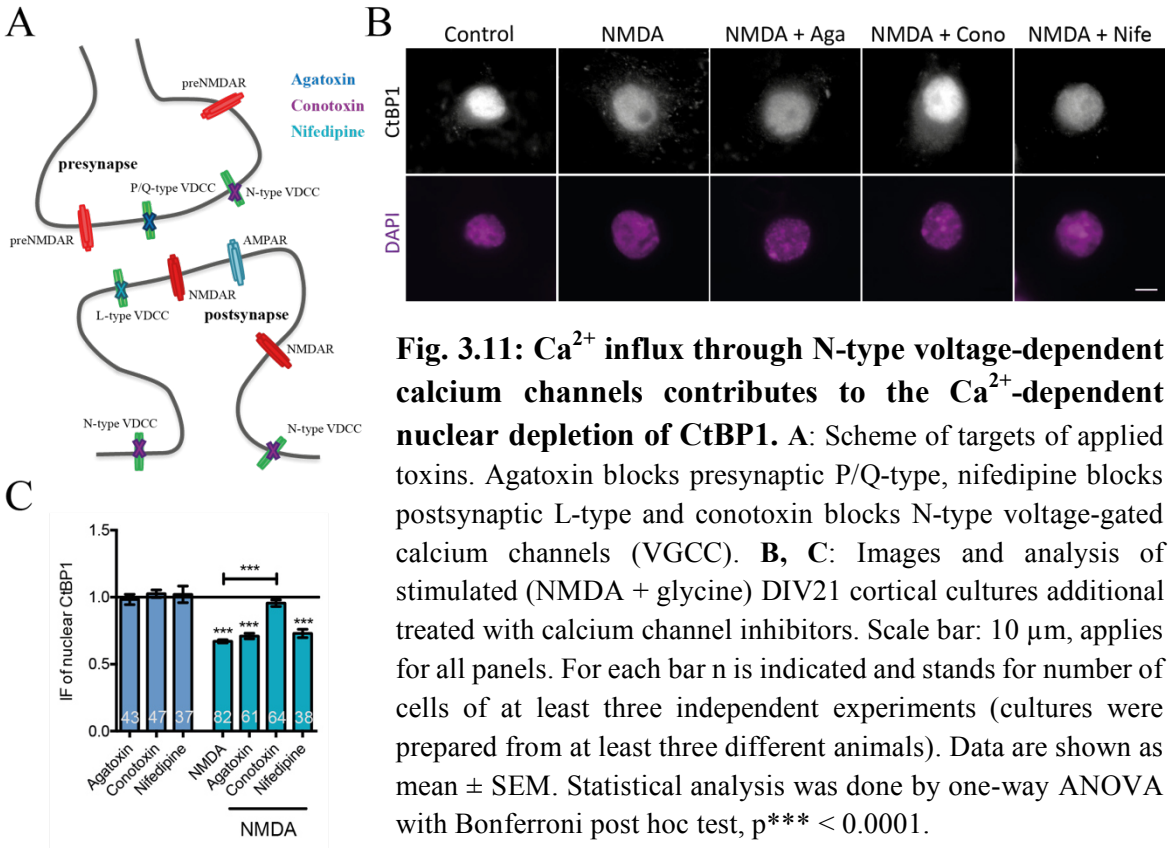

Fig. 3.11: Ca^{2+} influx through N-type voltage-dependent calcium channels contributes to the Ca^{2+}-dependent nuclear depletion of CtBP1. A: Scheme of targets of applied toxins. Agatoxin blocks presynaptic P/Q-type, nifedipine blocks postsynaptic L-type and conotoxin blocks N-type voltage-gated calcium channels (VGCC). **B, C**: Images and analysis of stimulated (NMDA + glycine) DIV21 cortical cultures additional treated with calcium channel inhibitors. Scale bar: 10 µm, applies for all panels. For each bar n is indicated and stands for number of cells of at least three independent experiments (cultures were prepared from at least three different animals). Data are shown as mean ± SEM. Statistical analysis was done by one-way ANOVA with Bonferroni post hoc test, p*** < 0.0001.

The quantification of the nuclear GFP reporter signal controlled by activity- and CtBP1-regulated Arc and BDNF promoters revealed an increased nuclear GFP IF signal in NMDA-stimulated cells which was abolished in cells treated with both NMDA and ω-conotoxin (Fig. 3.12 A, B: BDNF: NMDA: 195.7 ± 20.2 %; NMDA + Cono: 96.3 ± 10.6 %; Arc: NMDA: 157.2 ± 11.3 %; NMDA+ Cono: 103.4 ± 7.9 %, normalized to control cells expressing GFP).

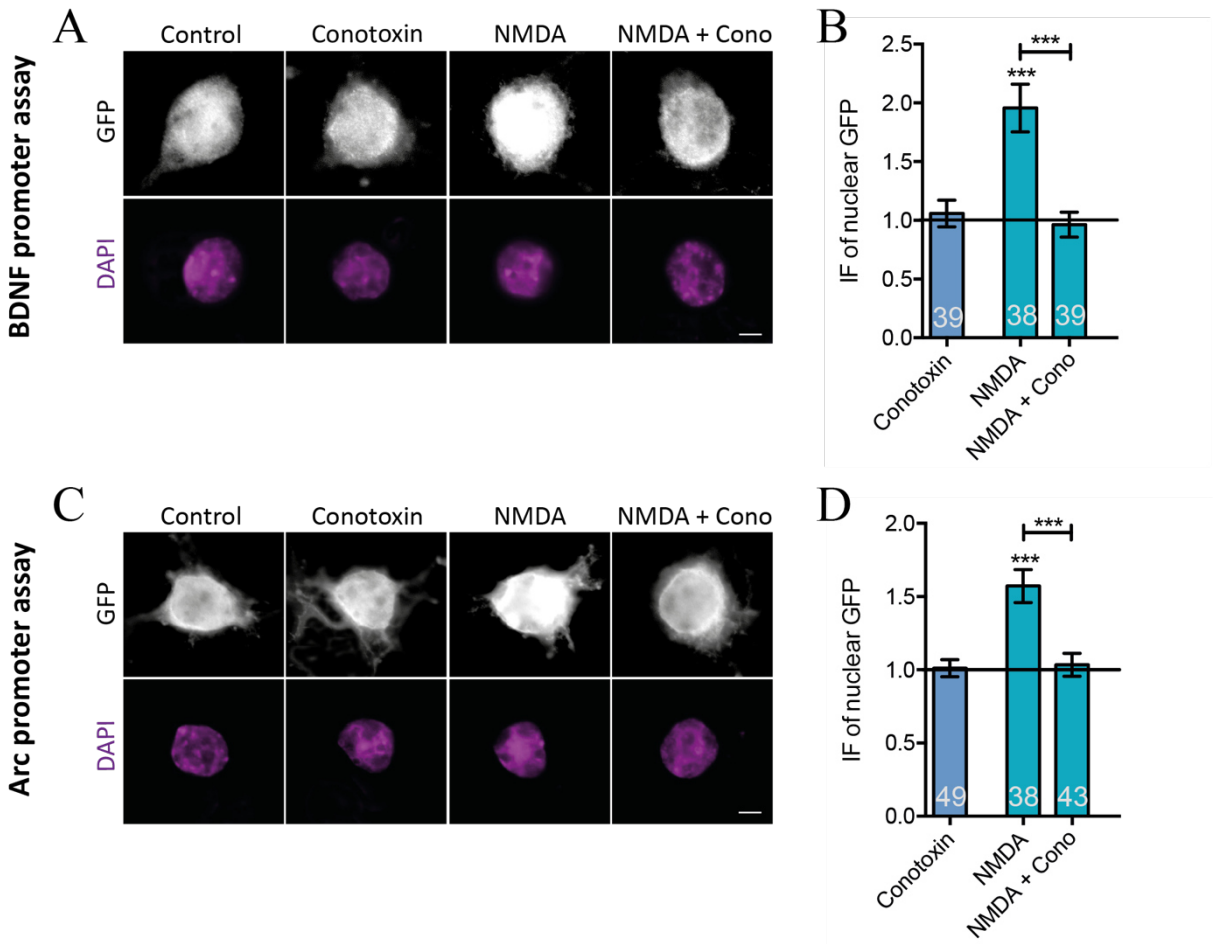

Fig. 3.12: Ca^{2+} influx through N-type voltage-dependent calcium channels is required for the regulation of activity-dependent genes by CtBP1. **A, C**: Representative images of pBDNFpI+II and pArc promoter assays using GFP protein under activity-controlled Arc and BDNF promoters. N-type VGCC blocker (conotoxin) was applied 20 min before and during NMDA receptor stimulation (NMDA + glycine). Scale bar: 10 µm, applies for all panels. **B, D**: Image analyses. For each graph n is indicated and stands for number of cells of at least three independent experiments (cultures were prepared from at least three different animals). Data are shown as mean ± SEM. Statistical analyses were done by one-way ANOVA with Bonferroni post hoc test, p*** <

These results suggest Ca^{2+} influx coming from N-type VGCCs to be important for the regulation of CtBP1 nuclear abundance. N-type VGCC activation might lead to a concentration of Ca^{2+} in the cytoplasm and subsequently to a Ca^{2+} wave towards the nucleus causing CtBP1 nuclear depletion resulting in increased gene expression.

3.4.3. Intracellular Ca^{2+} in regulation of CtBP1 nuclear abundance

To identify the role of Ca^{2+} in CtBP1 nuclear abundance, the cell-permeable calcium chelator BAPTA-AM was used to bind intracellular Ca^{2+} (Jordan *et al.*, 2007). The application of 10 µM BAPTA-AM to mature cortical neurons resulted in CtBP1 nuclear accumulation (Fig. 3.13 A, B: 120.1 ± 4.9 %, normalized to control cells). Additionally, Ca^{2+} influx through activated NMDA receptors (cells treated with 100 µM NMDA + 2 µM glycine) induced nuclear depletion of CtBP1 which was prevented by simultaneous application of BAPTA-AM (Fig. 3.13 A, B: NMDA: 64.6 ± 2.4 %; NMDA + BAPTA-AM: 95.4 ± 5.4 %, normalized to control cells).

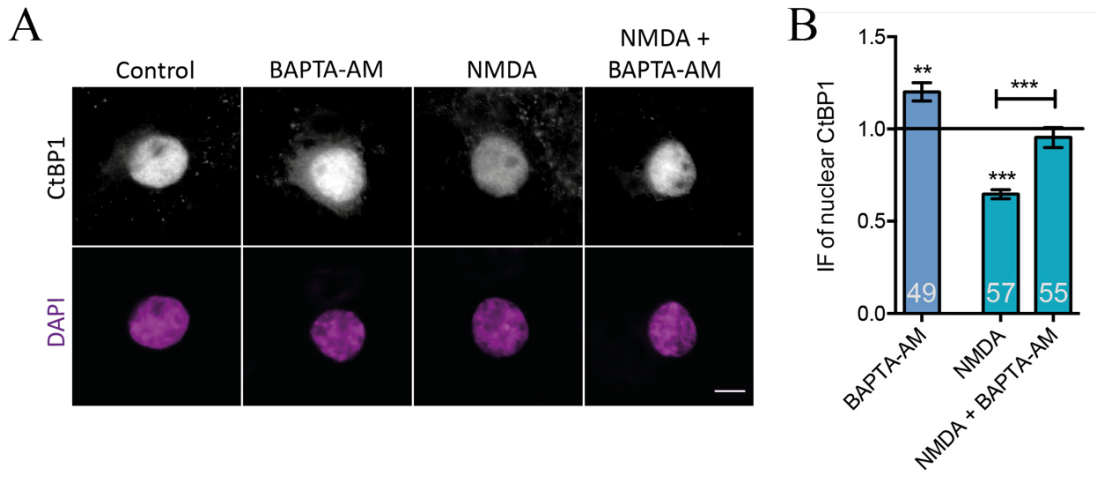

Fig. 3.13: Intracellular Ca^{2+} is required for the nuclear depletion of CtBP1 after activation of NMDA receptors. A: Representative images of cell bodies and nuclei of DIV21 cortical neurons treated with NMDA + glycine (NMDA receptor activation), BAPTA-AM (cell-permeable calcium chelator) or both. Scale bar: 10 µm, applies for all panels. Analysis of images is shown in **B**. For each bar n is indicated and stands for number of cells of at least three independent experiments (cultures were prepared from at least three different animals). Data are shown as mean ± SEM. Statistical analysis was done by one-way ANOVA with Bonferroni post hoc test, p** < 0.01 and p*** < 0.0001.

Next I examined whether mobilization of Ca^{2+} from internal stores also contributes to the activity-induced CtBP1 translocation in mature cortical neurons as Ca^{2+} release from IP_3-receptors is shown to be involved in the regulation of activity-dependent gene transcription (Jaimovich and Carrasco, 2002). To this end, DIV21 cortical cultures were stimulated with NMDA to allow Ca^{2+} influx into the cells and the subsequent induction of calcium-induced-calcium-release from internal stores such as IP_3-mediated Ca^{2+} release from the endoplasmic reticulum (Young *et al.*, 2004). To inhibit the IP_3-mediated Ca^{2+} release, the cells were treated

with xestospongin C (Xesto, 1 µM) (Fig. 3.14). Blocking of IP_3-dependent Ca^{2+} release during basal neuronal network activity showed no effect on CtBP1 translocation, but it rescued the NMDA-induced attenuated nuclear abundance of CtBP1 (Fig. 3.14 A, B: Xesto: 99.5 ± 2.0 %; NMDA: 63.9 ± 2.5 %; NMDA + Xesto: 99.5 ± 3.5 %, normalized to control cells).

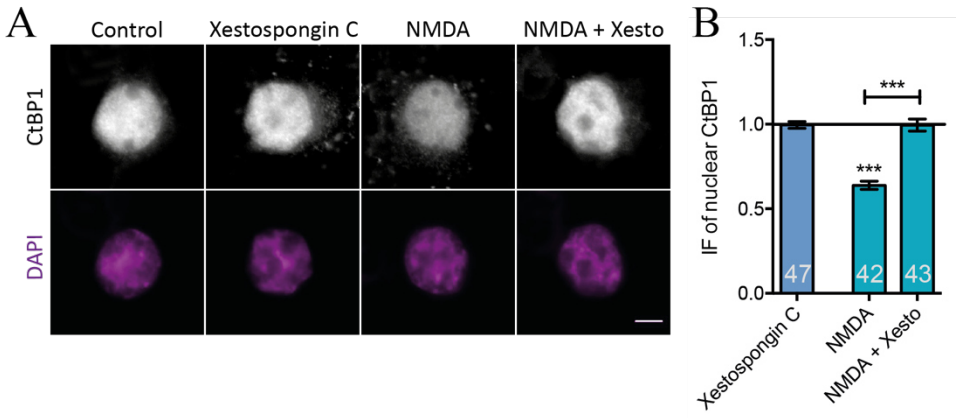

Fig. 3.14: Ca^{2+} released from intracellular stores is required for the nuclear depletion of CtBP1. A: Representative images of cell bodies and nuclei of DIV21 cortical neurons treated with NMDA + glycine (NMDA receptor activation), xestospongin C (blocks IP_3-dependent Ca^{2+} release) or both. Scale bar: 10 µm, applies for all panels. Analysis of images is shown in **B**. For each bar n is indicated and stands for number of cells of at least three independent experiments (cultures were prepared from at least three different animals). Data are shown as mean ± SEM. Statistical analysis was done by one-way ANOVA with Bonferroni post hoc test, p*** < 0.0001.

Taken together, GluN2B-containing NMDA receptor modulation and downstream Ca^{2+} signaling might lead to an elevation of intracellular Ca^{2+} concentrations. Moreover, an increase in intracellular Ca^{2+} levels can induce Ca^{2+} release through IP_3-receptors in the smooth endoplasmic reticulum resulting in Ca^{2+} signaling towards the nucleus which influences the nuclear abundance of CtBP1 and thus likely the downstream regulation of gene expression.

3.5. Activity-dependent nuclear export of CtBP1 in neurons is mediated by exportin 1

After revealing intracellular Ca^{2+} signaling crucial for the nuclear abundance of CtBP1, I assessed the molecular basis of the CtBP1 nuclear export. *In silico* analyses suggested that the sequence of CtBP1 contains a putative NES (Verger *et al.*, 2006). This type of NES comprises a core of large hydrophobic amino acids and can be recognized by exportins, which are shown to mediate nuclear export in a Ca^{2+}-dependent manner (Bogerd *et al.*, 1996; Henderson and Eleftheriou, 2000; Kaur *et al.*, 2014).

Despite the likely existence of an interaction motif for exportin 1, published experiments of applying leptomycin B (LMB), a potent inhibitor of the interaction between exportin 1 and the NES, did not show any effect on CtBP1 nuclear abundance (Verger *et al.*, 2006). In case of neuronal cells, nuclear accumulation of endogenous CtBP1 upon inhibition of exportin 1-mediated export under basal conditions was first observed after 24-hours incubation with the drug (Fig. 3.15 A, B: LMB 24 h: 137.7 ± 5.7 %, normalized to control cells) (Ivanova *et al.*, 2015).

In contrast, block of exportin 1-dependent nuclear export by LMB (3 nM) 20 minutes before activation of neuronal networks by application of the NMDA receptor agonist NMDA (100 µM NMDA + 2 µM glycine) abolished the activity-induced nuclear export of CtBP1 in DIV21 cortical cultures (Fig. 3.15 C, D: NMDA: 68.0 ± 2.0 %; NMDA + LMB: 101.6 ± 2.8 %, normalized to control cells). Further, quantitative analysis of the synaptic CtBP1 immunofluorescence signal revealed a 30 % decrease in comparison to NMDA-treated cells, similar to control levels (Fig. 3.15 E, F: NMDA: 134.2 ± 9.9 %; NMDA + LMB: 100.9 ± 5.9 %, normalized to control cells). These results suggest that NMDA receptor activation is crucial for an exportin 1-mediated nuclear export of CtBP1.

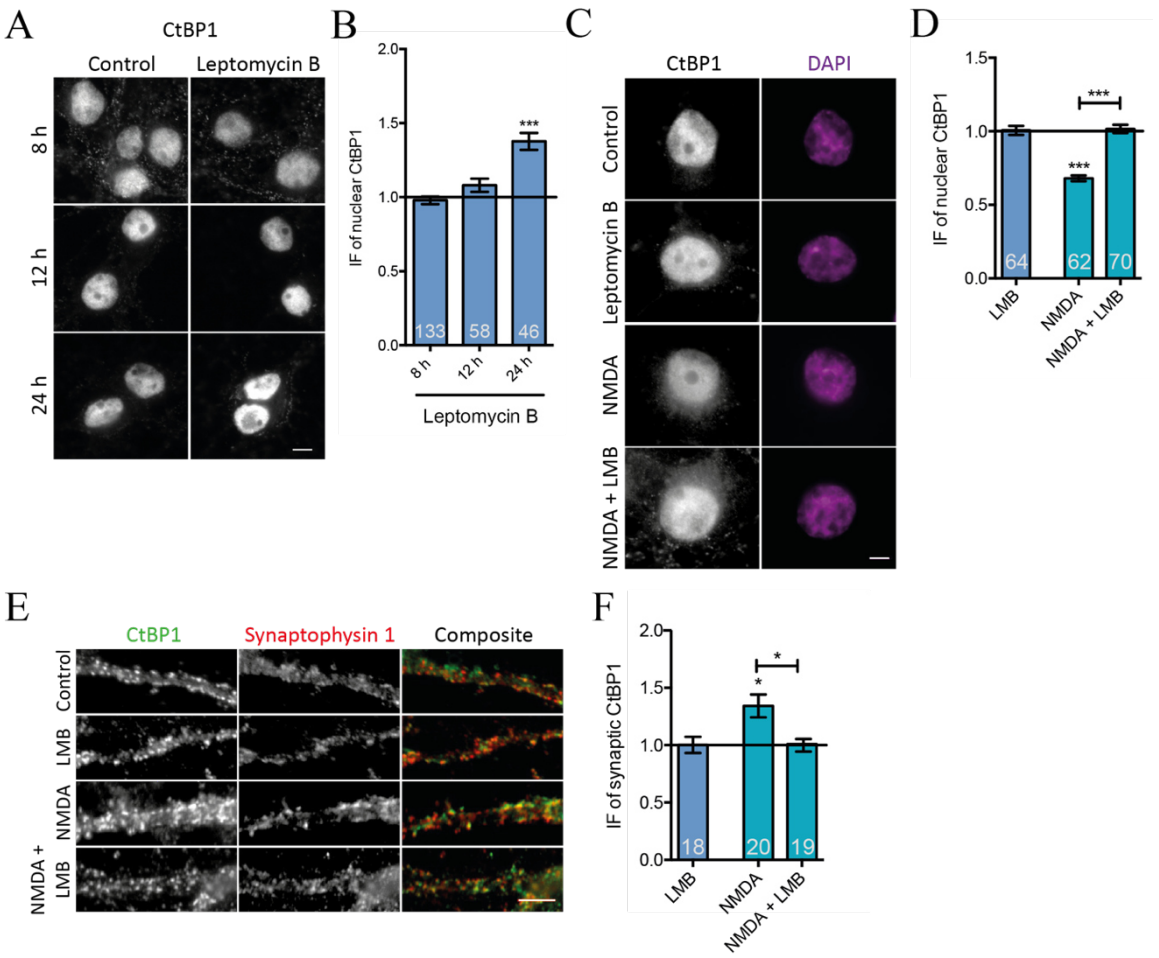

Fig. 3.15: Exportin 1 is crucial for the activity-dependent nuclear export of CtBP1 in cultured cortical neurons. A: Representative images of DIV21 mature cortical cultures stained with antibody towards CtBP1 after different periods of block of exportin 1-mediated nuclear export (leptomycin B). Analysis of time lapse is shown in **B**. This experiment was contributed by Dr. Daniela Ivanova. Scale bar: 10 µm, applies for all panels. **C, E**: Images displaying nuclear (**C**) and synaptic (**E**) effects of leptomycin B (LMB) on NMDA stimulated cells (NMDA + glycine). Analyses are shown in **D** and **F**. For each graph n is indicated and stands for number of cells (approximately 20 synapses per cell) of at least three independent experiments (cultures were prepared from at least three different animals). Data are shown as mean ± SEM. Statistical analyses were done by one-way ANOVA with Bonferroni post hoc test, $p^* < 0.05$ and $p^{***} < 0.0001$.

To finally prove the importance of the NES in the NMDA-induced nuclear export of CtBP1, a mutant (CtBP1intEGFP_NESmut) was generated (Fig. 3.16 A). Therefore, the two critical amino acids leucine 75 and leucine 81 in the NES signal sequence of CtBP1 were mutated to alanine residues (Fig. 3.16 A: L75A, L81A). This mutation was previously shown to interfere with the binding of exportin 1 and consequently with exportin 1-mediated nuclear export (Wen *et al.*, 1995). The mutation was inserted into a CtBP1intEGFP construct containing an internal EGFP-tag, shown to not influence the cellular distribution of CtBP1 (Ivanova *et al.*, 2015). DIV16 cortical neurons were stained with anti-GFP antibody to visualize both CtBP1intEGFP

and CtBP1intEGFP_NESmut. CtBP1intEGFP_NESmut showed a slight, but not significant accumulation in the nucleus and less synaptic fluorescence puncta compared to CtBP1intEGFP (Fig. 3.16 B, C: CtBP1intEGFP_NESmut: 125.1 ± 11.7 %, normalized to control cells overexpressing CtBP1intEGFP).

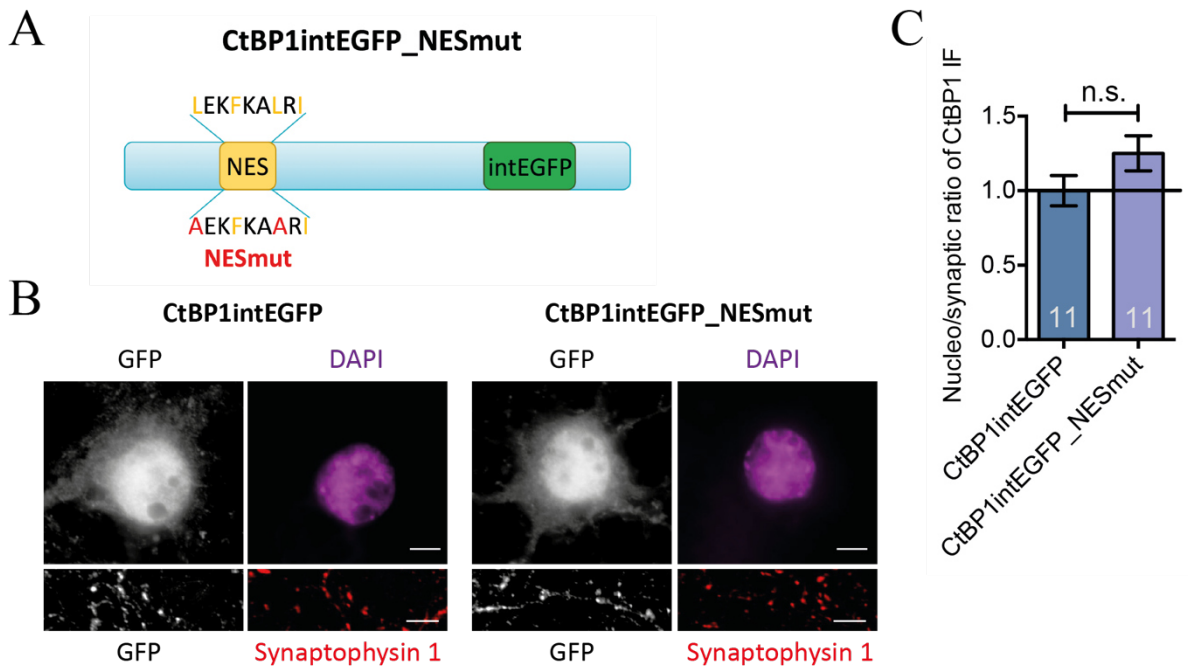

Fig. 3.16: Characterization of the lentiviral construct CtBP1intEGFP_NESmut. **A**: Scheme of the CtBP1intEGFP construct with depicted NES position. The inserted point mutations (L75A and L81A) are shown in yellow. **B:** Representative images of DIV16 primary cortical neurons stained with an antibody against the GFP-tag for the analysis of the distribution of CtBP1intEGFP_NESmut in comparison to CtBP1intEGFP. Analysis is shown in **C**. Scale bar: 10 µm, applies for all panels. For each graph n is indicated and stands for number of cells of at least three independent experiments (cultures were prepared from at least three different animals). Data are shown as mean ± SEM. Statistical analysis was done by unpaired t-test, n.s.: $p > 0.05$.

To examine the impact of the NES mutation on the activity-induced nuclear export of CtBP1, mature cortical cultures infected with the two constructs were treated with NMDA as described above (workflow Fig. 2.1). Quantitative immunofluorescence analysis showed the NMDA-induced nuclear export of CtBP1intEGFP even after blocking of protein synthesis with anisomycin (10 µM) or protein degradation with lactacystin (0.5 µM) (Fig. 3.17 A, B: NMDA + Aniso: 64.9 ± 2.1 %; NMDA + Lacta: 63.8 ± 1.7 %, normalized to control cells).

This implied that the results obtained by experiments with the CtBP1intEGFP construct are comparable to experiments on endogenous CtBP1. The mutations in the NES of CtBP1 abolished the activity-induced nuclear export of CtBP1intEGFP_NESmut completely (Fig. 3.17 C, D: NMDA: 100.7 ± 4.7 %, normalized to control cells). The mutation did not cause

degradation of the protein during the experimental procedure and compensation by new protein synthesis (Fig 3.16 C, D: NMDA + Aniso: 99.2 ± 3.5 %; NMDA + Lacta: 98.1 ± 4.5 %, normalized to control cells).

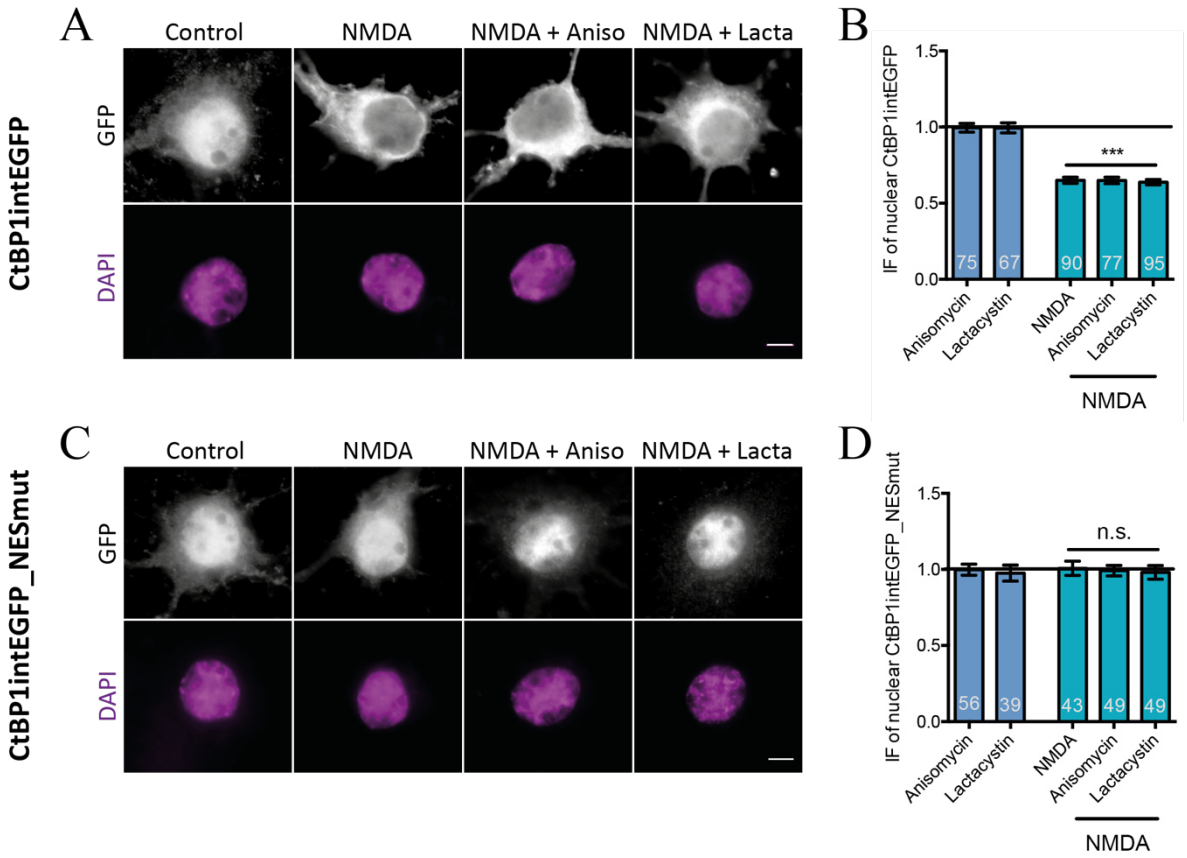

Fig. 3.17: Mutation in the NES of CtBP1 prevents its activity-induced nucleo-cytoplasmic redistribution. A: Representative images stained with GFP antibody to visualize CtBP1intEGFP after NMDA receptor stimulation (NMDA + glycine) and treatment of cortical neurons at DIV21with anisomycin (block of protein synthesis) or lactacystin (block of proteasomal degradation). Analyses are shown in **B**. **C**: Images representing properties of CtBP1intEGFP_NESmut upon indicated treatments. Analyses are shown in **D**. Scale bar: 10 µm, applies for all panels. For each graph n is indicated and stands for number of cells of at least three independent experiments (cultures were prepared from at least three different animals). Data are shown as mean ± SEM. Statistical analyses were done by one-way ANOVA with Bonferroni post hoc test, p*** < 0.0001 and n.s.: p > 0.05.

In addition, live-imaging experiments were performed to visualize the NMDA treatment-induced nuclear export of overexpressed CtBP1intEGFP and CtBP1intEGFP_NESmut (Fig. 3.18). At 37 °C and under constant perfusion, the cellular distribution of CtBP1intEGFP and CtBP1intEGFP_NESmut was imaged over time before and after NMDA stimulation (workflow Fig. 2.1). Images were acquired five minutes before treatment and every five minutes after NMDA wash out with 3-4 % laser power to minimize bleaching.

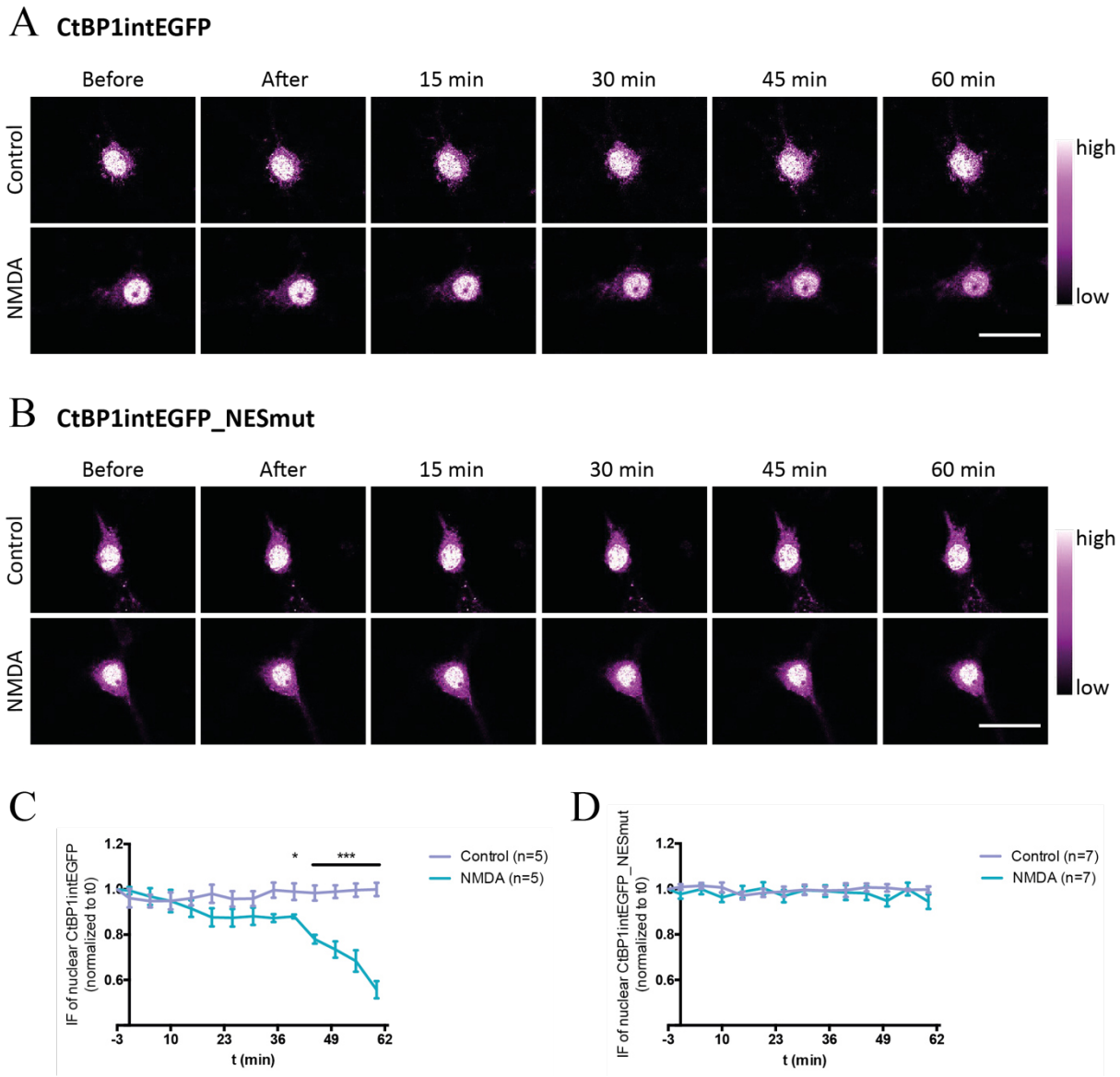

Fig. 3.18: Live-imaging experiments performed in mature hippocampal neurons demonstrate the activity-induced nuclear export of CtBP1 dependent on its NES. A, B: Recorded time lapse of overexpressed CtBP1intEGFP and CtBP1intEGFP_NESmut. Imaging of DIV16 hippocampal neurons started before stimulation with either water or NMDA (+ glycine) at 37 °C and with a perfusion system (flow 2 ml/min of Tyrodes Buffer). Scale bar: 30 µm, applies for all panels. **C, D**: Image analysis was performed for each time point (every five minutes, -3 minutes represents the time point before stimulation) over one hour. For each experiment n is indicated and stands for number of cells of at least three independent experiments (cultures were prepared from at least three different animals). Data are shown as mean ± SEM. Statistical analyses were done by one-way ANOVA with unpaired t-test, $p^* < 0.05$ and $p^{***} < 0.0001$.

40 minutes after NMDA treatment, a significant drop in the nuclear GFP immunofluorescence signal was measured for CtBP1intEGFP (Fig. 3.18: A, C: 40 min after NMDA: 88.0 ± 0.9 %, normalized to control cells). After 60 minutes the GFP IF decreased about 45 % suggesting a nuclear export of CtBP1intEGFP (Fig. 3.18 A, C: 60 min after NMDA: 55.7 ± 3.9 %, normalized to control cells). Over the imaged time, the nuclear immunofluorescence intensities of CtBP1intEGFP_NESmut stayed unchanged in both control and NMDA-treated conditions (Fig. 3.18 B, D: 60 min after water: 99.74 ± 1.3 %; 60 min after NMDA: 99.9 ± 2.8 %, normalized to control cells) implying the necessity of an exportin 1-facilitated nuclear export of CtBP1 in response to NMDA receptor stimulation in neurons.

Next, I tested whether CtBP1 and exportin 1 can physically interact. To this end, I performed co-immunoprecipitations (Co-IPs) of CtBP1intEGFP and CtBP1intEGFP_NESmut overexpressed in dissociated cortical cultures (Fig. 3.19). After separating the nuclear (NF) and cytoplasmic (CF, contains cytoplasmic and synaptic proteins) fraction from DIV16 cultures (see 3.2, Fig. 3.5), CtBP1 constructs from the nuclear enriched fraction were purified using magnetic beads labeled with an antibody towards GFP. Western blot analysis revealed exportin 1 to be in a complex with CtBP1intEGFP in the nuclear-enriched fraction (Fig. 3.19 A: exportin 1: 125 kDa, CtBP1intEGFP: 75 kDa). For the construct CtBP1intEGFP_NESmut no band was detected at 125 kDa, implying that the interaction between CtBP1 and exportin 1 is mediated by the NES signal sequence in CtBP1 (Fig. 3.19 A). To prove the specificity of the IP, IPs from cells expressing GFP only (27 kDa) were performed and did not reveal any cross-reaction of exportin 1 with the GFP-tag (Fig. 3.19 B).

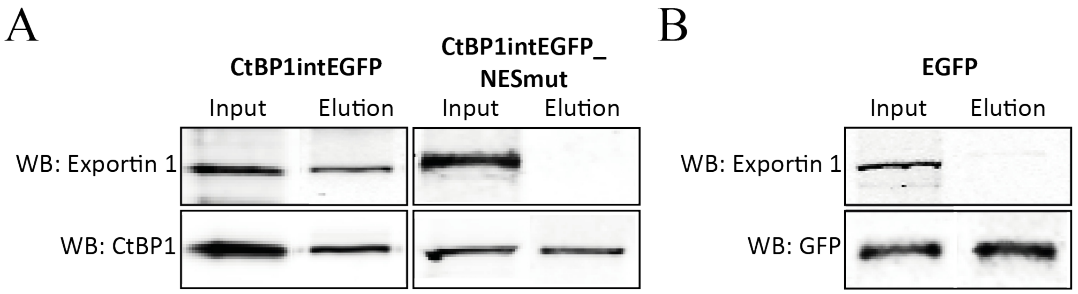

Fig. 3.19: Co-immunoprecipitations of overexpressed CtBP1 constructs revealed CtBP1 interaction with exportin 1 mediated by its NES. A, B: Co-immunoprecipitation (co-IP) of CtBP1intEGFP (75 kDa), CtBP1intEGFP_NESmut (75 kDa), or EGFP (27 kDa) with exportin 1 (125 kDa) from extracted nuclear-enriched fractions from DIV16 cortical cultures. Input fractions represent samples before co-IP with µMacs magnetic beads towards GFP, elution fractions contain purified constructs and bound proteins to CtBP1. As indicated, antibody against CtBP1 was used to detect CtBP1 constructs and for detection of GFP, GFP antibody was used. Four independent experiments (cultures were prepared from four different animals) were performed, whereby samples were loaded in triplicates.

Taken together, the nuclear export of CtBP1 is mediated by exportin 1 and depends on intracellular Ca^{2+} levels as shown in previous experiments. To link Ca^{2+} and the exportin 1-mediated nuclear export of CtBP1, I examined the contribution of posttranslational modifications by Ca^{2+}-sensitive kinases to its activity-induced nuclear export.

3.6. CtBP1 phosphorylation by PKA and Pak1 regulates its nuclear export in cortical neurons

In non-neuronal cells, phosphorylation of CtBP1 by different kinases is important for the function of CtBP1 in regulation of gene expression and in membrane fission (Barnes *et al.*, 2003; Liberali *et al.*, 2008). Potential phosphorylation sites of CtBP1 in neurons and their sequence positions are summarized below (Fig. 3.20 A, B).

A

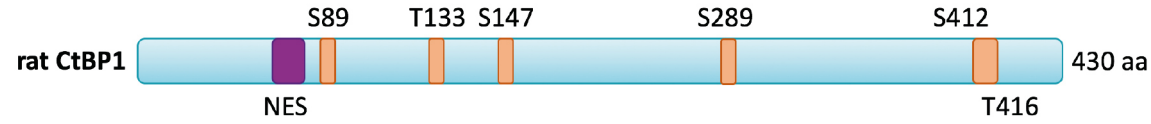

B

Residue	Kinase	Function
S89	PAK6	regulation of transcription
T133	PKA	CtBP1 dimerization and nuclear export
S147	Pak1	nuclear export
T165	Akt1	degradation
S289	ATM and ATR	in response to DNA damage
S412	HIPK2	proteasomal degradation

Fig. 3.20: Potential phosphorylation sites of CtBP1 in neurons. **A**: Position of phosphorylated residues and the nuclear export signal (NES) in rat CtBP1. **B**: List of potentially phosphorylated residues, their predicted kinases and functional consequences. Data collected from UniProt: Q13363.

In neurons, many Ca^{2+}-sensitive kinases are known to facilitate phosphorylation of proteins. Well-characterized Ca^{2+} sensors are CAMKII and MAPKK (phosphorylates and activates MAPK), both involved in classical Ca^{2+} signaling pathways and synaptic plasticity (Hudmon and Schulman, 2002; Thomas and Huganir, 2004). To investigate the potential role of these pathways in the NMDA treatment-induced CtBP1 nuclear export, the specific inhibitors calmidazolium chloride (CCl, 10 µM) and PD098059 (PD, 50 µM) blocking CAMKII and

MAPK kinase, respectively, were applied to DIV21 cortical neurons (Fig. 3.21). The quantitative analysis of immunofluorescence intensities of anti-CtBP1 antibody revealed no effect of the pharmacological reagents on the Ca^{2+}-induced CtBP1 nuclear export upon NMDA receptor activation (Fig. 3.21 A: NMDA: 65.6 ± 2.4 %; NMDA + CCl: 68.8 ± 2.3 %; NMDA + PD: 70.6 ± 2.9 %, normalized to control cells).

In silico analyses and previous studies revealed phosphorylation of CtBP1 at threonine 133 by PKA and at serine 147 by Pak1 (Dammer and Sewer, 2008; Thomas *et al.*, 2015). To test the role of these modifications in NMDA-induced nuclear export of CtBP1, the two kinases were inhibited by application of IPA3 (20 µM) to inhibit Pak1 enzymatic activity and of H89 (10 µM) or KT5720 (1 µM), which both block the PKA activity. These pharmacological reagents prevented the NMDA-induced nuclear export of CtBP1 (Fig. 3.21 B: NMDA: 67.8 ± 1.4 %; NMDA + IPA3: 90.3 ± 2.9 %; NMDA + H89: 95.5 ± 2.2 %; NMDA + KT5720: 95.4 ± 2.6 %, normalized to control cells), implying PKA and Pak1 involvement in the NMDA-mediated nuclear export mechanism of CtBP1. As these kinases are known to be regulated by intracellular Ca^{2+} (Dammer and Sewer, 2008; Leisner *et al.*, 2005), the PKA- and Pak1-dependent phosphorylation might link the increased intracellular Ca^{2+} levels in response to NMDA receptor activation to CtBP1 nuclear export.

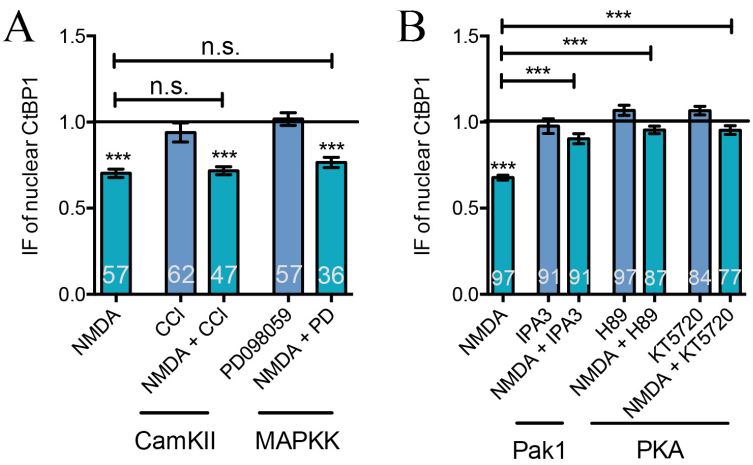

Fig. 3.21: Potential signaling pathways involved in CtBP1 relocalization.
A: Calcium/calmodulin-dependent kinase II (CAMKII) and MAP kinase kinase (MAPKK) blockers were used to identify their contribution to the nuclear export of CtBP1. **B**: P21-activated kinase (Pak1) and cAMP-dependent protein kinase A (PKA) inhibitors were used to identify their contribution to the nuclear export of CtBP1 in DIV21 mature cortical cultures. For each graph n is indicated and stands for number of cells of at least three independent experiments (cultures were prepared from at least three different animals). Data are shown as mean ± SEM. Statistical analyses were done by one-way ANOVA with Bonferroni post hoc test, p*** < 0.0001 and n.s.: p > 0.05.

To confirm the contribution of PKA to the nuclear export of CtBP1, the effect of induced activation of PKA was studied. Indeed, the activation of PKA by forskolin (Forsk, 50 µM) led to CtBP1 nuclear export under basal activity in mature neuronal cultures (Fig. 3.22 A, B: Forsk: 79.4 ± 1.7 %, normalized to control cells). Additionally, a combination of forskolin and NMDA (100 µM NMDA + 2 µM glycine) enhanced the NMDA-induced nuclear export of CtBP1 (Fig. 3.22 A, B: NMDA: 68.8 ± 1.8 %; NMDA + Forsk: 59.4 ± 1.7 %, normalized to control cells). Interestingly, PKA activation by forskolin was not sufficient to induce nuclear export of CtBP1 by simultaneous blockage of N-type VGCCs through application of ω-conotoxin (Fig. 3.22 A, B: Forsk + Cono: 96.8 ± 3.2 %, normalized to control cells). Together with previous results (see 3.4), the nuclear export of CtBP1 is dependent on its phosphorylation by PKA and Pak1 and is initiated by NMDA receptor signaling and activation of N-type VGCCs.

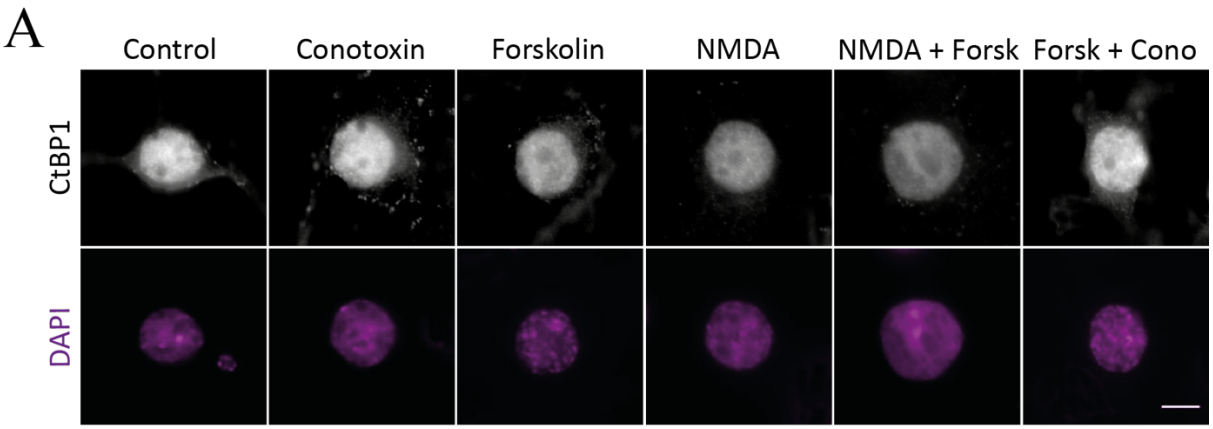

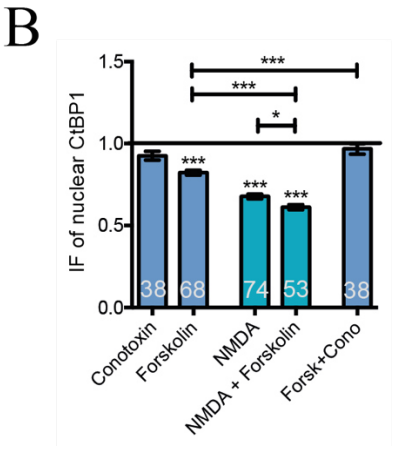

Fig. 3.22: Nuclear export of CtBP1 requires both PKA phosphorylation and activity-induced adaptations of intracellular Ca^{2+} levels. **A**: Representative images of DIV21 cortical neurons stimulated with NMDA (+ glycine) and treated with conotoxin (N-type VGCC blocker), and/or forskolin (activates PKA by elevating cAMP level). Scale bar: 10 µm, applies for all panels. Analysis of data is shown in **B**. For each bar n is indicated and stands for number of cells of at least three independent experiments (cultures were prepared from at least three different animals). Data are shown as mean ± SEM. Statistical analysis was done by one-way ANOVA with Bonferroni post hoc test, $p^* < 0.05$ and $p^{***} < 0.0001$.

To confirm this hypothesis, mutants based on CtBP1intEGFP lacking PKA (T133A) and Pak1 (S147A) phosphorylation sites were generated. Although not explicitly studied in terms of the co-repressor function of CtBP1 (Barnes *et al.*, 2003; Liberali *et al.*, 2008), the phospho-mimetic mutant (S147D) was shown to not have any functional impact on the endocytosis mediated by CtBP1 (Haga *et al.*, 2009). In contrast, the S147A mutant profoundly affects the nuclear as well as the cytoplasmic functions of the protein. Therefore, I focused my analysis on phospho-deficient mutants to further characterize the role of Pak1 and PKA phosphorylation in the activity-induced nuclear export of CtBP1.

To analyze the CtBP1 nuclear export mechanism on the basis of neuronal signaling-induced phosphorylation, DIV4 cortical cultures were infected with CtBP1intEGFP (mimicking endogenous CtBP1 distribution), CtBP1intEGFP_T133A (threonine to alanine mutation in PKA phosphorylation site), CtBP1intEGFP_S147A (serine to alanine mutation in Pak1 phosphorylation site), or with the double mutant CtBP1intEGFP_T133A_S147A. Quantitative measurements of immunofluorescence intensities of nuclear GFP signal at DIV16 illustrated the nucleo/synaptic distribution of mutants similar to CtBP1intEGFP (Fig. 3.23 A, B: CtBP1intEGFP: 100.0 ± 11.7 %; CtBP1intEGFP_T133A: 109.9 ± 20.2 %; CtBP1intEGFP_S147A: 103.5 ± 9.4 %; CtBP1intEGFP_T133A_S147A: 102.9 ± 9.9 %, normalized to control cells overexpressing CtBP1intEGFP).

Interestingly, none of the phospho-mutants showed a nuclear export in response to increased neuronal network activity (Fig. 3.24 A, B: CtBP1intEGFP NMDA: 62.5 ± 2.3 %; CtBP1intEGFP_T133A NMDA: 102.2 ± 4.4 %; CtBP1intEGFP_S147A NMDA: 96.2 ± 5.9 %; CtBP1intEGFP_T133A_S147A NMDA: 98.7 ± 4.4 %, normalized to control cells for each construct individually). This suggests that the nuclear export of CtBP1 depends on phosphorylation by both PKA and Pak1, which might influence compartment-specific functions of CtBP1 as already shown for non-neuronal cells (Dammer and Sewer, 2008; Liberali *et al.*, 2008).

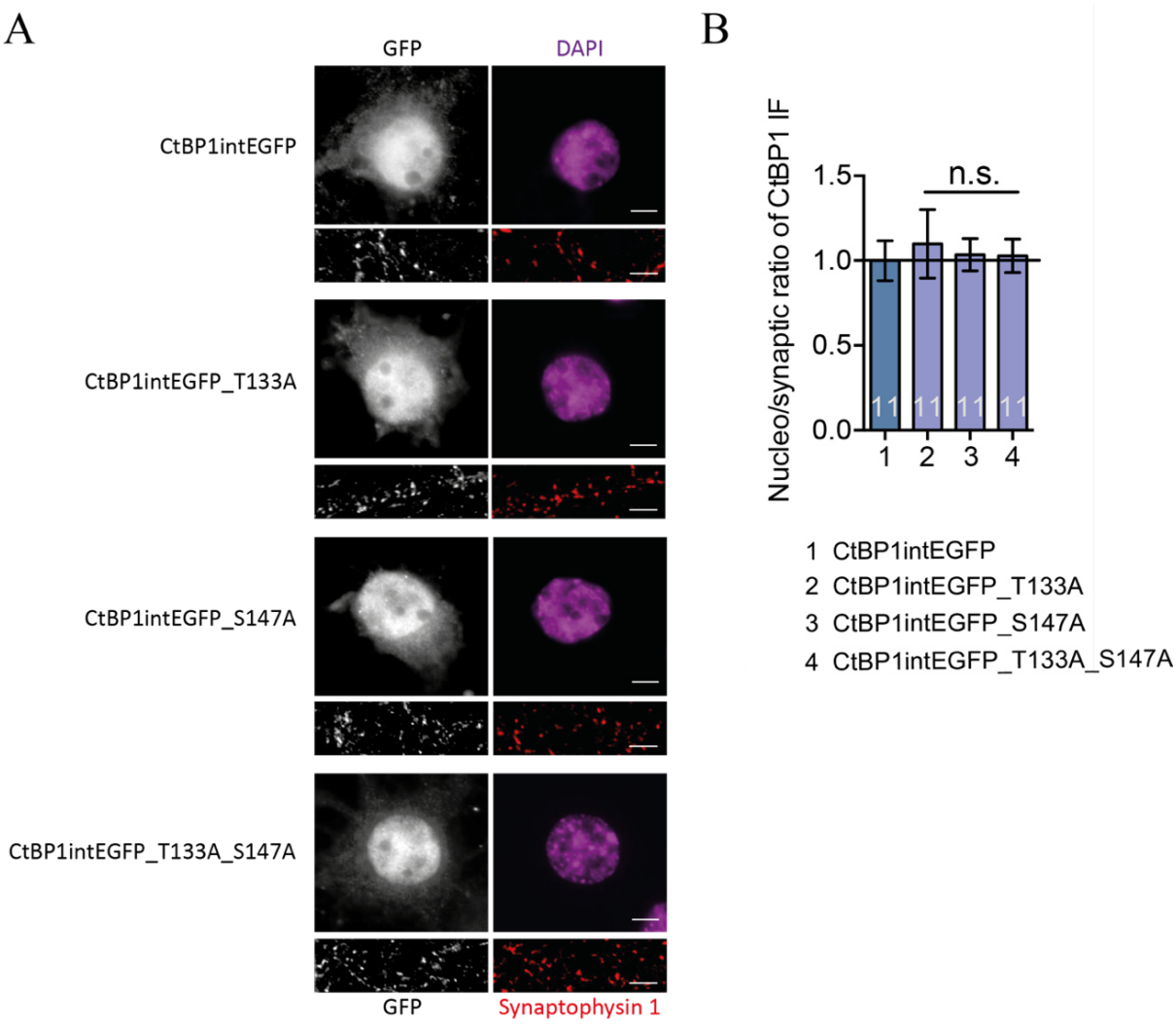

Fig. 3.23: Characterization of CtBP1 constructs lacking phosphorylation sites of PKA and Pak1. Representative images of cell bodies/nuclei (**A**) and synapses (**B**) of DIV16 cortical neurons infected with CtBP1intEGFP, CtBP1intEGFP_T133A (mutation of PKA phosphorylation site), CtBP1intEGFP_S147A (mutation of Pak1 phosphorylation site) or with the double mutant and stimulated with NMDA (+ glycine). Scale bar: 10 µm, applies for all panels. Analysis of data is shown in **B**. For each graph n is indicated and stands for number of cells of at least three independent experiments (cultures were prepared from at least three different animals). Data are shown as mean ± SEM. Statistical analysis was done by unpaired t-test, n.s.: $p > 0.05$.

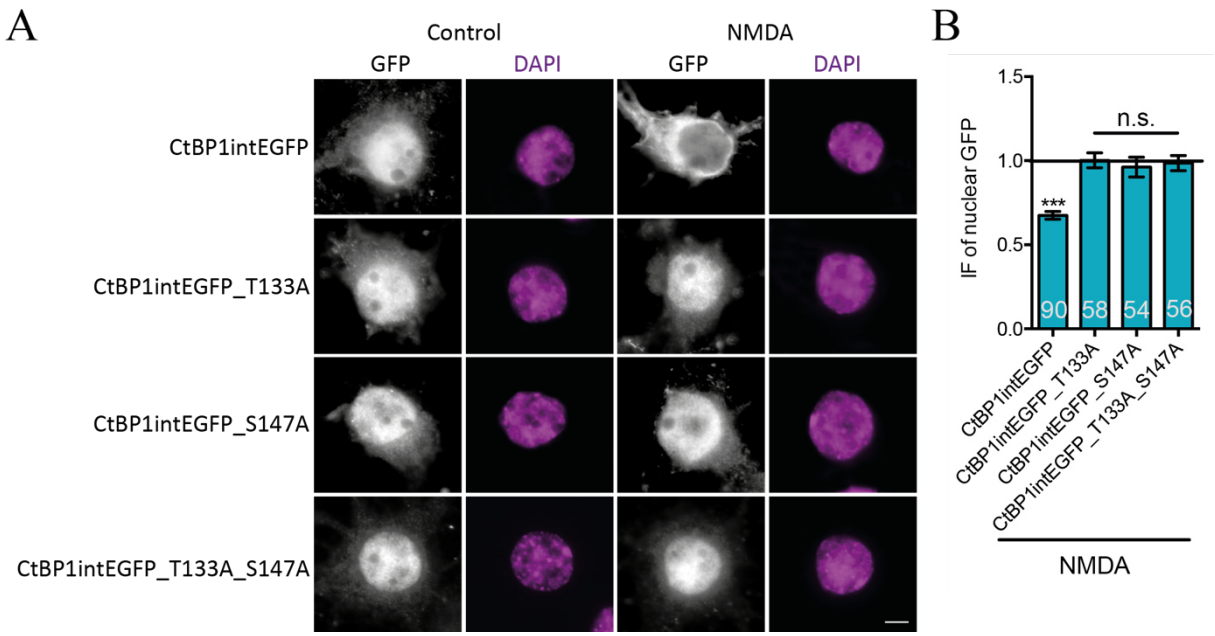

Fig. 3.24: Phosphorylation of CtBP1 by PKA and Pak1 is required for the activity-induced nucleo-cytoplasmic translocation of CtBP1. **A**: Representative images of DIV16 cortical neurons infected with CtBP1intEGFP, CtBP1intEGFP_T133A (mutation of PKA phosphorylation site), CtBP1intEGFP_S147A (mutation of Pak1 phosphorylation site) and double mutant. Scale bar: 10 µm, applies for all panels. Dissociated cultures were stimulated with NMDA (+ glycine) or water as Control. Analysis of data is shown in **B**. For each graph n is indicated and stands for number of cells of at least three independent experiments (cultures were prepared from at least three different animals). Data are shown as mean ± SEM. Statistical analysis was done by unpaired t-test, p*** < 0.0001 and n.s.: p > 0.05.

Taken together, phosphorylation of CtBP1 by the Ca^{2+}-sensitive kinases PKA and Pak1 is important for the CtBP1 nuclear export in response to increased neuronal activity.

3.7. Importin β1 and microtubules play a role in the activity-induced retrograde translocation and nuclear import of CtBP1

Besides the observed effects of neuronal activity, NMDA receptor modulation, and Ca^{2+} signaling on CtBP1 nuclear abundance, silencing of cultures by either TTX or APV and CNQX was shown to induce nuclear accumulation of CtBP1. The observed increase in the nuclear CtBP1 levels are caused by either diffusion or importins, whereas the latter is important in the regulation of nuclear import of proteins (Pemberton and Paschal, 2005). At first I assessed, whether the nuclear import of CtBP1 is facilitated by importins and in particular by importin β, the most prominent isoform in mammals (Perry *et al.*, 2012). Indeed, inhibition of this pathway by employing importazole (Imp, 20 µM) on mature cortical cultures (Fig. 3.25) (Soderholm *et al.*, 2011) revealed significantly lower anti-CtBP1 antibody immunofluorescence levels in the nucleus after 80 minutes of treatment (Fig. 3.25 A, B: 82.4 ± 2.0 %, normalized to control cells). Even induction of CtBP1 nuclear translocation by applying TTX did not trigger CtBP1 nuclear import in the presence of importazole (Fig. 3.25 A, B: 89.0 ± 2.2 %, normalized to control cells). That suggests importin β as a target molecule for the CtBP1 nuclear import.

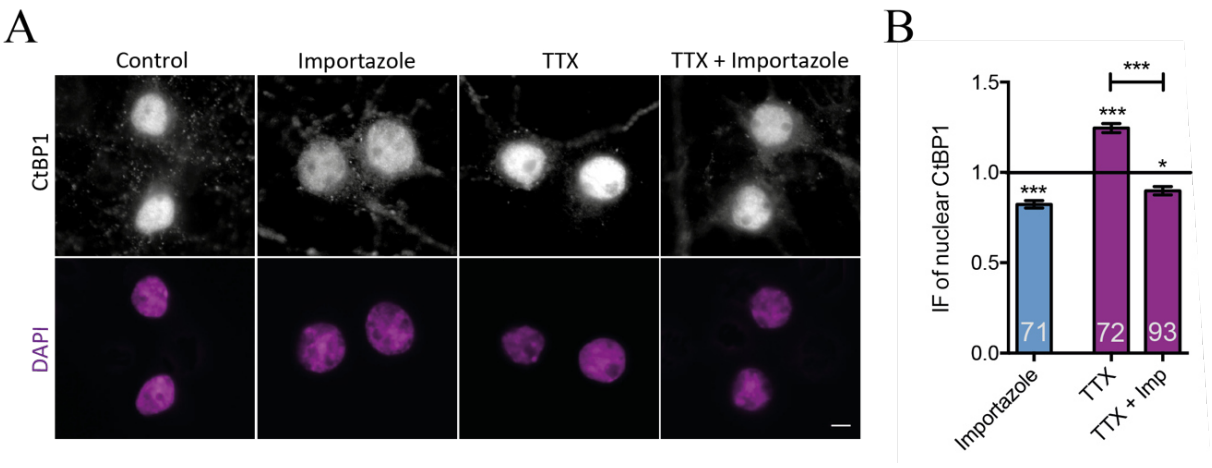

Fig. 3.25: Importin β plays a key role in the nuclear import mechanism of CtBP1 in mature cortical neurons. **A**: Representative images of cell bodies and nuclei stained with antibody towards CtBP1 and DAPI as a mask. Analysis is shown in **B**. Scale bar: 10 µm, applies for all panels. Importazole prevents importin β1 mediated nuclear import of proteins. For each bar n is indicated and stands for number of cells of at least three independent experiments (cultures were prepared from at least three different animals). Data are shown as mean ± SEM. Statistical analysis was done by one-way ANOVA with Bonferroni post hoc test, $p^* < 0.05$ and $p^{***} < 0.0001$.

Moreover, importin β was shown to play an essential role in the fast synapse-to-nucleus signaling of translocating molecules by mediating tight binding to the motorprotein dynein and subsequent nuclear import (Ambron *et al.*, 1992; Hanz *et al.*, 2003; Perry *et al.*, 2012; Thompson *et al.*, 2004; Xiao *et al.*, 2000; Yudin *et al.*, 2008). It is likely that the observed shift in the presynaptic, cytoplasmic and nuclear levels of CtBP1 in response to network silencing is based on a retrograde translocation of CtBP1 dependent on importin β and thus the microtubule machinery. To prove the hypothesis about a microtubule-dependent retrograde shuttling of CtBP1, I observed its behavior under the antimitotic agent nocodazole. The pharmacological reagent disrupts microtubules by binding to β-tubulin (Eilers *et al.*, 1989), thereby preventing a transport of molecules along microtubules. Indeed, after application of nocodazole (Noco, 20 µM) to DIV21 cortical cultures and analysis of anti-CtBP1 antibody immunofluorescence, nuclear CtBP1 levels were decreased back to control levels in comparison to TTX treated condition (Fig. 3.26 A, B: TTX: 129.6 ± 4.6 %; TTX + Noco: 102.2 ± 2.8 %, normalized to control cells). In addition, CtBP1 synaptic levels were decreased after TTX treatment (Fig. 3.26 C, D: 70.1 ± 3.9 %, normalized to control cells), but remained unchanged in comparison to control cells by additional application of nocodazole (Fig. 3.26 C, D: 98.44 ± 6.0 %, normalized to control cells).

The interference with microtubules may have pleiotropic effects on cells. Therefore, I estimated the contribution of importin β to the axon-to-soma retrograde translocation of CtBP1 using an importin β1 (KPNB1) subcellular KO mouse model. KPNB1 Δ3´UTR subcellular KO mice were received from Prof. Dr. Mike Fainzilber from Weizmann Institute of Science in Rehovot, Israel. They lack importin β1 mRNA and protein in axons, whereas its nuclear function is not affected (Perry *et al.*, 2012). Quantitative immunofluorescence analysis of DIV16 primary hippocampal cultures from KPNB1 Δ3´UTR subcellular KO mice revealed decreased nuclear CtBP1 levels (Fig. 3.27 A, B: 86.5 ± 2.1 %, normalized to wild-type cells) and increased presynaptic concentrations of CtBP1 (Fig. 3.27 C, D: 126.8 ± 5.3 %, normalized to wild-type cells). That implies a shift in the synapto-nuclear distribution of CtBP1 in KPNB1 Δ3´UTR subcellular KO mice.

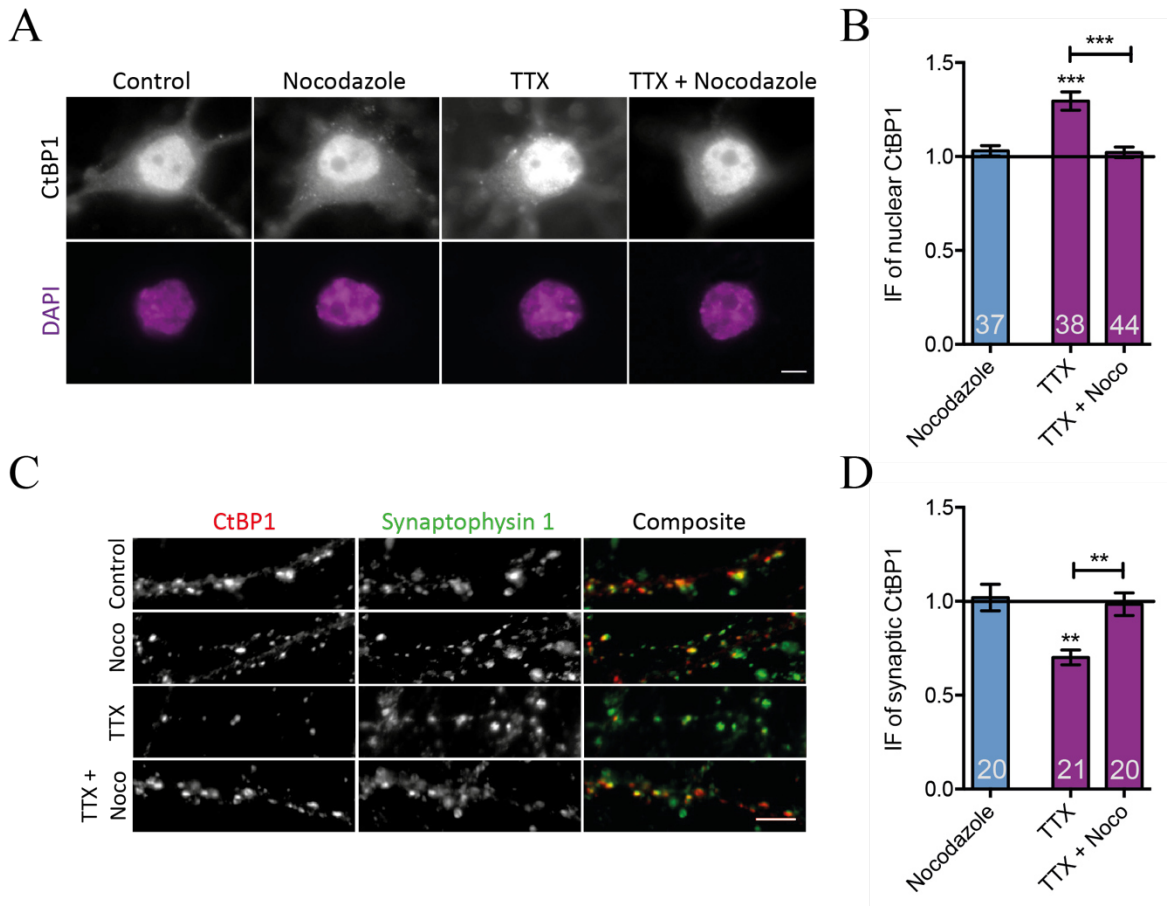

Fig. 3.26: Microtubule transport machinery is required for the activity-induced synapse-to-nucleus translocation of CtBP1. **A**: Representative images of cell bodies and nuclei stained with an anti-CtBP1 antibody and DAPI as a mask. Scale bar: 10 µm, applies for all panels. The analysis is shown in **B**. Analyzed groups of DIV21 primary cortical cultures were treated with either TTX to silence cultures, nocodazole to inhibit microtubule association, or both. **C**: Images showing presynaptic distribution of CtBP1, synaptophysin 1 was used as a presynaptic marker. Analysis is shown in **D**. For each graph n is indicated and stands for number of cells (at least 20 synapses per cell were analyzed) of at least three independent experiments (cultures were prepared from at least three different animals). Data are shown as mean ± SEM. Statistical analysis was done by one-way ANOVA with Bonferroni post hoc test, $p^{**} < 0.01$ and $p^{***} < 0.0001$.

The application of the glutamate receptor antagonists APV (50 µM) and CNQX (10 µM) for 48 hours chronically silenced the neuronal cultures and induced CtBP1 nuclear accumulation (Ivanova *et al.*, 2015) which was prevented in mice lacking axonal importin β1 (Fig. 3.27 E, F: WT APV+CNQX: 121.5 ± 5.2 %; KO Control: 84.7 ± 2.3%; KO APV + CNQX: 86.7 ± 2.9 %, normalized to wild-type control cells).

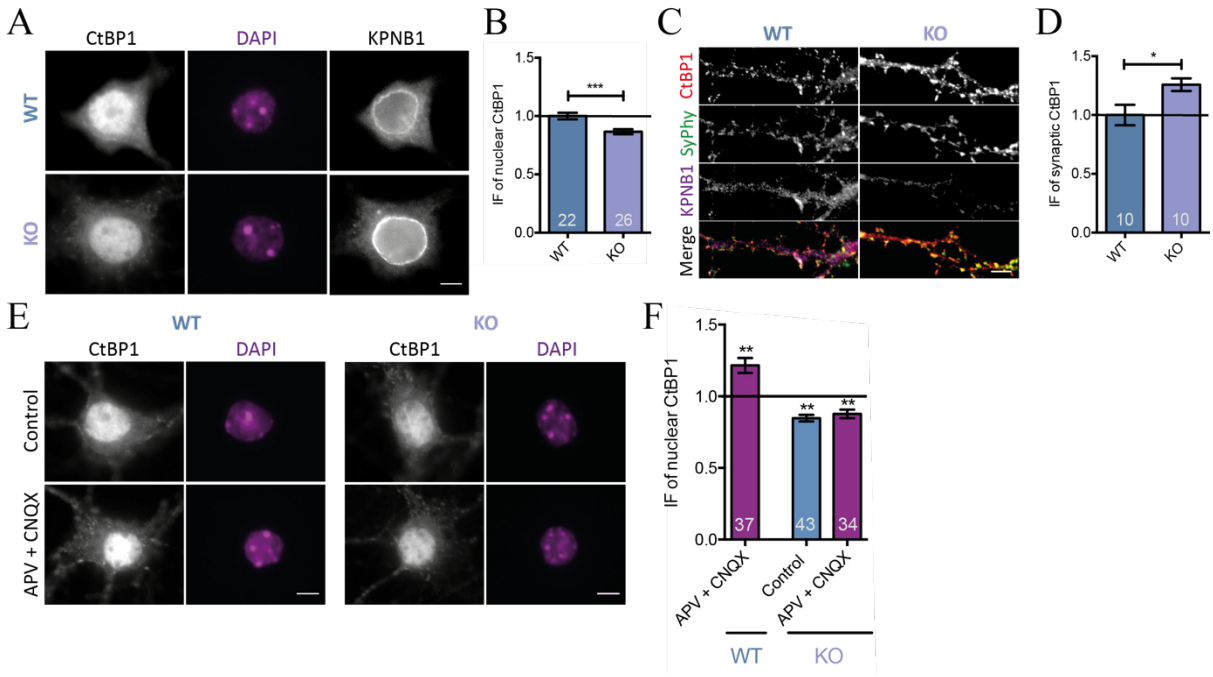

Fig. 3.27: Shift of CtBP1 distribution towards presynapses in primary dissociated hippocampal cultures from KPNB1 Δ3´UTR subcellular KO mice. Representative images of cell bodies/ nuclei (**A**) and synapses (**C**) of wild-type (WT) and subcellular knock-out (KO) of DIV21 cultures stained with antibodies towards CtBP1 and importin β1 (KPNB1) as well as the nuclear marker DAPI. Scale bar: 10 µm, applies for all panels. **B, D:** Analysis of immunofluorescence intensities of CtBP1 in both nuclei (**B**) and synapses (**D**). **E, F**: Comparison of activity-dependent (APV + CNQX for 48 hours) CtBP1 nuclear abundance in WT and KO neurons. For each graph n is indicated and stands for number of cells (at least 20 synapses per cell analyzed) of at least three independent experiments (cultures were prepared from at least three different animals). Data are shown as mean ± SEM. Statistical analyses were done by unpaired t-test (B, D) or one-way ANOVA with Bonferroni post hoc test (F), p* < 0.05, p** < 0.01 and p*** < 0.0001.

Due to the shift of CtBP1 levels towards the presynapses in KPNB1 Δ3´UTR subcellular KO mice, I investigated presynaptic adaptations in these mice by performing synaptotagmin 1 antibody live-uptake as a readout for synaptic activity (Kraszewski *et al.,* 1995; Lazarevic *et al.*, 2011; Piccoli *et al.*, 2011). Mature hippocampal cultures were incubated for 30 minutes with a fluorescently labeled antibody towards the lumenal domain of the synaptic vesicle protein synaptotagmin 1 (Fig. 3.28 A).

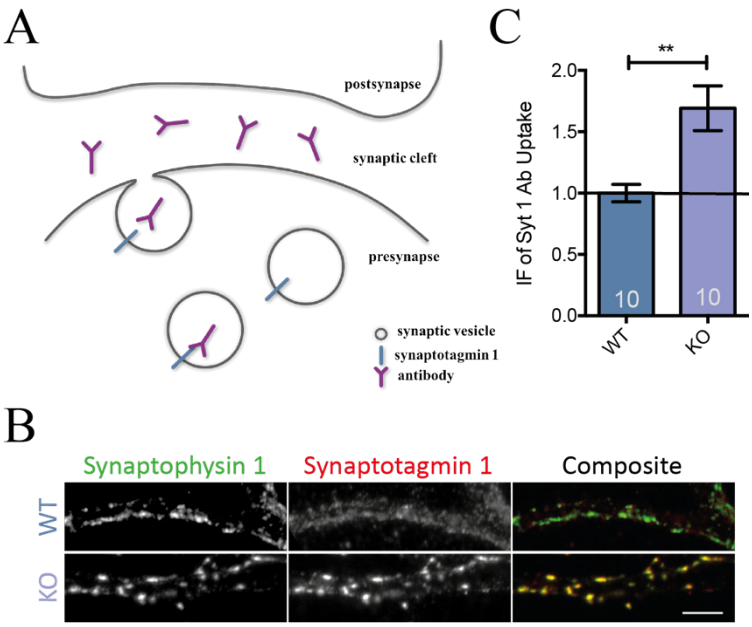

Fig. 3.28: Increased synaptic activity in KPNB1 Δ3´UTR subcellular KO mouse model. **A**: Scheme of the synaptotagmin 1 antibody live-uptake (Syt 1 Ab Uptake). **B**: Representative images of synapses of wild-type (WT) and knock-out (KO) cultures at DIV21 stained with synaptophysin 1. Scale bar: 10 µm, applies for all panels. **C**: Analysis of immunofluorescence intensities of synaptotagmin 1 as readout for synaptic activity. For each bar n is indicated and stands for number of cells with approximately 20 synapses of at least three independent experiments (cultures were prepared from at least three different animals). Data are shown as mean ± SEM. Statistical analysis was done by unpaired t-test, p** < 0.01.

The detected immunofluorescence intensities of the synaptotagmin 1 antibody represented the amount internalized during synaptic vesicle recycling. KPNB1 Δ3´UTR subcellular KO mice showed an increased synaptotagmin 1 antibody live-uptake in comparison to wild-type mice (Fig. 3.28 B, C: 169.2 ± 18.2 %, normalized to wild-type cells) implying increased synaptic activity in the subcellular KO mice which might explain the observed shift in CtBP1 protein concentration from the nucleus to presynapses in these cultures.

In summary, the results propose a mechanism for the nuclear import and retrograde translocation of CtBP1 dependent on microtubules and importin β1.

4. Discussion

The central nervous system contains millions of specialized cells generating a network for communication on the basis of electrochemical signaling. Thus, cells transmit the received information from synapses to the nucleus resulting in adaptations of gene expression pattern important for survival, development and plasticity. Synapse-to-nucleus communication can be mediated by Ca^{2+} signaling or by soluble molecules shuttling between distal subcellular compartments and the nucleus. The transport of signaling messengers through the nuclear pore represents an essential control point in the activity-dependent regulation of gene expression.
This study addressed signaling pathways and molecular mechanisms controlling the activity-induced nuclear import and export of the transcriptional co-repressor CtBP1 via modulation of neuronal network activity. The present work reveals Ca^{2+} signaling, GluN2B-containing NMDA receptor modulation and karyopherins as important for the regulation of the CtBP1 nuclear pool size, crucial for its co-repressor activity and neuronal function. Thus, the study provides a link between synaptic activity and regulation of gene expression representing an important step towards the understanding of the role of CtBP1 in the integration of synaptic signals into transcriptional regulation in neurons.

4.1. CtBP1 activity-regulated nuclear abundance is crucial for neuronal function

A number of studies has shown the importance of the integration of synaptic signals in the nucleus for neuronal development, plasticity and survival (Brunet *et al.*, 2005; Cohen and Greenberg, 2008; Rishal and Fainzilber, 2010). This includes shuttling of transcription factors between distal subcellular compartments and the nucleus. Initially, we observed a redistribution of CtBP1 between its nuclear and presynaptic location within two hours after disinhibition (4AP and bicuculline) and 24 hours after silencing (APV and CNQX) of mature cortical rat cultures. This was not affected by pharmacological inhibition of proteasomal degradation or *de-novo* protein synthesis (Ivanova *et al.,* 2015) suggesting interconnected CtBP1 pools, where the protein can shuttle between presynapses and the nucleus in response to altered neuronal network activity. The transport of signaling messengers, such as CtBP1, through the nuclear pore might represent a crucial step in the activity-dependent gene regulation as already shown for other transcription factors (Dieterich *et al.*, 2008; Gorlich and Kutay, 1999; Jordan and Kreutz, 2009; McBride *et al.*, 2002; Shen *et al.*, 2007; Strambio-De-Castillia *et al.*, 2010). To study CtBP1 nucleo-cytoplasmic translocation, new stimulation and silencing protocols were established.

Modulation of neuronal activity with either NMDA or TTX led to a shift in the CtBP1 nuclear as well as cytoplasmic and synaptic abundance within one hour in excitatory neurons. This time range is comparable with other shuttling transcriptional factors such as AIDA-1 (Jordan *et al.,* 2007) and suggests an activity-regulated nuclear redistribution of CtBP1 dependent on microtubules, actin filaments, or diffusion (Franker and Hoogenraad, 2013).

The nuclear role of CtBP1 is well-characterized (Chinnadurai, 2007; Ivanova *et al.*, 2015) allowing me to investigate the consequences of changes in neuronal activity on CtBP1 co-repressor functions. To that end, I used constitutive CtBP1 KO mice as a model (Hildebrand and Soriano, 2002). Previous studies described CtBP1 mutant mice as viable, fertile, smaller, and with deficits in development due to the deregulation of the transcriptional machinery (Hildebrand and Soriano, 2002). Experiments on CtBP1 KO mice revealed decreased protein levels of the CtBP1 paralog CtBP2, which had been shown to have similar functions and sequence homology (Hubler *et al.*, 2012). This suggests CtBP1 nuclear functions cannot be fully compensated by CtBP2. Both proteins function as transcriptional repressors, and they were shown to act as dimers in the nucleus (Kuppuswamy *et al.*, 2008; Nardini *et al.*, 2003). Thus, one possible explanation is that CtBP2 requires CtBP1 for its stabilization, which presumably protecting CtBP2 against protein degradation. To link CtBP1 activity-dependent nuclear abundance with its co-repressor function, I used the Arc and BDNF promoter reporter assays in primary neuronal cultures from CtBP1 KO mice as these promoters were shown to be regulated by this co-repressor (Ivanova *et al.,* 2015). In cultures lacking CtBP1, the induction of *GFP* reporter expression under activity-inducible Arc promoter and BDNF promoters I and II as seen in the WT neurons was abrogated. This demonstrates a CtBP1-mediated gene regulation of *Arc* and *BDNF* dependent on the activity state of neurons. However, the increased GFP immunofluorescence signal controlled by the Arc promoter in NMDA-treated KO cultures is lower than in stimulated WT neurons suggesting that further activity-dependent signaling pathways are involved in the regulation of *Arc* and presumably also *BDNF* expression (Cohen and Greenberg, 2008). Moreover, these changes in the promoter activity were achieved within one hour implying fast adaptations of CtBP1 co-repressor functions due to regulation of its nuclear abundance by modulation of neuronal activity. This could imply a regulated activity-dependent nuclear import and export of CtBP1.

4.2. Mechanisms facilitating the nuclear export of CtBP1 in neurons

The mechanisms underlying the observed redistribution of CtBP1 between the nucleus, the cytoplasm and presynapses represent crucial steps in the regulation of the co-repressor function of CtBP1. So far, only the anterograde transport of CtBP1 from the cytoplasm to presynapses was studied and revealed Piccolo-Bassoon transport vesicles (PTVs) as mediator for the movement of CtBP1 towards axon terminals (Ivanova *et al.*, 2016; Maas *et al.*, 2012). My work shows that nuclear depletion of CtBP1 can be triggered by stimulation of excitatory neurons with the NMDA receptor agonist NMDA without affecting the cell viability. To identify the mechanisms facilitating the nuclear depletion of CtBP1 in neurons, I have assessed the contribution of NMDA receptors, Ca^{2+} flux from different cell entry routes, exportin 1 and posttranslational modifications to the nuclear export of CtBP1.

4.2.1. NMDA receptor signaling and global Ca^{2+} routes regulate the nuclear abundance of CtBP1

Neuronal cells adjust their functions in response to surrounding stimuli through numerous intracellular signal transduction mechanisms. Synaptic activity-induced Ca^{2+} influx plays a crucial role in this process (Greer and Greenberg, 2008; Hagenston and Bading, 2011) by triggering transcription-regulating signaling pathways in the cytoplasm and in the nucleus (Hardingham *et al.*, 1997; Kaur *et al.*, 2014; Schlumm *et al.*, 2013; Xiang *et al.*, 2007).

The Ca^{2+}-dependent signaling cascade induced by NMDA receptor activation highly depends on the NMDA receptor composition. In brain areas with higher function, most of the NMDA receptors comprise GluN2A and GluN2B subunits (Sheng *et al.,* 1994). The exact distribution of these NMDA receptor subtypes is still under discussion. However, GluN2A is found at the postsynaptic membrane of neurons (Gladding and Raymond, 2011) and its subunit contribution arises during synapse maturation and cortical circuit refinement (Monyer *et al.*, 1994; Sakimura *et al.*, 1995; Sheng *et al.*, 1994). GluN2B subunits are highly expressed in young neurons and are found in post-, peri-, and extrasynaptic areas in mature neuronal cells. Extrasynaptic GluN2B-containing NMDA receptors were shown to contribute to the induction of CREB shut off and cell death pathways (Hardingham and Bading, 2010). Additionally, GluN2B-containing NMDA receptors are also found at presynapses where they seem to be important for synaptic transmission and plasticity (Corlew *et al.,* 2008). Pharmacological inhibition of GluN2B subunits in mature dissociated cultures abolished the NMDA-induced depletion of nuclear CtBP1 levels. In contrast, specific GluN2A inhibitors did not affect the activity-dependent

nuclear abundance of CtBP1. This suggests that GluN2B-containing NMDA receptor signaling is critical for activity-induced shuttling of CtBP1. These experiments did not allow discrimination between pre-, post, peri-, and extrasynaptic NMDA receptors. It might be interesting to study the contribution of presynaptic NMDA receptors to the CtBP1 co-repressor function, e.g. by using microfluidic chambers. They allow the separate stimulation of axons and thus only presynaptic NMDA receptors. Gene expression studies of CtBP1 activity-regulated genes (Ivanova *et al.,* 2015) in mice lacking GluN2B subunits might help to further investigate which NMDA receptor composition is required for the CtBP1 signaling. Additionally, it might be interesting to evaluate functional consequences of GluN2B subunit inhibition in CtBP1 KO mice by using the described promoter reporter assays.

Moreover, Ca^{2+} signaling can be mediated via VGCCs (Catterall, 2011), another potential regulator of CtBP1 Ca^{2+}-dependent shuttling. Ca^{2+} influx through VGCCs serves as a major messenger initiating posttranslational modifications of proteins and gene transcription (Catterall, 2011). Postsynaptic L-type VGCCs are important for the signaling of shuttling transcription factors such as CREB and CRTC1 (Ch'ng *et al.,* 2012; Deisseroth *et al.,* 1996), and they are shown to be important for the regulation of many activity-regulated genes (Xiang *et al.,* 2007). But not all Ca^{2+}-regulated transcription processes depend on L-type VGCCs as shown for AIDA-1 activity-dependent synapse-to-nucleus translocation and regulation of gene expression (Jordan *et al.,* 2007). Moreover, selective influx of Ca^{2+} through presynaptic P/Q-type VGCCs is shown to activate the expression of syntaxin-1A, a presynaptic protein involved in neurotransmitter release (Sutton *et al.,* 1999). Another group of VGCCs, which is present in neurons, are the N-type VGCCs. Besides their localization at presynapses and function in neurotransmitter release (Dolphin, 2012), they were shown to facilitate Ca^{2+} waves in the cytoplasm and in dendrites in response to action potential firing (Catterall, 2011; Dolphin, 2012; Mills *et al.*, 1994; Scholz and Miller, 1995). Inhibition of L-, P/Q-, and N-type VGCCs and subsequent NMDA stimulation of mature cortical cultures revealed only N-type VDCCs as crucial for the activity-induced nuclear depletion of CtBP1. Additional experiments in mature cortical cultures overexpressing Arc and BDNF promoters fused to a GFP reporter showed a correlation between N-type VGCC-dependent nuclear abundance of CtBP1 and the expression of the reporter. This suggests that CtBP1 induces changes in gene expression, which require a Ca^{2+} wave towards the nucleus, maybe even caused by back-propagating action potentials achieved via activation of N-type VGCCs and subsequent Ca^{2+} influx into the cytoplasm (Kuczewski *et al.,* 2008; Staley, 2004). However, my results do not indicate L-type VGCC

contribution to the regulation of Arc promoter and BDNF promoter I + II in the assays. This stands in contrast with studies that revealed *Arc* and *BDNF* expression regulated by this type of postsynaptic VGCCs (Cohen and Greenberg, 2008). However, it is shown that *BDNF* is controlled by a total of nine promoters. Promoter IV is also modulated in an activity-dependent manner by different Ca^{2+}-sensitive transcriptional regulators and was not considered in the present work (Tao *et al.*, 2002; Zhou *et al.*, 2006). In addition, the Arc promoter used in the present study was shortened and possibly some regulatory sequences which are controlled by other transcription factors might be missing (Kawashima *et al.*, 2009). Moreover, Ca^{2+} waves towards the nucleus facilitated by N-type VGCCs might play an important role in the Ca^{2+}-dependent regulation of *Arc* and *BDNF* expression. This has not been considered so far.

In addition, NMDA receptor and VGCC activation elevates intracellular Ca^{2+} levels. My experiments revealed that the activity-induced nuclear export of CtBP1 is abolished in the presence of BAPTA-AM, a cell-permeable calcium chelator. This implies that changes in intracellular Ca^{2+} concentrations are important for the activity-induced nuclear depletion of CtBP1 as shown for the shuttling of other transcription factors such as CRTC1 and HDACs (Ch'ng *et al.*, 2012; Chawla *et al.*, 2003). The elevation in intracellular Ca^{2+} can subsequently trigger Ca^{2+} release from internal stores like the endoplasmic reticulum through IP_3-receptors. They can be activated by the Ca^{2+}-dependent second messenger IP_3 and are involved in the regulation of activity-dependent gene transcription (Jaimovich and Carrasco, 2002). In my experiments, the pharmacological inhibition of IP_3-receptors at the endoplasmic reticulum revealed Ca^{2+} release through these receptors as important for the induction of CtBP1 nuclear export. The elevation of intracellular Ca^{2+} leads to an increase of the nuclear Ca^{2+} levels shown to be essential for the regulation of other transcription regulators such as HDAC4 and 5 (Hardingham *et al.*, 1997; Schlumm *et al.*, 2013). To fill this last gap in the Ca^{2+}-mediated nuclear export of CtBP1, the contribution of nuclear Ca^{2+} has to be examined by generating a calcium chelator fused to an NLS (NLS-CaMBP4 for instance).

Taken together, pharmacological modulation of mature dissociated rat cortical cultures and promoter assays revealed that CtBP1 nuclear export and thus its co-repressor function depends on GluN2B-containing NMDA receptor signaling and Ca^{2+} influx through N-type VGCCs. Consequently, the elevation in intracellular Ca^{2+} triggers Ca^{2+} release from IP_3-receptors, which might be involved in the depletion of nuclear CtBP1 levels mediated by Ca^{2+}-sensitive karyopherins (Kaur *et al.*, 2014).

4.2.2. Exportin 1 mediates the activity-induced nuclear export of CtBP1

After revealing Ca^{2+}-regulated nuclear abundance of CtBP1, I assessed the molecular basis of the CtBP1 nuclear export. There is evidence that nuclear export mediated by exportins is dependent on Ca^{2+} (Kaur *et al.*, 2014), and correspondingly, CtBP1 carries a putative NES in its protein sequence (Henderson and Eleftheriou, 2000; Verger *et al.*, 2006). This classical NES has been shown to interact with exportin 1 for many other proteins (Bogerd *et al.,* 1996; Henderson and Eleftheriou, 2000; Verger *et al.,* 2006).

Previously, exportin 1 was thought not to be involved in CtBP1 nuclear export due to work done in non-neuronal cells. There, LMB - a potent inhibitor of the interaction between exportin 1 and the NES sequence of CtBP1 - did not influence the nuclear CtBP1 levels (Verger *et al.,* 2006). In the present work, stimulation of neurons with NMDA and application of LMB completely abolished the decrease of the nuclear CtBP1 levels confirming its activity-induced nuclear export via exportin 1. Interestingly, time-lapse experiments with LMB revealed that nuclear accumulation of CtBP1 required a 24-hour treatment with the compound. Different effects were observed when blocking the nuclear accumulation of CtBP1 with the importin β inhibitor importazole. This treatment led to decreased nuclear CtBP1 levels within one hour under basal activity suggesting a continuous nuclear export of CtBP1 and a slow nuclear import independent of neuronal activity. Inhibition of protein synthesis and degradation did not alter the activity-induced shuttling of CtBP1. Thus, I can exclude proteasomal degradation or new protein synthesis of CtBP1 as explanation for the observed effects. More likely, the nuclear export of CtBP1 by exportin 1 is facilitated upon increase of neuronal activity, which might occur via diffusion in inactive neurons. The size for proteins diffusing through the nuclear pore is up to approximately 60 kDa in general, but even 90 kDa proteins were shown to enter the nucleus in this way (Ghavami *et al.,* 2016; Wang and Brattain, 2007). CtBP1 is 50 kDa in size, and its diffusion through nuclear pores might be a less energy-demanding alternative to keep a constant equilibrium between its nuclear, cytoplasmic, and presynaptic pools under basal activity. Thus, the active nuclear export of CtBP1 mediated by exportin 1 might only be used in cases of increased network activity where fast adaptations in gene expression are required. To confirm the data obtained in this experiment, I generated CtBP1intEGFP_NESmut where the two critical leucine residues within the NES signal peptide were mutated to alanine (Wen *et al.*, 1995). Indeed, the previously observed NMDA-induced nuclear export of CtBP1 was abolished in CtBP1intEGFP_NESmut. This result was confirmed in live-imaging experiments. Here, I studied CtBP1 nuclear export over time by imaging single cells overexpressing either

CtBP1intEGFP (representing wild-type CtBP1) or CtBP1intEGFP_NESmut. 40 minutes after NMDA receptor stimulation, I recorded a significant drop in the nuclear immunofluorescence of CtBP1intEGFP. This decrease of the nuclear CtBP1 immunofluorescence was most likely not due to protein degradation since the same effect was observed after inhibition of the proteasome activity in experiments using immunocytochemistry of fixed cultured neurons. This activity-induced nuclear export was abolished in the NES mutant. Additionally, western blot analyses of nuclear fractions from dissociated cortical cultures revealed CtBP1 in a complex with exportin 1. Thus, NMDA receptor-induced nuclear export of CtBP1 requires exportin 1 to pass the nuclear pore resulting in its decreased nuclear levels and increased cytoplasmic abundance.

These results indicate that the nuclear export of CtBP1 in neurons is controlled by Ca^{2+} signaling and mediated by exportin 1. In addition, posttranslational modifications might be important to enable CtBP1 nuclear export by causing conformational changes of the transcriptional co-repressor and exposure of its NES as shown for the shuttling transcription factor NF-AT4 (Hogan and Rao, 1999; Zhu and McKeon, 1999).

4.2.3. Posttranslational modifications of CtBP1

The nuclear levels of CtBP1 can be regulated by posttranslational modifications. SUMOylation by homeodomain interacting protein kinase 2 (HIPK2) retains CtBP1 in the nucleus and enhances its repressor function. Phosphorylation by PKA and Pak1 triggers its nuclear export and consequently gene expression (Barnes *et al.*, 2003; Dammer and Sewer, 2008). The present study strongly suggests that the nuclear export of CtBP1 is dependent on Ca^{2+} signaling. Thus, I addressed the contribution of the in neurons well-characterized Ca^{2+}-sensitive kinases CaMKII and MAPKK (phosphorylates MAPK) to the CtBP1 nuclear export as they are known to influence gene expression (Bayer *et al.,* 2001; Lee *et al.,* 2005; Papadia *et al.,* 2005; Strack *et al.,* 2000). However, inhibition of these signaling pathways did not alter the activity-induced decrease of the nuclear CtBP1 levels. Instead, CtBP1 nuclear export was abolished by inhibition of PKA and Pak1, while PKA activation even increased the nuclear export of CtBP1. To prevent CtBP1 phosphorylation by PKA and Pak1 phospho-mutants were generated. The expression of the mutant constructs did not show the expected accumulation of the overexpressed proteins in the nucleus under basal activity similar to the observations of Liberali *et al.* (2008). Diffusion of CtBP1 from the nucleus to the cytoplasm to keep the equilibrium between the three CtBP1 pools under basal activity might explain the observed results (see 4.2.2). NMDA receptor

stimulation of mature cortical cultures infected with the mutants revealed CtBP1 nuclear export to be dependent on the phosphorylation by both kinases. This suggests that the enzymatic activity of both proteins is required to mediate the nuclear export of CtBP1, possibly due to subsequent conformational changes of the co-repressor that might expose its NES.

Several studies suggest that both PKA and Pak1 can phosphorylate CtBP1 in the nucleus (Barnes *et al.,* 2003; Dammer and Sewer, 2008). Detection of phosphorylated endogenous CtBP1 in the nuclear fraction of cortical neurons might be one of the key experiments to confirm this hypothesis. Unfortunately, there are no specific phospho-antibodies against the two phosphorylation sites (T133 and S147) available, and generation of phospho-specific antisera in our lab was unsuccessful to-date. Alternatively, pull-down assays of CtBP1 from nuclear fractions might help to show PKA and Pak1 interacting with the co-repressor in the nucleus.

Taken together, the activity-dependent nuclear export of CtBP1 is driven by Ca^{2+} signaling and posttranslational modifications and facilitated by exportin 1. As CtBP1 is shown to shuttle bidirectionally between the nucleus as well as the cytoplasm and presynapses, the mechanism behind the nuclear import of CtBP1 is discussed in the following chapter.

4.3. Nuclear import of CtBP1 in neurons

Nuclear import of proteins can be mediated via diffusion or is regulated by importins. The importin-family members recognize the NLS of proteins and subsequent mediate their transport through the nuclear pore. The classical nuclear import pathway requires importin α to bind NLS-containing cargos and importin β for tight cargo binding and the nuclear import (Pemberton and Paschal, 2005). Moreover, it was shown that direct interaction with importin β is sufficient for nuclear import of a number of cargos (Chook and Suel, 2011; Palmeri and Malim, 1999; Xiao *et al.*, 2000).

First experiments in neuronal cultures, where the importin β-mediated nuclear import pathway was blocked by importazole, revealed decreased CtBP1 levels in comparison to control. Additionally, nuclear CtBP1 levels were significantly decreased upon importazole treatment within one hour under basal activity. That was not observed in case of applying LMB giving some indication of the nuclear import of CtBP1 (see 4.2.2). The slow accumulation of CtBP1 in the nucleus after inhibition of its nuclear export correlates with the nuclear import rate of CtBP1, which seems to be very slow under basal activity. However, Rishal *et al.* (2012) brought up the idea of a frequency encoded synapse-to-nucleus signaling in axon-length sensing and growth. Computational simulations were used to model this hypothesis suggesting that

microtubule-based synapse-to-nucleus communication can be encoded by the frequency of an oscillating retrograde signal arising from a negative feedback loop with a time delay between the bidirectional motor protein-dependent signals (Kam *et al.,* 2009; Rishal *et al.,* 2012). Hence, CtBP1 nuclear import under basal activity is slow, but constant, and the silencing-induced nuclear accumulation of the protein is significantly enhanced to intensify the signal coming from synapses in turn enabling the adjustment of activity-dependent gene expression.

Two scenarios are conceivable to explain my observation that nuclear accumulation of CtBP1 depends on importin β. CtBP1 import may either depend on the importin α/β complex or on importin β alone. As shown for other proteins such as human GW proteins, also both pathways can facilitate nuclear accumulation (Schraivogel *et al.,* 2015). The contribution of importin α to the nuclear import of CtBP1 might be examined in future studies in importin α KO mice, for instance.

The nuclear import mediated by importin α/β or β classically occurs via interaction with the NLS of cargo proteins, which is not present in CtBP1. Interestingly, its homolog CtBP2 contains an NLS, and it is conceivable that they can enter the nucleus as a dimer (Verger *et al.,* 2006). Further, the formation of dimers of CtBP1 with other NLS-containing proteins of the transcription machinery, such as BKLF, is feasible, but it is still under investigation whether this interaction can already take place in the cytoplasm (Verger *et al.*, 2006). Another molecule, which might be involved in the facilitation of importin β-mediated nuclear import of CtBP1, is the huntingtin protein. It contains an NLS recognized by importin β (Desmond *et al.,* 2012), and both proteins interact via the PLDLS binding motif (Kegel *et al.,* 2002). Thus, huntingtin might function as an adapter molecule between CtBP1 and importin β mediating its nuclear import. Additionally, both CtBP1 and huntingtin are present at excitatory synapses where the latter regulates synaptic vesicle release and localizes along microtubules to attend the transport of several cargos (McKinstry *et al.*, 2014). These characteristics together with the described CtBP1 shuttling from presynapses to the nucleus in response to decreased neuronal activity in excitatory neurons allow speculations about importin β-mediated retrograde translocation of CtBP1.

The observed retrograde shuttling of CtBP1 in silenced neuronal cultures might depend on microtubules, actin filaments, or diffusion (Franker and Hoogenraad, 2013). A retrograde shuttling of CtBP1 based on diffusion might be inefficient due to information loss in case of randomly axonal translocation of the transcriptional co-repressor (Kholodenko *et al.,* 2000; Lim *et al.,* 2016). More likely, the retrograde shuttling of CtBP1 is controlled by either microtubules or actin filaments. If its retrograde shuttling depends on microtubules, it is likely that importins

are involved in both the retrograde translocation and nuclear accumulation of CtBP1. This contributes to the idea that CtBP1 might play a role in fast adaptations of gene expression in response to synaptic stimuli as shown for other postsynapse-to-nucleus translocating signaling messengers such as Jacob. There, importin α facilitates its retrograde transport and functions as an adapter molecule by binding both importin β and Jacob to mediate its nuclear import (Dieterich *et al.,* 2008). Hence, I examined the hypothesis of an importin β1-mediated retrograde translocation and nuclear import of CtBP1 in KPNB1 Δ3`UTR subcellular KO mice lacking axonal importin β1, the most prominent isoform in mammals (Perry *et al.,* 2012). Indeed, the retrograde shuttling of CtBP1 upon network silencing was abolished in KPNB1 Δ3`UTR subcellular KO neurons, leading to synaptic accumulation of the protein and decreased its nuclear levels. This points to an importin β1-facilitated retrograde translocation and nuclear import of CtBP1 dependent on neuronal network activity. Additionally, I observed an increased synaptic activity due to an elevated vesicle recycling in hippocampal cultures from the KPNB1 Δ3`UTR subcellular KO mice compared to WT. The observed shift in nuclear versus synaptic distribution of CtBP1 might be due to either missing axonal importin β1 or increased basal activity in these KO cultures inducing the CtBP1 translocation from the nucleus to presynapses. The hypothesis about a retrograde translocation of CtBP1 based on microtubules was confirmed by nocodazole treatment of neuronal cultures, where interference with the dynamics of microtubules impaired CtBP1 presynapse-to-nucleus shuttling. This suggests that the microtubule transport machinery is involved in CtBP1 retrograde shuttling as shown for ATFs and the postsynapse-to-nucleus shuttling transcription factor Abi-1 (Baleriola et al., 2014; Proepper et al., 2007).

Although importin β1 seems to be important for an efficient retrograde translocation by tight cargo binding (Hanz *et al.,* 2003; Perry *et al.,* 2012; Soderholm *et al.,* 2011) and the nuclear import of CtBP1, there is presumably no direct interaction between the two proteins. Moreover, it is unclear whether the nuclear CtBP1 imported after TTX treatment derives from presynaptic or cytoplasmic pools. I suggest that activity-induced imported CtBP1 initially comes from the cytoplasm to allow fast adaptations in gene expression and after that it might arrive from presynapses to either influence gene expression by nuclear import or to refill its cytoplasmic pool. Whether the observed changes in presynaptic, cytoplasmic and nuclear CtBP1 levels are based on activity-dependent retrograde transport mechanisms via the microtubule transport machinery has to be addressed in future studies. Dynein-mutants can be used to interrupt the retrograde transport based on the microtubule transport machinery. Further, microfluidic chambers would allow observing axonal movement of GFP-tagged CtBP1.

4.4. Conclusion

The present study identifies new molecular mechanisms for the control of CtBP1 nuclear abundance in neurons. The regulation of the nuclear import and export of CtBP1 revealed to be crucial for its function as transcriptional co-repressor in excitatory neurons.

CtBP1 nuclear abundance is modulated by network activity, whereas alterations cause a shift in the equilibrium between its interconnected presynaptic, cytoplasmic and nuclear pools (Fig. 4.1).

The nuclear export and cytoplasmic accumulation of CtBP1 is facilitated by GluN2B-containing NMDA receptor signaling, Ca^{2+} influx through N-type VGCCs and IP_3-receptors resulting in CtBP1 phosphorylation by PKA and Pak1 which might mediate its Ca^{2+}-dependent nuclear export via exportin 1.

The activity-dependent nuclear import of CtBP1 is initiated by network silencing and facilitated by importin β1. The imported CtBP1 molecules are coming either from axon terminals, the cytoplasm, or a mixture of both which might depend on the input signals and time frame. The retrograde transport of CtBP1 might be mediated by importin β1 and microtubules. However, the exact mechanism of CtBP1 retrograde shuttling between presynapses and the cytoplasm (Fig. 4.1 indicated in blue) remains a challenging question for future studies.

This work suggests CtBP1 as a molecule linking synaptic activity to the regulation of gene expression, which is shown to be important for neuronal plasticity and brain function. Thus, it is of general interest to study CtBP1 in the context of neurological diseases such as epilepsy. It is shown that CtBP1 synapse-to-nucleus translocation is dependent on the activity state of the neuron and, thus, its metabolic status, represented by the NAD/NADH ratio. Changes in the NAD/NADH ratio can be sensed by CtBP1 and trigger its redistribution (Ivanova *et al.,* 2015). Typical for epilepsy is a higher excitability which leads to elevated cellular NADH level and increased expression of genes. One protein shown to be involved in epileptic seizures is BDNF. Its expression can be facilitated among others by CtBP1 nuclear depletion (Garriga-Canut *et al.,* 2006).

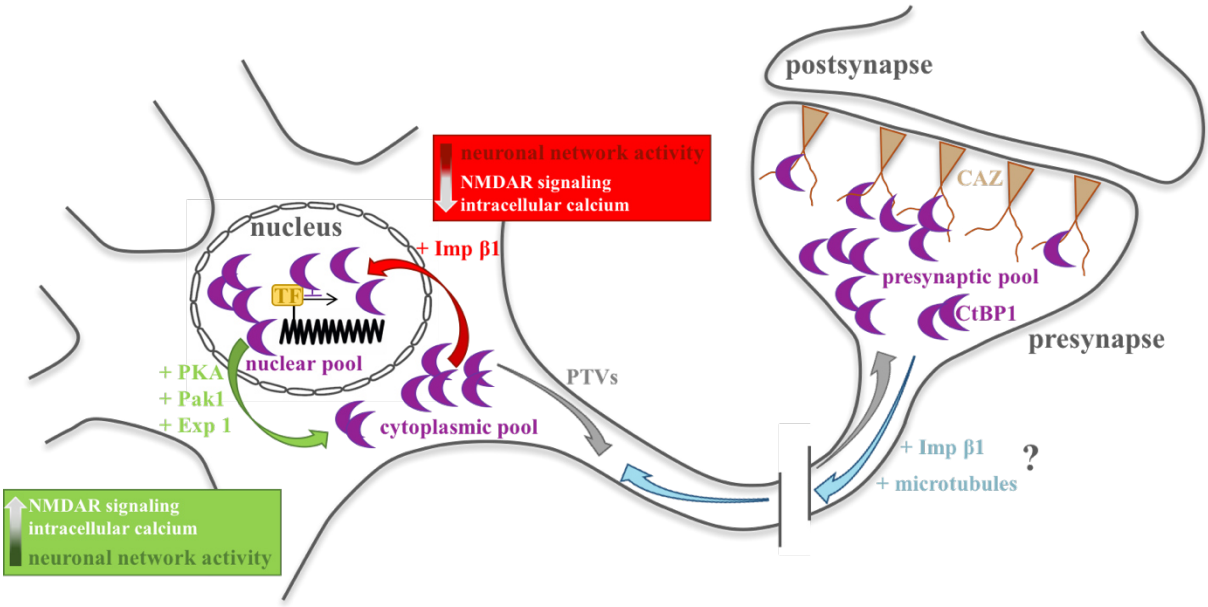

Fig. 4.1: Model for the activity-induced nuclear import and export of CtBP1 in neurons. Under basal activity, CtBP1 is present in the nucleus interacting with transcription factors (TF), at the cytoplasm, and at presynapses either bound to Bassoon and Piccolo (belonging to the cytomatrix at the active zone (CAZ)) or as soluble molecule. Increased neuronal network activity, NMDA receptor (NMDAR) signaling and an elevation in intracellular Ca^{2+} levels (green) lead to phosphorylation of CtBP1 (purple) by PKA and Pak1 and subsequent nuclear export via exportin 1 (Exp 1). In contrast, decreased neuronal activity (red) promotes CtBP1 nuclear import via importin β1 (Imp β1). The anterograde transport (grey) is supposed to take place via Piccolo-Bassoon transport vesicles (PTVs) and the retrograde shuttling of CtBP1 between presynapses and the cytoplasm/nucleus (blue) might be facilitated by microtubules and importin β1. However, the detailed mechanism of CtBP1 synapse-to-nucleus translocation remains a challenging question for future studies.

Many patients with drug-resistant temporal lobe epilepsy respond to the so-called ketogenic diet comprising few carbohydrates, high fat and adequate amounts of protein (Lauritzen *et al.,* 2015; Stafstrom, 2004). This reduces the cellular NADH level shown to balance CtBP1 co-repressor function and gene expression resulting in normal brain function (Ivanova *et al.,* 2016). It will be intriguing to elucidate the CtBP1 contribution to other forms of epilepsy and how its Ca^{2+}-dependent and karyopherin-regulated nuclear import and export triggers or diminishes seizures. Therefore, the control of CtBP1-mediated regulation of gene expression might represent a future target for therapeutic approaches in the treatment of neurological diseases.

5. Literature

Adams, J. P., and S. M. Dudek. 2005. 'Late-phase long-term potentiation: getting to the nucleus', *Nat Rev Neurosci*, 6: 737-43.

Ambron, R. T., R. Schmied, C. C. Huang, and M. Smedman. 1992. 'A signal sequence mediates the retrograde transport of proteins from the axon periphery to the cell body and then into the nucleus', *J Neurosci*, 12: 2813-8.

Baleriola, J., C. A. Walker, Y. Y. Jean, J. F. Crary, C. M. Troy, P. L. Nagy, and U. Hengst. 2014. 'Axonally synthesized ATF4 transmits a neurodegenerative signal across brain regions', *Cell*, 158: 1159-72.

Barnes, C. J., R. K. Vadlamudi, S. K. Mishra, R. H. Jacobson, F. Li, and R. Kumar. 2003. 'Functional inactivation of a transcriptional corepressor by a signaling kinase', *Nat Struct Biol*, 10: 622-8.

Bayer, K. U., P. De Koninck, A. S. Leonard, J. W. Hell, and H. Schulman. 2001. 'Interaction with the NMDA receptor locks CaMKII in an active conformation', *Nature*, 411: 801-5.

Ben-Yaakov, K., S. Y. Dagan, Y. Segal-Ruder, O. Shalem, D. Vuppalanchi, D. E. Willis, D. Yudin, I. Rishal, F. Rother, M. Bader, A. Blesch, Y. Pilpel, J. L. Twiss, and M. Fainzilber. 2012. 'Axonal transcription factors signal retrogradely in lesioned peripheral nerve', *EMBO J*, 31: 1350-63.

Bengtson, C. P., and H. Bading. 2012. 'Nuclear calcium signaling', *Adv Exp Med Biol*, 970: 377-405.

Bengtson, C. P., H. E. Freitag, J. M. Weislogel, and H. Bading. 2010. 'Nuclear calcium sensors reveal that repetition of trains of synaptic stimuli boosts nuclear calcium signaling in CA1 pyramidal neurons', *Biophys J*, 99: 4066-77.

Berridge, M. J. 1998. 'Neuronal calcium signaling', *Neuron*, 21: 13-26.

Bhattacharya, S., and C. Schindler. 2003. 'Regulation of Stat3 nuclear export', *J Clin Invest*, 111: 553-9.

Birnboim, H. C., and J. Doly. 1979. 'A rapid alkaline extraction procedure for screening recombinant plasmid DNA', *Nucleic Acids Res*, 7: 1513-23.

Bogerd, H. P., R. A. Fridell, R. E. Benson, J. Hua, and B. R. Cullen. 1996. 'Protein sequence requirements for function of the human T-cell leukemia virus type 1 Rex nuclear export signal delineated by a novel in vivo randomization-selection assay', *Mol Cell Biol*, 16: 4207-14.

Bonazzi, M., S. Spano, G. Turacchio, C. Cericola, C. Valente, A. Colanzi, H. S. Kweon, V. W. Hsu, E. V. Polishchuck, R. S. Polishchuck, M. Sallese, T. Pulvirenti, D. Corda, and A. Luini. 2005. 'CtBP3/BARS drives membrane fission in dynamin-independent transport pathways', *Nat Cell Biol*, 7: 570-80.

Brasier, D. J., and D. E. Feldman. 2008. 'Synapse-specific expression of functional presynaptic NMDA receptors in rat somatosensory cortex', *J Neurosci*, 28: 2199-211.

Brennan, A. M., J. A. Connor, and C. W. Shuttleworth. 2006. 'NAD(P)H fluorescence transients after synaptic activity in brain slices: predominant role of mitochondrial function', *J Cereb Blood Flow Metab*, 26: 1389-406.

Briggs, L. J., D. Stein, J. Goltz, V. C. Corrigan, A. Efthymiadis, S. Hubner, and D. A. Jans. 1998. 'The cAMP-dependent protein kinase site (Ser312) enhances dorsal nuclear import through facilitating nuclear localization sequence/importin interaction', *J Biol Chem*, 273: 22745-52.

Brunet, I., C. Weinl, M. Piper, A. Trembleau, M. Volovitch, W. Harris, A. Prochiantz, and C. Holt. 2005. 'The transcription factor Engrailed-2 guides retinal axons', *Nature*, 438: 94-8.

Catterall, W. A. 2011. 'Voltage-gated calcium channels', *Cold Spring Harb Perspect Biol*, 3: a003947.

Ch'ng, T. H., B. Uzgil, P. Lin, N. K. Avliyakulov, T. J. O'Dell, and K. C. Martin. 2012. 'Activity-dependent transport of the transcriptional coactivator CRTC1 from synapse to nucleus', *Cell*, 150: 207-21.

Chawla, S., P. Vanhoutte, F. J. Arnold, C. L. Huang, and H. Bading. 2003. 'Neuronal activity-dependent nucleocytoplasmic shuttling of HDAC4 and HDAC5', *J Neurochem*, 85: 151-9.

Chinnadurai, G. 2007. 'Transcriptional regulation by C-terminal binding proteins', *Int J Biochem Cell Biol*, 39: 1593-607.

Chook, Y. M., and K. E. Suel. 2011. 'Nuclear import by karyopherin-betas: recognition and inhibition', *Biochim Biophys Acta*, 1813: 1593-606.

Cimato, T. R., M. J. Ettinger, X. Zhou, and J. M. Aletta. 1997. 'Nerve growth factor-specific regulation of protein methylation during neuronal differentiation of PC12 cells', *J Cell Biol*, 138: 1089-103.

Cohen, S., and M. E. Greenberg. 2008. 'Communication between the synapse and the nucleus in neuronal development, plasticity, and disease', *Annu Rev Cell Dev Biol*, 24: 183-209.

Corda, D., A. Colanzi, and A. Luini. 2006. 'The multiple activities of CtBP/BARS proteins: the Golgi view', *Trends Cell Biol*, 16: 167-73.

Corlew, R., D. J. Brasier, D. E. Feldman, and B. D. Philpot. 2008. 'Presynaptic NMDA receptors: newly appreciated roles in cortical synaptic function and plasticity', *Neuroscientist*, 14: 609-25.

Cosker, K. E., S. L. Courchesne, and R. A. Segal. 2008. 'Action in the axon: generation and transport of signaling endosomes', *Curr Opin Neurobiol*, 18: 270-5.

Cowger, J. J., Q. Zhao, M. Isovic, and J. Torchia. 2007. 'Biochemical characterization of the zinc-finger protein 217 transcriptional repressor complex: identification of a ZNF217 consensus recognition sequence', *Oncogene*, 26: 3378-86.

Cull-Candy, S. G., and D. N. Leszkiewicz. 2004. 'Role of distinct NMDA receptor subtypes at central synapses', *Sci STKE*, 2004: re16.

Dammer, E. B., and M. B. Sewer. 2008. 'Phosphorylation of CtBP1 by cAMP-dependent protein kinase modulates induction of CYP17 by stimulating partnering of CtBP1 and 2', *J Biol Chem*, 283: 6925-34.

Das, S., M. Grunert, L. Williams, and S. R. Vincent. 1997. 'NMDA and D1 receptors regulate the phosphorylation of CREB and the induction of c-fos in striatal neurons in primary culture', *Synapse*, 25: 227-33.

de Marchena, J., A. C. Roberts, P. G. Middlebrooks, V. Valakh, K. Yashiro, L. R. Wilfley, and B. D. Philpot. 2008. 'NMDA receptor antagonists reveal age-dependent differences in the properties of visual cortical plasticity', *J Neurophysiol*, 100: 1936-48.

Deisseroth, K., H. Bito, and R. W. Tsien. 1996. 'Signaling from synapse to nucleus: postsynaptic CREB phosphorylation during multiple forms of hippocampal synaptic plasticity', *Neuron*, 16: 89-101.

Deisseroth, K., P. G. Mermelstein, H. Xia, and R. W. Tsien. 2003. 'Signaling from synapse to nucleus: the logic behind the mechanisms', *Curr Opin Neurobiol*, 13: 354-65.

Desmond, C. R., R. S. Atwal, J. Xia, and R. Truant. 2012. 'Identification of a karyopherin beta1/beta2 proline-tyrosine nuclear localization signal in huntingtin protein', *J Biol Chem*, 287: 39626-33.

Dieterich, D. C., A. Karpova, M. Mikhaylova, I. Zdobnova, I. Konig, M. Landwehr, M. Kreutz, K. H. Smalla, K. Richter, P. Landgraf, C. Reissner, T. M. Boeckers, W. Zuschratter, C. Spilker, C. I. Seidenbecher, C. C. Garner, E. D. Gundelfinger, and M. R. Kreutz. 2008. 'Caldendrin-Jacob: a protein liaison that couples NMDA receptor signalling to the nucleus', *PLoS Biol*, 6: e34.

Dillman, J. F., 3rd, and K. K. Pfister. 1994. 'Differential phosphorylation in vivo of cytoplasmic dynein associated with anterogradely moving organelles', *J Cell Biol*, 127: 1671-81.

Dolmetsch, R. E., U. Pajvani, K. Fife, J. M. Spotts, and M. E. Greenberg. 2001. 'Signaling to the nucleus by an L-type calcium channel-calmodulin complex through the MAP kinase pathway', *Science*, 294: 333-9.

Dolphin, A. C. 2012. 'Calcium channel auxiliary alpha2delta and beta subunits: trafficking and one step beyond', *Nat Rev Neurosci*, 13: 542-55.

Dzhura, I., Y. Wu, R. J. Colbran, J. R. Balser, and M. E. Anderson. 2000. 'Calmodulin kinase determines calcium-dependent facilitation of L-type calcium channels', *Nat Cell Biol*, 2: 173-7.

Eilers, U., J. Klumperman, and H. P. Hauri. 1989. 'Nocodazole, a microtubule-active drug, interferes with apical protein delivery in cultured intestinal epithelial cells (Caco-2)', *J Cell Biol*, 108: 13-22.

Fainzilber, M., V. Budnik, R. A. Segal, and M. R. Kreutz. 2011. 'From synapse to nucleus and back again--communication over distance within neurons', *J Neurosci*, 31: 16045-8.

Fields, R. D., P. R. Lee, and J. E. Cohen. 2005. 'Temporal integration of intracellular Ca2+ signaling networks in regulating gene expression by action potentials', *Cell Calcium*, 37: 433-42.

Franker, M. A., and C. C. Hoogenraad. 2013. 'Microtubule-based transport - basic mechanisms, traffic rules and role in neurological pathogenesis', *J Cell Sci*, 126: 2319-29.

Frischknecht, R., M. Heine, D. Perrais, C. I. Seidenbecher, D. Choquet, and E. D. Gundelfinger. 2009. 'Brain extracellular matrix affects AMPA receptor lateral mobility and short-term synaptic plasticity', *Nat Neurosci*, 12: 897-904.

Garriga-Canut, M., B. Schoenike, R. Qazi, K. Bergendahl, T. J. Daley, R. M. Pfender, J. F. Morrison, J. Ockuly, C. Stafstrom, T. Sutula, and A. Roopra. 2006. '2-Deoxy-D-glucose reduces epilepsy progression by NRSF-CtBP-dependent metabolic regulation of chromatin structure', *Nat Neurosci*, 9: 1382-7.

Ghavami, A., E. van der Giessen, and P. R. Onck. 2016. 'Energetics of Transport through the Nuclear Pore Complex', *PLoS One*, 11: e0148876.

Gladding, C. M., and L. A. Raymond. 2011. 'Mechanisms underlying NMDA receptor synaptic/extrasynaptic distribution and function', *Mol Cell Neurosci*, 48: 308-20.

Goelet, P., Castellucci, V.F., Schacher, S., and Kandel, E.R. (1986). The long and the short of long-term memory--a molecular framework. *Nature,* 322: 419-422.

Golbabapour, S., M. A. Abdulla, and M. Hajrezaei. 2011. 'A concise review on epigenetic regulation: insight into molecular mechanisms', *Int J Mol Sci*, 12: 8661-94.

Gorlich, D., and U. Kutay. 1999. 'Transport between the cell nucleus and the cytoplasm', *Annu Rev Cell Dev Biol*, 15: 607-60.

Green, M. R., and J. Sambrook. 2012. 'Molecular Cloning: A Laboratory Manual', *CSH Press*.

Greer, P. L., and M. E. Greenberg. 2008. 'From synapse to nucleus: calcium-dependent gene transcription in the control of synapse development and function', *Neuron*, 59: 846-60.

Haga, Y., N. Miwa, S. Jahangeer, T. Okada, and S. Nakamura. 2009. 'CtBP1/BARS is an activator of phospholipase D1 necessary for agonist-induced macropinocytosis', *EMBO J*, 28: 1197-207.

Hagenston, A. M., and H. Bading. 2011. 'Calcium signaling in synapse-to-nucleus communication', *Cold Spring Harb Perspect Biol*, 3: a004564.

Hanz, S., E. Perlson, D. Willis, J. Q. Zheng, R. Massarwa, J. J. Huerta, M. Koltzenburg, M. Kohler, J. van-Minnen, J. L. Twiss, and M. Fainzilber. 2003. 'Axoplasmic importins enable retrograde injury signaling in lesioned nerve', *Neuron*, 40: 1095-104.

Hara, D., T. Miyashita, M. Fukuchi, H. Suzuki, Y. Azuma, A. Tabuchi, and M. Tsuda. 2009. 'Persistent BDNF exon I-IX mRNA expression following the withdrawal of neuronal activity in neurons', *Biochem Biophys Res Commun*, 390: 648-53.

Hardingham, G. E., F. J. Arnold, and H. Bading. 2001. 'Nuclear calcium signaling controls CREB-mediated gene expression triggered by synaptic activity', *Nat Neurosci*, 4: 261-7.

Hardingham, G.E., and Bading, H. (2002). Coupling of extrasynaptic NMDA receptors to a CREB shut-off pathway is developmentally regulated. *Biochim Biophys Acta,* 1600:148-153.

Hardingham, G. E., and H. Bading. 2010. 'Synaptic versus extrasynaptic NMDA receptor signalling: implications for neurodegenerative disorders', *Nat Rev Neurosci*, 11: 682-96.

Hardingham, G. E., S. Chawla, C. M. Johnson, and H. Bading. 1997. 'Distinct functions of nuclear and cytoplasmic calcium in the control of gene expression', *Nature*, 385: 260-5.

Harrington, A. W., C. St Hillaire, L. S. Zweifel, N. O. Glebova, P. Philippidou, S. Halegoua, and D. D. Ginty. 2011. 'Recruitment of actin modifiers to TrkA endosomes governs retrograde NGF signaling and survival', *Cell*, 146: 421-34.

Harvey, C. D., R. Yasuda, H. Zhong, and K. Svoboda. 2008. 'The spread of Ras activity triggered by activation of a single dendritic spine', *Science*, 321: 136-40.

Henderson, B. R., and A. Eleftheriou. 2000. 'A comparison of the activity, sequence specificity, and CRM1-dependence of different nuclear export signals', *Exp Cell Res*, 256: 213-24.

Hidalgo Carcedo, C., M. Bonazzi, S. Spano, G. Turacchio, A. Colanzi, A. Luini, and D. Corda. 2004. 'Mitotic Golgi partitioning is driven by the membrane-fissioning protein CtBP3/BARS', *Science*, 305: 93-6.

Hildebrand, J. D., and P. Soriano. 2002. 'Overlapping and unique roles for C-terminal binding protein 1 (CtBP1) and CtBP2 during mouse development', *Mol Cell Biol*, 22: 5296-307.

Hogan, P. G., and A. Rao. 1999. 'Transcriptional regulation. Modification by nuclear export?', *Nature*, 398: 200-1.

Howe, C. L., and W. C. Mobley. 2005. 'Long-distance retrograde neurotrophic signaling', *Curr Opin Neurobiol*, 15: 40-8.

Hubler, D., M. Rankovic, K. Richter, V. Lazarevic, W. D. Altrock, K. D. Fischer, E. D. Gundelfinger, and A. Fejtova. 2012. 'Differential spatial expression and subcellular localization of CtBP family members in rodent brain', *PLoS One*, 7: e39710.

Hudmon, A., and H. Schulman. 2002. 'Neuronal CA2+/calmodulin-dependent protein kinase II: the role of structure and autoregulation in cellular function', *Annu Rev Biochem*, 71: 473-510.

Ivanova, D., A. Dirks, and A. Fejtova. 2016. 'Bassoon and piccolo regulate ubiquitination and link presynaptic molecular dynamics with activity-regulated gene expression', *J Physiol*.

Ivanova, D., A. Dirks, C. Montenegro-Venegas, C. Schone, W. D. Altrock, C. Marini, R. Frischknecht, D. Schanze, M. Zenker, E. D. Gundelfinger, and A. Fejtova. 2015. 'Synaptic activity controls localization and function of CtBP1 via binding to Bassoon and Piccolo', *EMBO J*, 34: 1056-77.

Jaimovich, E., and M. A. Carrasco. 2002. 'IP3 dependent Ca2+ signals in muscle cells are involved in regulation of gene expression', *Biol Res*, 35: 195-202.

Johnson, B. N., A. K. Berger, G. P. Cortese, and M. J. Lavoie. 2012. 'The ubiquitin E3 ligase parkin regulates the proapoptotic function of Bax', *Proc Natl Acad Sci U S A*, 109: 6283-8.

Jordan, B. A., B. D. Fernholz, L. Khatri, and E. B. Ziff. 2007. 'Activity-dependent AIDA-1 nuclear signaling regulates nucleolar numbers and protein synthesis in neurons', *Nat Neurosci*, 10: 427-35.

Jordan, B. A., and M. R. Kreutz. 2009. 'Nucleocytoplasmic protein shuttling: the direct route in synapse-to-nucleus signaling', *Trends Neurosci*, 32: 392-401.

Kaltschmidt, C., B. Kaltschmidt, and P. A. Baeuerle. 1995. 'Stimulation of ionotropic glutamate receptors activates transcription factor NF-kappa B in primary neurons', *Proc Natl Acad Sci U S A*, 92: 9618-22.

Kam, N., Y. Pilpel, and M. Fainzilber. 2009. 'Can molecular motors drive distance measurements in injured neurons?', *PLoS Comput Biol*, 5: e1000477.

Karpova, A., Bar, J., and Kreutz, M.R. (2012). Long-distance signaling from synapse to nucleus via protein messengers. Adv Exp Med Biol *970*, 355-376.

Karpova, A., M. Mikhaylova, S. Bera, J. Bar, P. P. Reddy, T. Behnisch, V. Rankovic, C. Spilker, P. Bethge, J. Sahin, R. Kaushik, W. Zuschratter, T. Kahne, M. Naumann, E. D. Gundelfinger, and M. R. Kreutz. 2013. 'Encoding and transducing the synaptic or extrasynaptic origin of NMDA receptor signals to the nucleus', *Cell*, 152: 1119-33.

Kasischke, K. A., H. D. Vishwasrao, P. J. Fisher, W. R. Zipfel, and W. W. Webb. 2004. 'Neural activity triggers neuronal oxidative metabolism followed by astrocytic glycolysis', *Science*, 305: 99-103.

Kaur, G., J. D. Ly-Huynh, and D. A. Jans. 2014. 'Intracellular calcium levels can regulate Importin-dependent nuclear import', *Biochem Biophys Res Commun*, 450: 812-7.

Kawashima, T., Okuno, H., Nonaka, M., Adachi-Morishima, A., Kyo, N., Okamura, M., Takemoto-Kimura, S., Worley, P.F., and Bito, H. (2009). Synaptic activity-responsive element in the Arc/Arg3.1 promoter essential for synapse-to-nucleus signaling in activated neurons. *Proc Natl Acad Sci U S A*, 106: 316-321.

Kegel, K. B., A. R. Meloni, Y. Yi, Y. J. Kim, E. Doyle, B. G. Cuiffo, E. Sapp, Y. Wang, Z. H. Qin, J. D. Chen, J. R. Nevins, N. Aronin, and M. DiFiglia. 2002. 'Huntingtin is present in the nucleus, interacts with the transcriptional corepressor C-terminal binding protein, and represses transcription', *J Biol Chem*, 277: 7466-76.

Kholodenko, B. N., G. C. Brown, and J. B. Hoek. 2000. 'Diffusion control of protein phosphorylation in signal transduction pathways', *Biochem J*, 350 Pt 3: 901-7.

Kim, J. H., S. Y. Choi, B. H. Kang, S. M. Lee, H. S. Park, G. Y. Kang, J. Y. Bang, E. J. Cho, and H. D. Youn. 2013. 'AMP-activated protein kinase phosphorylates CtBP1 and down-regulates its activity', *Biochem Biophys Res Commun*, 431: 8-13.

Korsak, L.I., Mitchell, M.E., Shepard, K.A., and Akins, M.R. (2016). Regulation of neuronal gene expression by local axonal translation. *Curr Genet Med Rep,* 4: 16-25.

Kraszewski, K., O. Mundigl, L. Daniell, C. Verderio, M. Matteoli, and P. De Camilli. 1995. 'Synaptic vesicle dynamics in living cultured hippocampal neurons visualized with CY3-conjugated antibodies directed against the lumenal domain of synaptotagmin', *J Neurosci*, 15: 4328-42.

Kuczewski, N., C. Porcher, N. Ferrand, H. Fiorentino, C. Pellegrino, R. Kolarow, V. Lessmann, I. Medina, and J. L. Gaiarsa. 2008. 'Backpropagating action potentials trigger dendritic release of BDNF during spontaneous network activity', *J Neurosci*, 28: 7013-23.

Kumar, V., J. E. Carlson, K. A. Ohgi, T. A. Edwards, D. W. Rose, C. R. Escalante, M. G. Rosenfeld, and A. K. Aggarwal. 2002. 'Transcription corepressor CtBP is an NAD(+)-regulated dehydrogenase', *Mol Cell*, 10: 857-69.

Kuppuswamy, M., S. Vijayalingam, L. J. Zhao, Y. Zhou, T. Subramanian, J. Ryerse, and G. Chinnadurai. 2008. 'Role of the PLDLS-binding cleft region of CtBP1 in recruitment of core and auxiliary components of the corepressor complex', *Mol Cell Biol*, 28: 269-81.

Kutsuwada, T., K. Sakimura, T. Manabe, C. Takayama, N. Katakura, E. Kushiya, R. Natsume, M. Watanabe, Y. Inoue, T. Yagi, S. Aizawa, M. Arakawa, T. Takahashi, Y. Nakamura, H. Mori, and M. Mishina. 1996. 'Impairment of suckling response, trigeminal neuronal pattern formation, and hippocampal LTD in NMDA receptor epsilon 2 subunit mutant mice', *Neuron*, 16: 333-44.

Laemmli, U. K. 1970. 'Cleavage of structural proteins during the assembly of the head of bacteriophage T4', *Nature*, 227: 680-5.

Lauritzen, F., T. Eid, and L. H. Bergersen. 2015. 'Monocarboxylate transporters in temporal lobe epilepsy: roles of lactate and ketogenic diet', *Brain Struct Funct*, 220: 1-12.

Lazarevic, V., C. Schone, M. Heine, E. D. Gundelfinger, and A. Fejtova. 2011. 'Extensive remodeling of the presynaptic cytomatrix upon homeostatic adaptation to network activity silencing', *J Neurosci*, 31: 10189-200.

Lee, B., G. Q. Butcher, K. R. Hoyt, S. Impey, and K. Obrietan. 2005. 'Activity-dependent neuroprotection and cAMP response element-binding protein (CREB): kinase coupling, stimulus intensity, and temporal regulation of CREB phosphorylation at serine 133', *J Neurosci*, 25: 1137-48.

Lee, S. H., C. S. Lim, H. Park, J. A. Lee, J. H. Han, H. Kim, Y. H. Cheang, S. H. Lee, Y. S. Lee, H. G. Ko, D. H. Jang, H. Kim, M. C. Miniaci, D. Bartsch, E. Kim, C. H. Bailey, E. R. Kandel, and B. K. Kaang. 2007. 'Nuclear translocation of CAM-associated protein activates transcription for long-term facilitation in Aplysia', *Cell*, 129: 801-12.

Leisner, T. M., M. Liu, Z. M. Jaffer, J. Chernoff, and L. V. Parise. 2005. 'Essential role of CIB1 in regulating PAK1 activation and cell migration', *J Cell Biol*, 170: 465-76.

Liberali, P., E. Kakkonen, G. Turacchio, C. Valente, A. Spaar, G. Perinetti, R. A. Bockmann, D. Corda, A. Colanzi, V. Marjomaki, and A. Luini. 2008. 'The closure of Pak1-dependent macropinosomes requires the phosphorylation of CtBP1/BARS', *EMBO J*, 27: 970-81.

Lim, A. F., W. L. Lim, and T. H. Ch'ng. 2016. 'Activity-dependent synapse to nucleus signaling', *Neurobiol Learn Mem*.

Lin, X., B. Sun, M. Liang, Y. Y. Liang, A. Gast, J. Hildebrand, F. C. Brunicardi, F. Melchior, and X. H. Feng. 2003. 'Opposed regulation of corepressor CtBP by SUMOylation and PDZ binding', *Mol Cell*, 11: 1389-96.

Lois, C., E. J. Hong, S. Pease, E. J. Brown, and D. Baltimore. 2002. 'Germline transmission and tissue-specific expression of transgenes delivered by lentiviral vectors', *Science*, 295: 868-72.

Maas, C., Torres, V.I., Altrock, W.D., Leal-Ortiz, S., Wagh, D., Terry-Lorenzo, R.T., Fejtova, A., Gundelfinger, E.D., Ziv, N.E., and Garner, C.C. (2012). Formation of Golgi-derived active zone precursor vesicles. *J Neurosci,* 32: 11095-11108.

McBride, K. M., G. Banninger, C. McDonald, and N. C. Reich. 2002. 'Regulated nuclear import of the STAT1 transcription factor by direct binding of importin-alpha', *EMBO J*, 21: 1754-63.

McKinstry, S. U., Y. B. Karadeniz, A. K. Worthington, V. Y. Hayrapetyan, M. I. Ozlu, K. Serafin-Molina, W. C. Risher, T. Ustunkaya, I. Dragatsis, S. Zeitlin, H. H. Yin, and C. Eroglu. 2014. 'Huntingtin is required for normal excitatory synapse development in cortical and striatal circuits', *J Neurosci*, 34: 9455-72.

Mills, L. R., C. E. Niesen, A. P. So, P. L. Carlen, I. Spigelman, and O. T. Jones. 1994. 'N-type Ca2+ channels are located on somata, dendrites, and a subpopulation of dendritic spines on live hippocampal pyramidal neurons', *J Neurosci*, 14: 6815-24.

Mirnezami, A. H., S. J. Campbell, M. Darley, J. N. Primrose, P. W. Johnson, and J. P. Blaydes. 2003. 'Hdm2 recruits a hypoxia-sensitive corepressor to negatively regulate p53-dependent transcription', *Curr Biol*, 13: 1234-9.

Monyer, H., N. Burnashev, D. J. Laurie, B. Sakmann, and P. H. Seeburg. 1994. 'Developmental and regional expression in the rat brain and functional properties of four NMDA receptors', *Neuron*, 12: 529-40.

Moore, D. L., and J. L. Goldberg. 2011. 'Multiple transcription factor families regulate axon growth and regeneration', *Dev Neurobiol*, 71: 1186-211.

Morrison, D. K. 2012. 'MAP kinase pathways', *Cold Spring Harb Perspect Biol*, 4.

Mullen, R. J., C. R. Buck, and A. M. Smith. 1992. 'NeuN, a neuronal specific nuclear protein in vertebrates', *Development*, 116: 201-11.

Nachury, M. V., and K. Weis. 1999. 'The direction of transport through the nuclear pore can be inverted', *Proc Natl Acad Sci U S A*, 96: 9622-7.

Nardini, M., S. Spano, C. Cericola, A. Pesce, A. Massaro, E. Millo, A. Luini, D. Corda, and M. Bolognesi. 2003. 'CtBP/BARS: a dual-function protein involved in transcription co-repression and Golgi membrane fission', *EMBO J*, 22: 3122-30.

Palmeri, D., and M. H. Malim. 1999. 'Importin beta can mediate the nuclear import of an arginine-rich nuclear localization signal in the absence of importin alpha', *Mol Cell Biol*, 19: 1218-25.

Paoletti, P. 2011. 'Molecular basis of NMDA receptor functional diversity', *Eur J Neurosci*, 33: 1351-65.

Papadia, S., P. Stevenson, N. R. Hardingham, H. Bading, and G. E. Hardingham. 2005. 'Nuclear Ca2+ and the cAMP response element-binding protein family mediate a late phase of activity-dependent neuroprotection', *J Neurosci*, 25: 4279-87.

Pemberton, L. F., and B. M. Paschal. 2005. 'Mechanisms of receptor-mediated nuclear import and nuclear export', *Traffic*, 6: 187-98.

Perry, R. B., E. Doron-Mandel, E. Iavnilovitch, I. Rishal, S. Y. Dagan, M. Tsoory, G. Coppola, M. K. McDonald, C. Gomes, D. H. Geschwind, J. L. Twiss, A. Yaron, and M. Fainzilber. 2012. 'Subcellular knockout of importin beta1 perturbs axonal retrograde signaling', *Neuron*, 75: 294-305.

Piccoli, G., S. B. Condliffe, M. Bauer, F. Giesert, K. Boldt, S. De Astis, A. Meixner, H. Sarioglu, D. M. Vogt-Weisenhorn, W. Wurst, C. J. Gloeckner, M. Matteoli, C. Sala, and M. Ueffing. 2011. 'LRRK2 controls synaptic vesicle storage and mobilization within the recycling pool', *J Neurosci*, 31: 2225-37.

Popov, N., M. Schmitt, S. Schulzeck, and H. Matthies. 1975. '[Reliable micromethod for determination of the protein content in tissue homogenates]', *Acta Biol Med Ger*, 34: 1441-6.

Postigo, A. A., and D. C. Dean. 1999. 'ZEB represses transcription through interaction with the corepressor CtBP', *Proc Natl Acad Sci U S A*, 96: 6683-8.

Powell, J. A., M. A. Carrasco, D. S. Adams, B. Drouet, J. Rios, M. Muller, M. Estrada, and E. Jaimovich. 2001. 'IP(3) receptor function and localization in myotubes: an unexplored Ca(2+) signaling pathway in skeletal muscle', *J Cell Sci*, 114: 3673-83.

Proepper, C., S. Johannsen, S. Liebau, J. Dahl, B. Vaida, J. Bockmann, M. R. Kreutz, E. D. Gundelfinger, and T. M. Boeckers. 2007. 'Abelson interacting protein 1 (Abi-1) is essential for dendrite morphogenesis and synapse formation', *EMBO J*, 26: 1397-409.

Quinlan, K. G., M. Nardini, A. Verger, P. Francescato, P. Yaswen, D. Corda, M. Bolognesi, and M. Crossley. 2006. 'Specific recognition of ZNF217 and other zinc finger proteins at a surface groove of C-terminal binding proteins', *Mol Cell Biol*, 26: 8159-72.

Quinlan, K. G., A. Verger, A. Kwok, S. H. Lee, J. Perdomo, M. Nardini, M. Bolognesi, and M. Crossley. 2006. 'Role of the C-terminal binding protein PXDLS motif binding cleft in protein interactions and transcriptional repression', *Mol Cell Biol*, 26: 8202-13.

Riefler, G. M., and B. L. Firestein. 2001. 'Binding of neuronal nitric-oxide synthase (nNOS) to carboxyl-terminal-binding protein (CtBP) changes the localization of CtBP from the nucleus to the cytosol: a novel function for targeting by the PDZ domain of nNOS', *J Biol Chem*, 276: 48262-8.

Rishal, I., and M. Fainzilber. 2010. 'Retrograde signaling in axonal regeneration', *Exp Neurol*, 223: 5-10.

Rishal, I., N. Kam, R. B. Perry, V. Shinder, E. M. Fisher, G. Schiavo, and M. Fainzilber. 2012. 'A motor-driven mechanism for cell-length sensing', *Cell Rep*, 1: 608-16.

Sakimura, K., T. Kutsuwada, I. Ito, T. Manabe, C. Takayama, E. Kushiya, T. Yagi, S. Aizawa, Y. Inoue, H. Sugiyama, and et al. 1995. 'Reduced hippocampal LTP and spatial learning in mice lacking NMDA receptor epsilon 1 subunit', *Nature*, 373: 151-5.

Sandler, V. M., and J. G. Barbara. 1999. 'Calcium-induced calcium release contributes to action potential-evoked calcium transients in hippocampal CA1 pyramidal neurons', *J Neurosci*, 19: 4325-36.

Schaeper, U., J. M. Boyd, S. Verma, E. Uhlmann, T. Subramanian, and G. Chinnadurai. 1995. 'Molecular cloning and characterization of a cellular phosphoprotein that interacts with a conserved C-terminal domain of adenovirus E1A involved in negative modulation of oncogenic transformation', *Proc Natl Acad Sci U S A*, 92: 10467-71.

Schlumm, F., D. Mauceri, H. E. Freitag, and H. Bading. 2013. 'Nuclear calcium signaling regulates nuclear export of a subset of class IIa histone deacetylases following synaptic activity', *J Biol Chem*, 288: 8074-84.

Schmitz, F., A. Konigstorfer, and T. C. Sudhof. 2000. 'RIBEYE, a component of synaptic ribbons: a protein's journey through evolution provides insight into synaptic ribbon function', *Neuron*, 28: 857-72.

Scholz, K. P., and R. J. Miller. 1995. 'Developmental changes in presynaptic calcium channels coupled to glutamate release in cultured rat hippocampal neurons', *J Neurosci*, 15: 4612-7.

Schraivogel, D., S. G. Schindler, J. Danner, E. Kremmer, J. Pfaff, S. Hannus, R. Depping, and G. Meister. 2015. 'Importin-beta facilitates nuclear import of human GW proteins and balances cytoplasmic gene silencing protein levels', *Nucleic Acids Res*, 43: 7447-61.

Shen, T., Z. Cseresnyes, Y. Liu, W. R. Randall, and M. F. Schneider. 2007. 'Regulation of the nuclear export of the transcription factor NFATc1 by protein kinases after slow fibre type electrical stimulation of adult mouse skeletal muscle fibres', *J Physiol*, 579: 535-51.

Sheng, M., J. Cummings, L. A. Roldan, Y. N. Jan, and L. Y. Jan. 1994. 'Changing subunit composition of heteromeric NMDA receptors during development of rat cortex', *Nature*, 368: 144-7.

Shi, Y., F. Lan, C. Matson, P. Mulligan, J. R. Whetstine, P. A. Cole, R. A. Casero, and Y. Shi. 2004. 'Histone demethylation mediated by the nuclear amine oxidase homolog LSD1', *Cell*, 119: 941-53.

Shi, Y., J. Sawada, G. Sui, B. Affar el, J. R. Whetstine, F. Lan, H. Ogawa, M. P. Luke, Y. Nakatani, and Y. Shi. 2003. 'Coordinated histone modifications mediated by a CtBP co-repressor complex', *Nature*, 422: 735-8.

Soderholm, J. F., S. L. Bird, P. Kalab, Y. Sampathkumar, K. Hasegawa, M. Uehara-Bingen, K. Weis, and R. Heald. 2011. 'Importazole, a small molecule inhibitor of the transport receptor importin-beta', *ACS Chem Biol*, 6: 700-8.

Spano, S., M. G. Silletta, A. Colanzi, S. Alberti, G. Fiucci, C. Valente, A. Fusella, M. Salmona, A. Mironov, A. Luini, and D. Corda. 1999. 'Molecular cloning and functional characterization of brefeldin A-ADP-ribosylated substrate. A novel protein involved in the maintenance of the Golgi structure', *J Biol Chem*, 274: 17705-10.

Stafstrom, C. E. 2004. 'Dietary approaches to epilepsy treatment: old and new options on the menu', *Epilepsy Curr*, 4: 215-22.

Staley, K. 2004. 'Neuroscience. Epileptic neurons go wireless', *Science*, 305: 482-3.

Strack, S., R. B. McNeill, and R. J. Colbran. 2000. 'Mechanism and regulation of calcium/calmodulin-dependent protein kinase II targeting to the NR2B subunit of the N-methyl-D-aspartate receptor', *J Biol Chem*, 275: 23798-806.

Strambio-De-Castillia, C., M. Niepel, and M. P. Rout. 2010. 'The nuclear pore complex: bridging nuclear transport and gene regulation', *Nat Rev Mol Cell Biol*, 11: 490-501.

Sun, L., D. Chiu, D. Kowal, R. Simon, M. Smeyne, R. S. Zukin, J. Olney, R. Baudy, and S. Lin. 2004. 'Characterization of two novel N-methyl-D-aspartate antagonists: EAA-090 (2-[8,9-dioxo-2,6-diazabicyclo [5.2.0]non-1(7)-en2-yl]ethylphosphonic acid) and EAB-318 (R-alpha-amino-5-chloro-1-(phosphonomethyl)-1H-benzimidazole-2-propanoic acid hydrochloride)', *J Pharmacol Exp Ther*, 310: 563-70.

Sutton, K. G., J. E. McRory, H. Guthrie, T. H. Murphy, and T. P. Snutch. 1999. 'P/Q-type calcium channels mediate the activity-dependent feedback of syntaxin-1A', *Nature*, 401: 800-4.

Tao, X., A. E. West, W. G. Chen, G. Corfas, and M. E. Greenberg. 2002. 'A calcium-responsive transcription factor, CaRF, that regulates neuronal activity-dependent expression of BDNF', *Neuron*, 33: 383-95.

Thiagalingam, A., A. De Bustros, M. Borges, R. Jasti, D. Compton, L. Diamond, M. Mabry, D. W. Ball, S. B. Baylin, and B. D. Nelkin. 1996. 'RREB-1, a novel zinc finger protein, is involved in the differentiation response to Ras in human medullary thyroid carcinomas', *Mol Cell Biol*, 16: 5335-45.

Thomas, G. M., and R. L. Huganir. 2004. 'MAPK cascade signalling and synaptic plasticity', *Nat Rev Neurosci*, 5: 173-83.

Thomas, J.L., Moncollin, V., Ravel-Chapuis, A., Valente, C., Corda, D., Mejat, A., and Schaeffer, L. (2015). PAK1 and CtBP1 Regulate the Coupling of Neuronal Activity to Muscle Chromatin and Gene Expression. *Mol Cell Biol,* 35: 4110-4120.

Thompson, K. R., K. O. Otis, D. Y. Chen, Y. Zhao, T. J. O'Dell, and K. C. Martin. 2004. 'Synapse to nucleus signaling during long-term synaptic plasticity; a role for the classical active nuclear import pathway', *Neuron*, 44: 997-1009.

tom Dieck, S., W. D. Altrock, M. M. Kessels, B. Qualmann, H. Regus, D. Brauner, A. Fejtova, O. Bracko, E. D. Gundelfinger, and J. H. Brandstatter. 2005. 'Molecular dissection of the photoreceptor ribbon synapse: physical interaction of Bassoon and RIBEYE is essential for the assembly of the ribbon complex', *J Cell Biol*, 168: 825-36.

Traynelis, S. F., L. P. Wollmuth, C. J. McBain, F. S. Menniti, K. M. Vance, K. K. Ogden, K. B. Hansen, H. Yuan, S. J. Myers, and R. Dingledine. 2010. 'Glutamate receptor ion channels: structure, regulation, and function', *Pharmacol Rev*, 62: 405-96.

Tsuriel, S., R. Geva, P. Zamorano, T. Dresbach, T. Boeckers, E. D. Gundelfinger, C. C. Garner, and N. E. Ziv. 2006. 'Local sharing as a predominant determinant of synaptic matrix molecular dynamics', *PLoS Biol*, 4: e271.

Valente, C., A. Luini, and D. Corda. 2013. 'Components of the CtBP1/BARS-dependent fission machinery', *Histochem Cell Biol*, 140: 407-21.

Vali, S., R. Carlsen, I. Pessah, and F. Gorin. 2000. 'Role of the sarcoplasmic reticulum in regulating the activity-dependent expression of the glycogen phosphorylase gene in contractile skeletal muscle cells', *J Cell Physiol*, 185: 184-99.

Vashishta, A., A. Habas, P. Pruunsild, J. J. Zheng, T. Timmusk, and M. Hetman. 2009. 'Nuclear factor of activated T-cells isoform c4 (NFATc4/NFAT3) as a mediator of antiapoptotic transcription in NMDA receptor-stimulated cortical neurons', *J Neurosci*, 29: 15331-40.

Verger, A., K. G. Quinlan, L. A. Crofts, S. Spano, D. Corda, E. P. Kable, F. Braet, and M. Crossley. 2006. 'Mechanisms directing the nuclear localization of the CtBP family proteins', *Mol Cell Biol*, 26: 4882-94.

Wang, C. C., R. G. Held, S. C. Chang, L. Yang, E. Delpire, A. Ghosh, and B. J. Hall. 2011. 'A critical role for GluN2B-containing NMDA receptors in cortical development and function', *Neuron*, 72: 789-805.

Wang, R., and M. G. Brattain. 2007. 'The maximal size of protein to diffuse through the nuclear pore is larger than 60kDa', *FEBS Lett*, 581: 3164-70.

Weichenhan, D., and C. Plass. 2013. 'The evolving epigenome', *Hum Mol Genet*, 22: R1-6.

Wen, W., J. L. Meinkoth, R. Y. Tsien, and S. S. Taylor. 1995. 'Identification of a signal for rapid export of proteins from the nucleus', *Cell*, 82: 463-73.

West, A. E., E. C. Griffith, and M. E. Greenberg. 2002. 'Regulation of transcription factors by neuronal activity', *Nat Rev Neurosci*, 3: 921-31.

Wiegert, J. S., C. P. Bengtson, and H. Bading. 2007. 'Diffusion and not active transport underlies and limits ERK1/2 synapse-to-nucleus signaling in hippocampal neurons', *J Biol Chem*, 282: 29621-33.

Xiang, G., L. Pan, W. Xing, L. Zhang, L. Huang, J. Yu, R. Zhang, J. Wu, J. Cheng, and Y. Zhou. 2007. 'Identification of activity-dependent gene expression profiles reveals specific subsets of genes induced by different routes of Ca(2+) entry in cultured rat cortical neurons', *J Cell Physiol*, 212: 126-36.

Xiao, Z., X. Liu, and H. F. Lodish. 2000. 'Importin beta mediates nuclear translocation of Smad 3', *J Biol Chem*, 275: 23425-8.

Yang, H., S. D. Chen, G. Q. Lu, B. Li, L. Liang, and J. Y. Xu. 2005. '[Proteasomal inhibitor lactacystin induces cell apoptosis and caspase 3 activation in PC12 cells]', *Zhonghua Yi Xue Za Zhi*, 85: 2058-61.

Yang, J. S., S. Y. Lee, S. Spano, H. Gad, L. Zhang, Z. Nie, M. Bonazzi, D. Corda, A. Luini, and V. W. Hsu. 2005. 'A role for BARS at the fission step of COPI vesicle formation from Golgi membrane', *EMBO J*, 24: 4133-43.

Young, K. W., M. A. Garro, R. A. Challiss, and S. R. Nahorski. 2004. 'NMDA-receptor regulation of muscarinic-receptor stimulated inositol 1,4,5-trisphosphate production and protein kinase C activation in single cerebellar granule neurons', *J Neurochem*, 89: 1537-46.

Yudin, D., S. Hanz, S. Yoo, E. Iavnilovitch, D. Willis, T. Gradus, D. Vuppalanchi, Y. Segal-Ruder, K. Ben-Yaakov, M. Hieda, Y. Yoneda, J. L. Twiss, and M. Fainzilber. 2008. 'Localized regulation of axonal RanGTPase controls retrograde injury signaling in peripheral nerve', *Neuron*, 59: 241-52.

Zanassi, P., M. Paolillo, A. Feliciello, E. V. Avvedimento, V. Gallo, and S. Schinelli. 2001. 'cAMP-dependent protein kinase induces cAMP-response element-binding protein phosphorylation via an intracellular calcium release/ERK-dependent pathway in striatal neurons', *J Biol Chem*, 276: 11487-95.

Zhang, Q., D. W. Piston, and R. H. Goodman. 2002. 'Regulation of corepressor function by nuclear NADH', *Science*, 295: 1895-7.

Zhang, Q., Y. Yoshimatsu, J. Hildebrand, S. M. Frisch, and R. H. Goodman. 2003. 'Homeodomain interacting protein kinase 2 promotes apoptosis by downregulating the transcriptional corepressor CtBP', *Cell*, 115: 177-86.

Zhou, Z., E. J. Hong, S. Cohen, W. N. Zhao, H. Y. Ho, L. Schmidt, W. G. Chen, Y. Lin, E. Savner, E. C. Griffith, L. Hu, J. A. Steen, C. J. Weitz, and M. E. Greenberg. 2006. 'Brain-specific phosphorylation of MeCP2 regulates activity-dependent Bdnf transcription, dendritic growth, and spine maturation', *Neuron*, 52: 255-69.

Zhou, X., Hollern, D., Liao, J., Andrechek, E., and Wang, H. (2013). NMDA receptor-mediated excitotoxicity depends on the coactivation of synaptic and extrasynaptic receptors. *Cell Death Dis,* 4: e560.

Zhu, J., and F. McKeon. 1999. 'NF-AT activation requires suppression of Crm1-dependent export by calcineurin', *Nature*, 398: 256-60.

Zou, H., C. Ho, K. Wong, and M. Tessier-Lavigne. 2009. 'Axotomy-induced Smad1 activation promotes axonal growth in adult sensory neurons', *J Neurosci*, 29: 7116-23.

6. Abbreviations

4-AP	4-aminopyridin
A	alanine
AMPAR	α-amino-3-hydroxy-5-methyl-4-isoxazolepropionic acid receptors
ANOVA	analysis of variance
APV	D-(-)-2-amino-5-phosphonopentanoic acid
ATF	activating transcription factor protein family
BDNF	brain-derived neurotrophic factor
BKLF	basic Krüppel-like factor
BSA	bovine serum albumin
CaMKII	calcium/calmodulin-dependent protein kinase II
cDNA	complementary DNA
CNQX	6-cyano-7-nitroquinoxaline-2,3-dione disodium
CRM1	exportin 1
DIV	day-*in-vitro*
DNA	deoxyribonucleic acid
E.coli	*Eschericia coli*
EDTA	ethylenediaminetetraacetic acid
EFGP	enhanced green fluorescent protein
e.g.	exempli gratia, for example
ERK1/2	extracellular-signal-regulated kinase
et al.	*et alias*
Fig.	Figure
GAPDH	glyceraldehyde 3-phosphate dehydrogenase
GFP	green fluorescent protein
GluN2A	N-methyl-D-aspartate receptor subunit A
GluN2B	N-methyl-D-aspartate receptor subunit A
gp	guinea pig
GTP	guanosine 5´-triphosphate
HAT	histone acetyltransferase
HBSS	Hank´s Balanced Salt
HDAC	histone deacetylases
HEK cells	human embryonic kidney cells
HEPES	4-(2-hydroxyethyl)-1-piperazineethansulfonic acid
HIPK2	homeodomain interacting protein kinase 2
HMT	histone methyltransferase
ICC	immunocytochemistry
IF	immunofluorescence
ID	integrated density
Imp β	importin β
$InsP_3$	inositol 1,4,5-triphosphate
IP_3-receptor	inositol 1,4,5-triphosphate receptor
kDa	kilo Dalton
KO	knock-out

KPNB1	gene encoding Importin β
MAPK	mitogen-activated kinase
mRNA	messenger RNA
NAD	nicotinamide adenine dinucleotide
ms	mouse
n.s.	not significant
NBD	nucleotide binding domain
NES	nuclear export signal
NF-κB	nuclear factor „kappa-light-chain-enhancer“ of activated B-cells
NGF	neurotrophic growth factor
NLS	nuclear localization signal
NMDA	N-methyl-D-aspartate
nNOS	neuronal nitric-oxide synthase
NPC	nuclear pore complex
NRSF/REST	neuron-restrictive silencer factor/RE1-silencing transcription factor
p	p-value (statistics)
pa	photoactivatable
PAGE	polyacrylamide gel electrophoresis
Pak1	group I p21-activated kinase
PBS	phosphate-buffered saline
PCR	polymerase chain reaction
PFA	paraformaldehyde
PKA	c-AMP-dependent protein kinase A
pS	phosphorylated serine
PTV	Piccolo-Bassoon transport vesicles
PVDF	polyvinyliden fluoride
rb	rabbit
RNA	ribonucleic acid
S	serine
SBD	substrate binding domain
SDS	sodium dodecyl sulfate
SEM	standard error of the mean
STAT	signal transducer and activator of transcription protein family
SUMO	small ubiquitin like modifier
T	threonine
TAE	tris-acetate-EDTA-buffer
TEMED	tetramethylethylenediamine
T_m	annealing temperature
TrkA	tropomyosin receptor kinase A
TTX	tetrodotoxin
VGCC	voltage-gated calcium channel
WB	western blot
WT	wild-type

7. Curriculum Vitae

Personal information

Name:	Anika Dirks
Date of birth:	20.05.1987
Family status:	Married
Nationality:	German

Education and qualification

since 10.2012	PhD thesis at the Leibniz Institute for Neurobiology, Magdeburg Title of PhD Thesis: "Identification of molecular mechanisms modulating nuclear abundance and co-repressor functions of CtBP1 in neurons"
10.2010 - 09.2012	Master of Science Biochemistry, University of Halle-Wittenberg Title of master thesis: "Generation, expression, purification and characterization of pyroglutamate-specific antibodies" at probiodrug AG Halle
05.2011 - 09.2011	Summer student at the University of Cambridge (UK), MRC/LMB, group leader: Prof. Dr. Ermanno Gherardi
10.2007 - 09.2010	Bachelor of Science Biochemistry, University of Halle-Wittenberg Title of bachelor thesis: "Analysis of OPMD-relevant protein conformation changes of the poly (A) binding protein nuclear 1"
10.2006 - 09.2007	Study of Dentist, University of Halle-Wittenberg
1999 - 2006	Grammar school Europagymnasium „Richard von Weizsäcker", Thale
1997 - 1999	Secondary school Sekundarschule „Käthe Kollwitz", Thale
1993 - 1997	Primary school Grundschule „Auf den Höhen", Thale

Magdeburg, 31.03.2017

Anika Dirks

8. List of publications

Synaptic activity controls localization and function of CtBP1 via binding to Bassoon and Piccolo. Ivanova D[1], **Dirks A**[2], Montenegro-Venegas C[2], Schöne C[2], Altrock WD[3], Marini C[2], Frischknecht R[3], Schanze D[4], Zenker M[4], Gundelfinger ED[5], Fejtova A[6]. *EMBO J.* 2015 Apr 15;34(8):1056-77.

Bassoon and piccolo regulate ubiquitination and link presynaptic molecular dynamics with activity-regulated gene expression. Ivanova D[1], **Dirks A**[2], Fejtova A[1,3]. *J Physiol.* 2016 Feb 24.

9. Eidesstattliche Erklärung

Hiermit versichere ich, dass ich die von mir eingereichte Dissertation selbstständig und ohne fremde Hilfe angefertigt und keine anderen als die angegebenen Quellen und Hilfsmittel verwendet habe.

Weiterhin erkläre ich, dass ich weder diese noch eine andere Arbeit zur Erlangung des akademischen Grades doctor rerum naturalium (Dr. rer. nat.) an anderen Einrichtungen eingereicht habe.

Magdeburg, 31.03.2017

Ort, Datum

Unterschrift Anika Dirks